



**British  
Geological Survey**

NATURAL ENVIRONMENT RESEARCH COUNCIL

# State of stress across UK Regions

GeoAnalytics and Modelling Directorate

Open Report OR/17/048



BRITISH GEOLOGICAL SURVEY

GEOANALYTICS and Modelling Directorate

OPEN REPORT OR/17/048

# State of stress across UK Regions

M.W. Fellgett, A. Kingdon, J.D.O. Williams, C.M.A. Gent

The National Grid and other  
Ordnance Survey data © Crown  
Copyright and database rights  
2017. Ordnance Survey Licence  
No. 100021290

## *Keywords*

UK stress field, Stress  
Magnitude, Legacy Data, Pore  
Pressure, Vertical stress,  
Minimum Horizontal Stress,  
Maximum Horizontal Stress.

## *Bibliographical reference*

M.W. FELLGETT, A. Kingdon,  
J.D.O. Williams, C.M.A. Gent.  
2017. State of stress across UK  
Regions. *British Geological  
Survey Open Report*, OR/17/048.  
64pp.

Copyright in materials derived  
from the British Geological  
Survey's work is owned by the  
Natural Environment Research  
Council (NERC) and/or the  
authority that commissioned the  
work. You may not copy or adapt  
this publication without first  
obtaining permission. Contact the  
BGS Intellectual Property Rights  
Section, British Geological  
Survey, Keyworth,  
e-mail [ipr@bgs.ac.uk](mailto:ipr@bgs.ac.uk). You may  
quote extracts of a reasonable  
length without prior permission,  
provided a full acknowledgement  
is given of the source of the  
extract.

Maps and diagrams in this book  
use topography based on  
Ordnance Survey mapping.

## BRITISH GEOLOGICAL SURVEY

The full range of our publications is available from BGS shops at Nottingham, Edinburgh, London and Cardiff (Welsh publications only) see contact details below or shop online at [www.geologyshop.com](http://www.geologyshop.com)

The London Information Office also maintains a reference collection of BGS publications, including maps, for consultation.

We publish an annual catalogue of our maps and other publications; this catalogue is available online or from any of the BGS shops.

*The British Geological Survey carries out the geological survey of Great Britain and Northern Ireland (the latter as an agency service for the government of Northern Ireland), and of the surrounding continental shelf, as well as basic research projects. It also undertakes programmes of technical aid in geology in developing countries.*

*The British Geological Survey is a component body of the Natural Environment Research Council.*

*British Geological Survey offices*

### **BGS Central Enquiries Desk**

Tel 0115 936 3143 Fax 0115 936 3276  
email [enquiries@bgs.ac.uk](mailto:enquiries@bgs.ac.uk)

### **Environmental Science Centre, Keyworth, Nottingham NG12 5GG**

Tel 0115 936 3241 Fax 0115 936 3488  
email [sales@bgs.ac.uk](mailto:sales@bgs.ac.uk)

### **The Lyell Centre, Research Avenue South, Edinburgh EH14 4AP**

Tel 0131 667 1000 Fax 0131 668 2683  
email [scotsales@bgs.ac.uk](mailto:scotsales@bgs.ac.uk)

### **Natural History Museum, Cromwell Road, London SW7 5BD**

Tel 020 7589 4090 Fax 020 7584 8270  
Tel 020 7942 5344/45 email [bgs london@bgs.ac.uk](mailto:bgs london@bgs.ac.uk)

### **Columbus House, Greenmeadow Springs, Tongwynlais, Cardiff CF15 7NE**

Tel 029 2052 1962 Fax 029 2052 1963

### **Maclean Building, Crowmarsh Gifford, Wallingford OX10 8BB**

Tel 01491 838800 Fax 01491 692345

### **Geological Survey of Northern Ireland, Department of Enterprise, Trade & Investment, Dundonald House, Upper Newtownards Road, Ballymiscaw, Belfast, BT4 3SB**

Tel 028 9038 8462 Fax 028 9038 8461

[www.bgs.ac.uk/gsni/](http://www.bgs.ac.uk/gsni/)

### *Parent Body*

### **Natural Environment Research Council, Polaris House, North Star Avenue, Swindon SN2 1EU**

Tel 01793 411500 Fax 01793 411501  
[www.nerc.ac.uk](http://www.nerc.ac.uk)

Website [www.bgs.ac.uk](http://www.bgs.ac.uk)

Shop online at [www.geologyshop.com](http://www.geologyshop.com)

# Foreword

New and emerging subsurface energy technologies and the extent to which they might make a major contribution to the energy security of the UK, the UK economy and to jobs is a subject of close debate. The complexity of geological conditions in the UK means that there is a need to better understand the impacts of energy technologies on the subsurface environment. Our vision is that the research facilities at the UK Geoenergy Observatories will allow us to carry out ground-breaking scientific monitoring, observation and experimentation to gather critical evidence on the impact on the environment (primarily in terms of the sub-surface and linking to the wider environment) of a range of geoenergy technologies.

The Natural Environment Research Council (NERC) through the British Geological Survey, the UK environmental science base and in collaboration with industry, will deliver the UK Geoenergy Observatories project comprised of two new world-class subsurface research facilities. These facilities will enable rigorous, transparent and replicable observations of subsurface processes, framed by the Energy Security Innovation and Observing System for the sub surface Science Plan. The two facilities will form the heart of a wider distributed network of sensors and instrumented boreholes for monitoring the subsurface across the UK. Scientific research will generate knowledge applicable to a wide range of energy technologies including: shallow geothermal energy, shale gas, underground gas storage, coal bed methane, underground coal gasification, and carbon capture and storage.

The UK Geoenergy Observatories project will create a first-of-its-kind set of national infrastructure research and testing facilities capable of investigating the feasibility of innovative unconventional and emerging energy technologies. Specifically, the project will allow us to:

- deploy sensors and monitoring equipment to enable world-class science and understanding of subsurface processes and interactions
- develop real-time, independent data capable of providing independent evidence to better inform decisions relating to unconventional, emerging and innovative energy technologies policy, regulatory practice and business operations in these technology areas.

This report is a published product of the UK Geoenergy Observatories project (formerly known as the ESIOS project), by the British Geological Survey (BGS) and forms part of the geological characterisation of the Cheshire site. The report describes the data available to characterise the onshore in-situ stress field near Cheshire and two other UK regions. This report also compiles all of the available data on the maximum horizontal stress. Key outputs include estimates of vertical, stress pore pressure and minimum horizontal stress in the Cheshire and Lancashire region.

This report is based on data as compiled by 31-Jan-2016, additional Hydraulic Fracture data from the Coal Authority may be available. It does not include any data from the World stress Map database (Heidbach et al., 2016) which could not be independently verified at the time of writing. Some data may since have been collected.

## Acknowledgements

The authors would like to thank David Evans and Edward Hough for their review and comments to improve this report and the BGS records team and Library team, in particular Catherine Oldham and Lesley Gerrett for help in collating the legacy stress field information from the Coal Authority and the Hot Dry Rock Project. Rose diagrams were produced using the ‘circular’ package in R, see; Agostinelli and Lund (2013) for details.

# Contents

<b>Foreword</b> .....	<b>i</b>
<b>Acknowledgements</b> .....	<b>i</b>
<b>Contents</b> .....	<b>ii</b>
<b>Summary</b> .....	<b>v</b>
<b>1 Introduction</b> .....	<b>6</b>
<b>2 Characterising the UK stress field and in-situ stresses</b> .....	<b>6</b>
2.1 Vertical stress .....	9
2.2 Minimum horizontal stress .....	12
2.3 Pore Pressure .....	13
2.4 Stress Field Orientation .....	13
2.5 Maximum horizontal stress .....	16
2.6 Well Data Quality Control .....	16
<b>3 Regions</b> .....	<b>17</b>
3.1 Eastern Yorkshire and North Nottinghamshire .....	17
3.2 The Weald .....	23
3.3 Cheshire and Lancashire .....	24
3.4 Additional Maximum Horizontal stress data.....	29
<b>4 Discussion</b> .....	<b>30</b>
<b>5 Conclusions</b> .....	<b>40</b>
<b>6 Further Work</b> .....	<b>41</b>
<b>Appendix 1</b> .....	<b>41</b>
<b>1.1 Wells with Stress field information</b> .....	<b>41</b>
<b>1.2 Wells with Stress field information</b> .....	<b>51</b>
<b>1.3 Stress field information from Mines and Quarries</b> .....	<b>56</b>
<b>Glossary</b> .....	<b>56</b>
<b>References</b> .....	<b>57</b>

## FIGURES

Figure 1: Map of the UK Landmass showing the distribution of: Wells drilled by the Coal Authority, Site investigation wells drilled by NIREX and Onshore hydrocarbon wells with digital geophysical log data. Note the low density of wells across central and Northern Wales, North Scotland and parts of the UK e.g. Devon and Cornwall. Contains British Geological Survey materials ©NERC 2017. ....	8
--	---

Figure 2: A 100 metre section of an onshore hydrocarbon well showing native digital data in blue and machine digitised (vectorised) data in green. Note the vectorised data is almost a perfect match for the native digital data. ....	10
Figure 3: Section of a wireline log plot from a UK oil well (depth in feet), the density trace (Right hand panel, solid black line) is cut off at $2.95 \text{ gcm}^{-3}$ , because of this vectorisation could not reproduce the source digital data accurately. ....	11
Figure 4: Extract from an End of Well Report from a UK hydrocarbons well. The text states that an FIT was performed but does not state a value. ....	12
Figure 5: Image and diagram showing an example of a borehole breakout and its relationship to the principle horizontal stresses. Left panel conventional logs including perpendicular dual-caliper and gamma-ray log. Centre: Unwrapped circumferential resistivity borehole imaging (CMI) (clockwise from north), breakouts highlighted by green boxes (orientation $54^\circ$ ). Right panel: Diagram showing the plan view of the breakout and the principle stresses, dotted circle represents the original hole/bit size; solid line represents the borehole wall. ....	14
Figure 6: A 10 m section of borehole imaging from Melbourne 1 in North Yorkshire showing both borehole breakouts and DIFs (after Kingdon et al., 2016). Left panel; conventional wireline logs including 4- arm caliper. Right Panel; Unwrapped Compact Micro Imager (CMI) resistivity image (clockwise from North), breakouts highlighted by green boxes indicate an $S_{\text{hmin}}$ orientation of NE-SW. ....	15
Figure 7: Map of East Yorkshire and North Nottinghamshire showing 120 wells in the area of interest which were investigated for stress field information (Blue) and the 54 wells with suitable information to aid stress field characterisation (Red). Contains Ordnance Survey data © Crown copyright and database rights 2017. ....	18
Figure 8: Compilation of vertical stress gradients from East Yorkshire and North Nottinghamshire. Dashed black line represents a gradient of $23 \text{ MPakm}^{-1}$ which is a good fit to the deepest wells in the region. ....	19
Figure 9: Compilation of available pressure data for East Yorkshire and North Nottinghamshire. With the exception of three data points from Marishes all of the data plot on or near the hydrostatic pressure gradient of $10 \text{ MPakm}^{-1}$ , indicating that pore pressure is hydrostatic... ..	20
Figure 10: Compilation of FIT, LOT and RFT data available for the East Yorkshire and North Nottinghamshire region. $S_v$ is the vertical (lithostatic) stress for the region and corresponds to a gradient of $23 \text{ MPakm}^{-1}$ after Figure 8. $PP$ is the pore pressure gradient for the area of $10.17 \text{ MPakm}^{-1}$ after Figure 9. $S_{\text{hmin}}$ plotted using the lower bound of the LOT's after Addis et al (1998). These gradients are based on regional data and may not be representative of the stress field at specific sites. Above 1500 m eleven of the values recorded from both FIT's and LOT's plot on or above the $S_v$ line. This may be the result of poor tests or it may indicate that at shallow depths $S_{\text{hmin}} \approx S_v$ . ....	21
Figure 11: A 10 m section of borehole imaging from the Melbourne 1 well showing both borehole breakouts and DIFs. Left hand panel; conventional wireline logs including Gamma Ray, Density and P-Wave Velocity. Right hand Panel; Unwrapped CMI resistivity image (clockwise from North), breakouts highlighted by green boxes and showing an $S_{\text{HMAX}}$ direction of $148.2^\circ$ . ....	22
Figure 12: Map of The Weald showing the distribution of the initial 118 wells in the area of interest screened for information to characterise the in-situ stress field (Blue) and the 18 wells used to calculate the vertical stress (Red). Contains Ordnance Survey data © Crown copyright and database rights 2017. ....	23
Figure 13: Compilation of vertical stress gradients from the Weald based on 13 wells. All of the curves fall in the range of $22 - 25 \text{ MPakm}^{-1}$ . Below 1000 metres there is a sharp change in the	

profile of Baxters Copse however this is associated with a large wash out rather than any change in the vertical stress gradient and the data from this well below 1100 m are excluded from the regional interpretation..... 24

- Figure 14: Map of Cheshire and Lancashire showing the distribution of the initial 67 wells in the area of interest thought to contain information to characterise the in-situ stress field (Blue) and the 21 Wells, which contained information to characterise the stress field (Red). Contains Ordnance Survey data © Crown copyright and database rights 2017. .... 25
- Figure 15: Compilation of vertical stress gradients from the proposed UKGEO Thornton Site and surrounding areas. Dashed black line represents a gradient of 23 MPakm<sup>-1</sup>. The vertical stress gradients range from 23 – 26 MPakm<sup>-1</sup>..... 26
- Figure 16: Compilation of available RFT pressure data for Cheshire and Lancashire. All of the data plot on or near the hydrostatic pressure gradient of 10 MPakm<sup>-1</sup>. Indicating that pore pressure is hydrostatic..... 27
- Figure 17: Compilation of FIT and LOT data available for Cheshire and Lancashire. S<sub>v</sub> (Green) is the vertical stress (lithostatic pressure) for the region and corresponds to a gradient of 23 MPakm<sup>-1</sup> after Figure 15. PP is the pore pressure gradient for the area of 10.80 MPakm<sup>-1</sup> after Figure 16. Sh<sub>min</sub> plotted using the lower bound of the LOT's after Addis et al (1998). These gradients may not be representative of the stress field at specific sites. These gradients are based on regional data and may not be representative of the stress field at specific sites. .... 28
- Figure 18: Distribution of additional S<sub>HMax</sub> data from publish literature and Coal Authority reports across the UK: HF – Hydraulic Fracturing, OC – Overcoring. Contains British Geological Survey materials ©NERC 2017. .... 30
- Figure 19: Map showing geographical location of borehole data available to characterise the UK stress field: FIT – Formation Integrity Test, LOT- Leak off test, HF – Hydraulic Fracturing, OC – Overcoring and Calc – S<sub>HMax</sub> calculation from borehole breakouts and DIFs. Contains British Geological Survey materials ©NERC 2017..... 31
- Figure 20: Vertical stress gradients for a variety of UK Regions. Dashed lines representing gradients of 23 and 26 MPakm<sup>-1</sup> are included for reference. Balcombe 1 is a well from the Weald, Marishes 1 is from North Yorkshire, Doe Green 1 is from Lancashire, Sellafield 2 was drilled in Cumbria and Dounreay 1 was drilled on the North Coast of Scotland..... 33
- Figure 21: Diagram showing the available pressure data from Cheshire, Lancashire, East Yorkshire and North Nottinghamshire. PP corresponds to a gradient of 10.19 MPakm<sup>-1</sup>. This data supports the assumption of hydrostatic pore pressure in these regions. .... 34
- Figure 22: Compilation of FIT and LOT data and estimates of S<sub>hmin</sub> from: Cheshire, Lancashire, East Yorkshire and North Nottinghamshire, S<sub>v</sub> is 23 MPakm<sup>-1</sup> after Figure 20. Figure 21 demonstrated that the pressure data for the region corresponded to hydrostatic pressure; PP represents a gradient of 10.19 MPakm<sup>-1</sup>. At depths of < 1000 m there are 12 FIT/LOT measurements which plot at or above the vertical stress line. This indicates that S<sub>hmin</sub> ≈ S<sub>v</sub> but more work is needed to confirm this. Regional Sh<sub>min</sub> gradients plotted using the lower bound of the LOT's after Addis et al (1998). These gradients are based on regional data and may not be representative of the stress field at specific sites. .... 35
- Figure 23: Compilation of all FIT, LOT and RFT data Which exceeds S<sub>v</sub> shown by the green line which corresponds to a gradient of 23 MPakm<sup>-1</sup>. Figure 21 demonstrated that the RFT data for the region corresponded to hydrostatic pressure and has not been plotted. PP represents a gradient of 10.19 MPakm<sup>-1</sup>. Nine of the eleven measurements were collected at depths of < 1000 m suggesting either changes in the stress field at this point of less heterogeneity in the strata. .... 36

Figure 24: Location of all of the measurements of  $S_{HMax}$  magnitude across the UK. These magnitudes have been estimated using: Overcoring (OC), Hydraulic Fracturing (HF) and calculations from observations of borehole breakouts and DIFs (Calc). Contains British Geological Survey materials ©NERC 2017..... 37

Figure 25: Compilation of all  $S_{HMax}$  magnitudes from: Overcoring (OC), Hydraulic Fracturing (HF) and calculations from observations of borehole breakouts and DIFs (Calc). With the exception of three overcoring measurements  $S_{HMax}$  magnitude is greater than the  $S_v$  of  $23 \text{ MPakm}^{-1}$  suggesting that  $S_{HMax} \geq S_v$  however this is based on data from a small number of locations.38

Figure 26:  $S_{hmin}$  values which exceed the vertical stress gradient of  $23 \text{ MPakm}^{-1}$  indicating possible reverse Faulting regimes.  $S_{hmin}$  values derived from hydraulic fracturing and overcoring methods. Values have been shaded broadly by lithology and age. Green: Unknown source and age, Red: Igneous source, Orange: Triassic Sediments, Blue: Carboniferous sediments ..... 38

Figure 27:  $S_{HMax}$  orientations from Hydraulic Fracturing and Overcoring binned at  $5^\circ$  intervals 39

## TABLES

Table 1: Table showing the principle stresses in different faulting regimes and their relationship to  $S_{HMax}$ ,  $S_{hmin}$  and  $S_v$ ..... 6

Table 2: Summary of the hydraulic fracture tests from two UK Coal Authority Boreholes in East Yorkshire and North Nottinghamshire ..... 21

Table 3: List of parameters from the Melbourne 1 well used in Equation 3 to calculate  $S_{HMax}$  from a unit with a DIF ..... 23

Table 4: Summary table of  $S_{HMax}$  data calculated using borehole breakouts from the Prees Hall 1 well (based on Baker Hughes, 2011). PPG – Pounds per Gallon. .... 28

## Summary

Knowledge of the in- situ stress field is a key constraint for a variety of sub surface activities and crucial for the safe and sustainable use of the sub surface. However is a lack of available stress magnitude data across the UK. This report assesses legacy stress magnitude data along with new analysis to characterise the UK onshore stress field.

To investigate the UK onshore in-situ stress field, three regions were studied. The regions were selected based on the potential availability of information to characterise the stress field and their resource potential for unconventional shale resources, highlighted by Andrews et al. (2013). The study focused on: East Yorkshire and North Nottinghamshire, Cheshire and Lancashire and the Weald.

The vertical stress across the UK varies between 23 and 26  $\text{MPakm}^{-1}$  with higher values recorded in Cheshire and Scotland compared to East Yorkshire, North Nottinghamshire and the Weald. Pore pressure measurements from Cheshire, Lancashire, East Yorkshire and North Nottinghamshire are hydrostatic with a gradient of  $10.19 \text{ MPakm}^{-1}$ . Leak off test and formation integrity test data has been used to estimate the gradient of minimum horizontal stress in Cheshire, Lancashire East Yorkshire and North Nottinghamshire. This estimates show that the minimum horizontal stress gradient is two to three  $\text{MPakm}^{-1}$  higher in Cheshire and Lancashire than East Yorkshire and North Nottinghamshire, which is similar to the differences in vertical stress gradients.

Legacy maximum horizontal stress data has been compiled from a variety of techniques from the Coal Authority and peer review publications. This data shows that the maximum horizontal stress  $>$  vertical stress, When combined with the leak off test and formation integrity test data (which shows vertical stress  $>$  minimum horizontal stress) this indicates that the UK is predominately a strike slip

faulting environment. Above 1200 m there are indications of reverse faulting though these are largely confined to igneous rocks in Cornwall, Leicestershire and Cumbria.

The available information shows that there are similarities in the stress field across the UK though due to the geographic and stratigraphic constraints on the data more information would help to better characterise the stress field.

# 1 Introduction

It has long been recognised that detailed knowledge of the in-situ stress field is crucial to the safe and sustainable use of the subsurface. The in-situ stress field is a key constraint for a variety of activities including civil engineering, radioactive waste disposal, mining, unconventional hydrocarbon exploration and fault stability (Nirex, 1997; Zoback et al., 2003; Tingay et al., 2005; Williams et al., 2016).

Despite this there is a lack of stress magnitude data at depth across the UK leading to uncertainty in stress magnitudes. The World Stress Map (WSM) 2016 release (Heidbach et al., 2016) lists 125 records of variable quality for stress field characterisation across the UK landmass, which include: borehole breakout studies, hydraulic fracture measurements, overcoring and focal plane mechanism studies.

Several studies have examined aspects of the stress field across the UK onshore and UK continental shelf areas (Baptie, 2010; Williams et al., 2015; 2016; Holford et al., 2016; Kingdon et al., 2016). Kingdon et al. (2016) characterised the orientation of the UK stress field based upon borehole breakout data largely from within the Carboniferous Pennine Coal Measures. The authors found the orientation of  $S_{HMax}$  to be 150.9 degrees or NW-SE.

Little information exists in the public domain regarding the magnitude of the principle stresses across the UK. A few notable exceptions to this include work on the Cretaceous Captain Sandstone Member of the North Sea Inner Moray Firth Basin (Williams et al., 2016) and the work undertaken during the assessment for radioactive waste disposal at Sellafield, Cumbria NW England (Nirex, 1997).

This report details the collection of the limited information in the public domain to characterise the in-situ stress from a variety of sources, before providing geographic summaries of the stress field.

# 2 Characterising the UK stress field and in-situ stresses

Zoback et al. (2003) states that stress is a tensor with six independent components but it can be assumed that at depth it is resolved to three principle stresses: a vertical stress ( $S_v$  = lithostatic pressure), a minimum horizontal stress ( $S_{hmin}$ ) and a maximum horizontal stress ( $S_{HMax}$ ). The other component required to fully characterise the stress field is the direction of  $S_{HMax}$  which is perpendicular to  $S_{hmin}$ . The magnitudes of the principle stress relative to each other determine which faulting regime is dominant (Table 1).

**Table 1: Table showing the principle stresses in different faulting regimes and their relationship to  $S_{HMax}$ ,  $S_{hmin}$  and  $S_v$**

Faulting Environment	Principle stress		
	$\sigma_1$	$\sigma_2$	$\sigma_3$
In Normal Faulting	$S_v$	$\geq S_{HMax}$	$\geq S_{hmin}$
In Strike Slip	$S_{HMax}$	$\geq S_v$	$\geq S_{hmin}$
In Reverse Faulting	$S_{HMax}$	$\geq S_{hmin}$	$\geq S_v$

Standard downhole geophysical logging and borehole tests can be used to estimate the magnitude of the principle stresses. Stress data is typically available from deep coal and hydrocarbon exploration wells in addition to a small number of boreholes drilled as part of the Sellafield project (Nirex 1997) and other research boreholes. Figure 1 shows the available Coal, Oil and Radioactive Waste boreholes across the UK landmass.

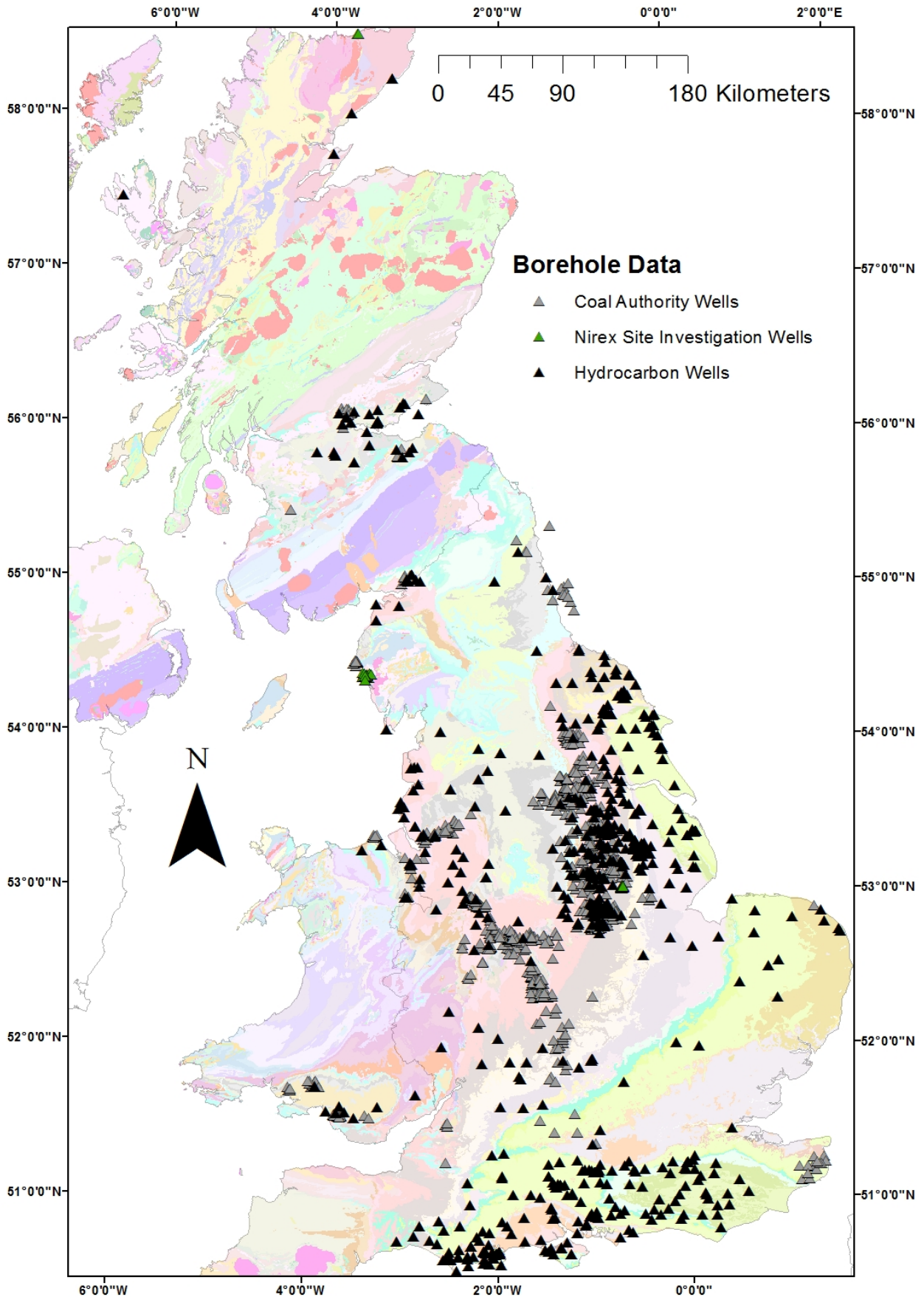


Figure 1: Map of the UK Landmass showing the distribution of: Wells drilled by the Coal Authority, Site investigation wells drilled by NIREX and Onshore hydrocarbon wells with digital geophysical log data. Note the low density of wells across central and Northern Wales, North Scotland and parts of the UK e.g. Devon and Cornwall. Contains British Geological Survey materials ©NERC 2017.

Figure 1 illustrates that for areas of the UK e.g. North Scotland, Central and Northern Wales there is a lack of data in the form of boreholes to quantify the in-situ stress field. It is also the case that even where deep boreholes have been drilled the necessary data required to characterise the stress field may not have been acquired. For example, between 1950 and 1995, Coal Authority data were often collected using non-standard tool, often with minimal metadata. The data available from onshore hydrocarbon wells were largely collected from 1960 to the present day, with the quality and variety of information available depending upon the operator, age and classification of the well. Because of this heterogeneity only a subset of the wells shown in Figure 1 will enable detailed characterisation of the principle stresses and the stress field orientation.

## 2.1 Vertical stress

The vertical stress is often used to predict fracture gradients and pore pressure in the absence of downhole, in-situ data (Tingay et al., 2003a). In a sedimentary basin with no supporting information it is common to assume a vertical stress gradient of 23 MPakm<sup>-1</sup> or 1 psift<sup>-1</sup> (e.g. Dickenson, 1953; Tingay et al., 2003a). This corresponds to a basin with a layer-cake stratigraphy, an average density of 2.3 gcm<sup>-3</sup> and 15% porosity (Zoback et al., 2003). However, this is based on data from the Gulf of Mexico and specifically for Tertiary deltas (Tingay et al., 2003a). Multiple studies document that the state of stress can be highly variable and where possible the vertical stress should be determined using in-situ data (e.g. Tingay et al., 2003a; Verweij et al., 2016; Williams et al., 2016).

### 2.1.1 Estimating vertical stress

The vertical stress can be estimated from wireline density logs using the method of Zoback et al (2003). This method integrates density logs from surface to total depth (TD). The method for estimating vertical stress is given in Equation 1:

$$S_v = \int_0^z \rho(z)g dz \approx \bar{\rho}gz$$

#### Equation 1

Where  $\bar{\rho}$  is the mean overburden density,  $\rho(z)$  is the density as a function of depth and  $g$  is the acceleration due to gravity (this study is limited to the UK landmass, thereby negating the need to correct for water depth). Density logging of hydrocarbon wells is often only collected through the strata of economic interest. The density log method requires densities information to the surface, this requires the user to estimate densities in the shallow sub-surface which are not sampled by the density tools. For wells drilled a body of water (usually offshore wells) the water depth must also be included.

Original native digital data for hydrocarbon wells is often unavailable, hardcopy logs can be machine digitised in a process known as vectorisation. This vectorised data has been shown to be a good match to native digital data (Figure 2), though quality is dependent on the quality of the scan of the original log data.

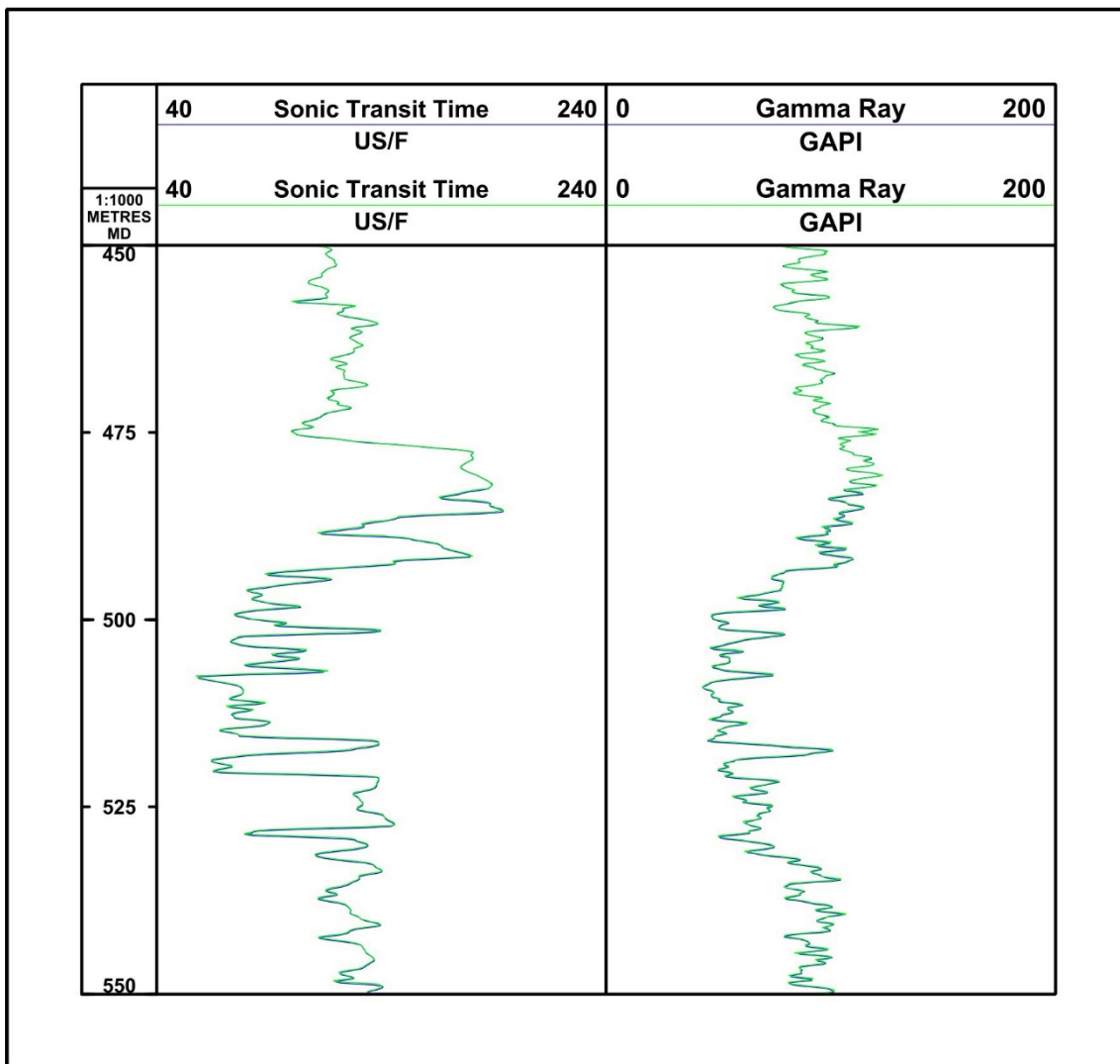


**Figure 2: A 100 metre section of an onshore hydrocarbon well showing native digital data in blue and machine digitised (vectorised) data in green. Note the vectorised data is almost a perfect match for the native digital data.**

In some cases the quality of the hardcopy log can cause problems and effect log data quality as shown in Figure 3. Even though the density log goes off scale at 4470 ft there is no backup / wrap-around on the scan. As a result the curve is 'top and tailed', degrading the signal quality and making it unsuitable for use in this work.

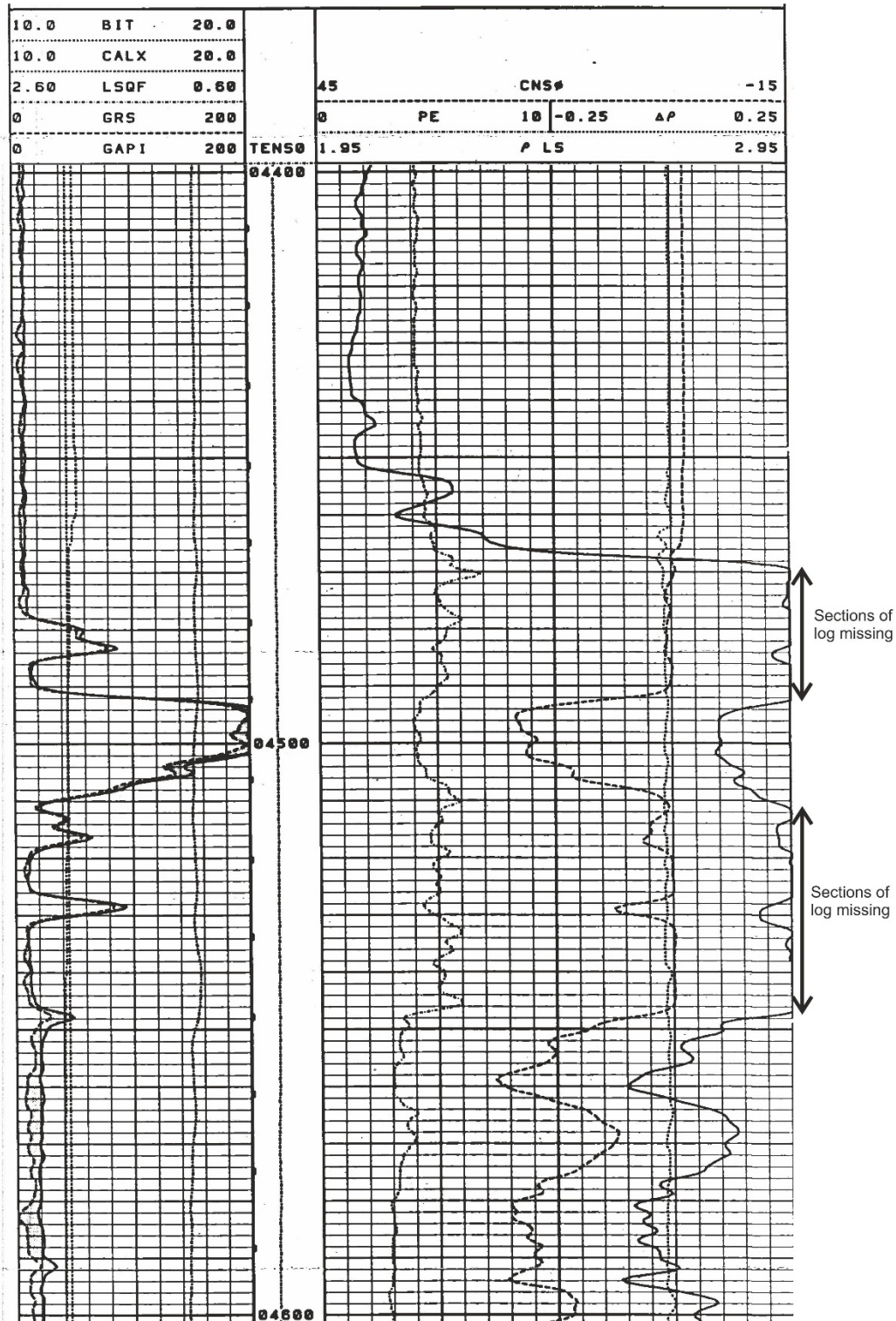


**Figure 3: Section of a wireline log plot from a UK oil well (depth in feet), the density trace (Right hand panel, solid black line) is cut off at 2.95  $\text{gcm}^{-3}$ , because of this vectorisation could not reproduce the source digital data accurately.**

Often density logs from Coal Authority wells were collected from near surface making them useful for estimating the shallow subsurface density values. However, many were logged with non-standard tools which returned densities in counts per second (CPS). Conversion factors between CPS to  $\text{gcm}^{-3}$  cause errors and often there is no record of the conversion factor. For this report, no density log in CPS has been converted to  $\text{gcm}^{-3}$  by the authors, where data had already been converted it was reviewed before being incorporated.

## 2.2 Minimum horizontal stress

The minimum horizontal stress ( $S_{hmin}$ ) is also the minimum principle stress ( $\sigma_3$ ) in both normal and strike slip environments. Baptie (2010) demonstrated that the UK is predominately a strike slip / reverse environment with NW-SE compression driven by the Mid Atlantic Ridge. The magnitude of  $\sigma_3$  (Table 1) is important for any hydraulic fracturing operation as this is the value that needs to be exceeded to induce a hydraulic fracture. The magnitude of  $\sigma_3$  is also important to minimise the likelihood of inducing hydraulic fractures during the drilling process. In normal and strike-slip environments, these fractures occur when the weight of the mud used to drill the hole exceeds  $S_{hmin}$ . A detailed knowledge of  $S_{hmin}$  allows drillers to alter the weight of the drilling mud and reduce the chances of inducing a hydraulic fracture.

In boreholes  $S_{hmin}$  can be determined by a specific type of hydraulic fracture known as a leak-off test (LOT). These tests are typically carried out below casing shoes and multiple tests can be carried out in individual boreholes. To carry out a leak-off test the well is shut in and the pressure is increased. If pumping occurs at a constant rate then the pressure should increase linearly with time (Zoback et al., 2003). At a specific point (known as the leak-off point) this linear relationship breaks down and the drilling mud is said to be “Leaking off” due to the formation of a hydraulic fracture, into which the fluid moves/invades. If the well is pressured but not taken to leak-off, then it is known as a Formation Integrity Test (FIT) or Limit Test (LT; Zoback et al., 2003). As a result FIT’s are considered a lower bound for  $S_{hmin}$ , with LOT’s giving a more reliable estimate of the magnitude of  $S_{hmin}$ . LOT’s are a function of  $S_{hmin}$  and rock tensile strength, they can be effected by drilling fluids and pre existing fractures. The most reliable estimates of  $S_{hmin}$  come from extended Leak-off Tests (XLOT’s) which are fully completed LOT’s. However no XLOT’s were available for this study and are not discussed further here. For a more detailed discussion of LOT’s and XLOT’s see: Addis et al., 1998; White et al., 2002.

LOT and FIT data are recorded either in units of psi, specific gravity or as an equivalent mud weight, for this study all values have been converted to MPa. They are typically found in well reports, mud logs and composite plots, but there is no consistent standard for their reporting. Collecting LOT’s/FIT’s in all boreholes is not standard industry practice. In a small hydrocarbon field it is typical to collect FIT/LOT data from one or two wells for characterisation purposes. In some cases, tests were performed but the mud weight not recorded (Figure 4).

<b>3 ¾” Hole Section</b>					
<b>MWD RUN</b>			<b>07</b>		
<b>Interval Drilled</b>			<b>7508 ft – 7694 ft</b>		
<b>Tool Type</b>			<b>NaviTrak</b>		
<b>Operational status</b>			<b>Performed to Specification</b>		
<b>MWD / RWD Service</b>	<b>Percentage Logged</b>		<b>MWD / RWD Service</b>	<b>Percentage Logged</b>	
	<b>MWD</b>	<b>RWD</b>		<b>MWD</b>	<b>RWD</b>

The 3 ¾” section was drilled using a 3 ⅛” NaviTrak with a 2 ⅞” National mud motor.

The cement and casing shoe were drilled out with no problems, formation was drilled from 7508 ft to 7519 ft then an FIT was performed. The rest of the 3 ¾” section was drilled with no major events. Well TD was called at 7694 ft 50 ft TVD into the Kirkham Abby formation.

Figure 4: Extract from an End of Well Report from a UK hydrocarbons well. The text states that an FIT was performed but does not state a value.

## 2.3 Pore Pressure

Pore Pressure ( $P_p$ ) relates to the pressure of the fluids within the pores of a rock. Usually this equates to the pressure of a water column from the depth of interest to the surface, also known as hydrostatic pressure. When the density of water is approximately  $1 \text{ gcm}^{-3}$  hydrostatic pressure increases at a rate of 0.44 psi/ft or  $10 \text{ MPakm}^{-1}$  (Zoback et al., 2003).

Pore pressure is typically recorded downhole in permeable formations using a number of conventional tools including: Formation Multi Tester (FMT), Repeat Formation Tester (RFT) and Modular Formation Dynamics Tester (MDT). In impermeable formations such as shales, geophysical logging tools fail. When this occurs, laboratory test data is often used to estimate pressure (Zoback, 2010).

Whilst pore pressure is not in itself a principle stress, it effects on  $S_{HMax}$  and is directly coupled to  $S_{hmin}$  (Hillis, 2000). In a porous elastic rock the behaviour is controlled by the effective stress (Zoback, 2010). The concept of effective stress was first noted by Terzaghi, (1923) and represents the difference between internal pore pressure and externally applied stresses (Zoback, 2010). By making assumptions about faults in bodies of rock at depth the concept of effective stress can be used to predict the magnitudes of the principle stresses at depth (Zoback et al., 2003).

Section 2.5 discusses the role of Pore Pressure in estimating  $S_{HMax}$  in the presence of well bore failure.  $S_v$  is unaffected by changes in pore pressure, however some changes can be indicative of processes which can affect  $S_v$  such as undercompaction and overpressure (Hillis, 2000; Tingay et al., 2003a). The ratio between the change in  $S_{hmin}$  and the change in  $P_p$  can also be used to evaluate whether increases in  $P_p$  will result in tensile fractures or fault reactivation (Tingay et al., 2003b).

## 2.4 Stress Field Orientation

The orientation of the stress field is an important component of subsurface characterisation as in normal and strike-slip environments it constrains the orientation of any hydraulic fracture. Hydraulic fractures propagate perpendicular to  $\sigma_3$  as this is the least energy configuration (Zoback et al., 2003). In the vertical plane the orientation of these features will be parallel to  $S_{HMax}$  (Brudy and Zoback, 1999).

There are two types of deformation that occur at the borehole wall which indicate the orientation of  $S_{hmin}$  or  $S_{HMax}$ : borehole breakouts and drilling-induced tensile fractures (DIFs). Stress concentrations at the borehole wall can lead to compressive failure which is termed a borehole breakout (Bell and Gough, 1979). Plumb and Hickman (1985) were able to demonstrate that these failures were orientated in the direction of  $S_{hmin}$  which in vertical boreholes is perpendicular to the direction of  $S_{HMax}$ . DIFs are the result of tensile fractures induced by the drilling process. These features are orientated in the direction of  $S_{HMax}$  (Moos and Zoback, 1990). Figure 5 shows a borehole breakout and its relationship to  $S_{HMax}$  and  $S_{hmin}$ .

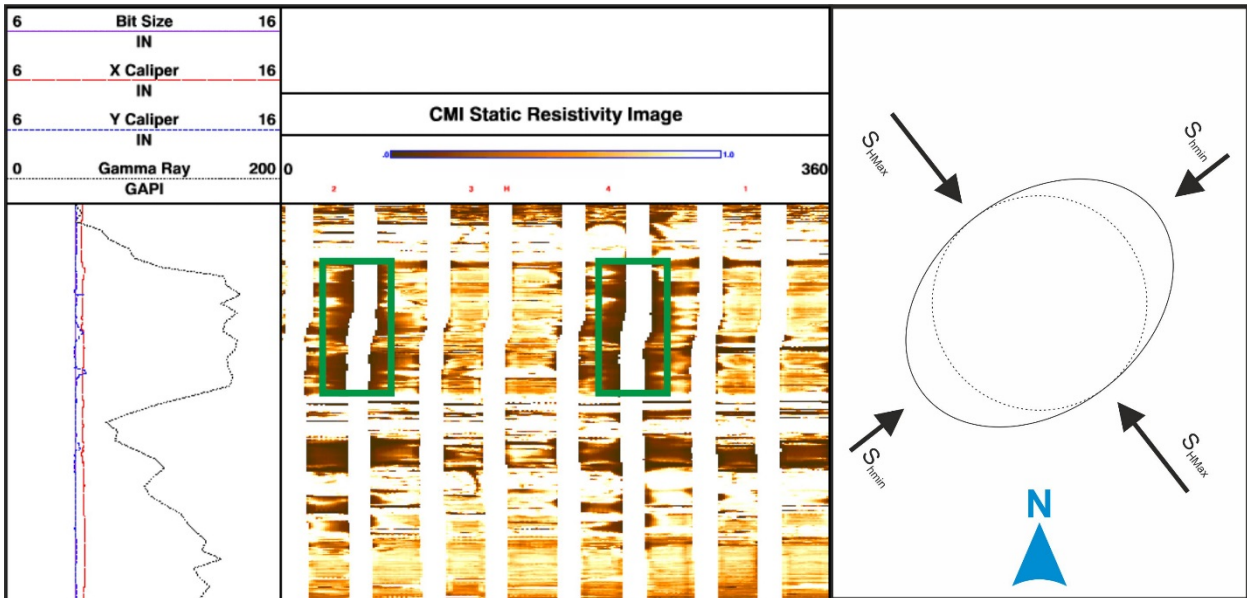


**Figure 5: Image and diagram showing an example of a borehole breakout and its relationship to the principle horizontal stresses. Left panel conventional logs including perpendicular dual-caliper and gamma-ray log. Centre: Unwrapped circumferential resistivity borehole imaging (CMI) (clockwise from north), breakouts highlighted by green boxes (orientation 54°). Right panel: Diagram showing the plan view of the breakout and the principle stresses, dotted circle represents the original hole/bit size; solid line represents the borehole wall.**

Borehole breakouts and DIFs are most reliably characterised using borehole imaging tools (see Figure 6 after; Kingdon et al., 2016). These generate high resolution false colour images using physical properties e.g. P-wave velocity or electrical resistivity. They can provide borehole wall coverage of 20% - 95% with a vertical resolution of up to 2.5 mm (Kingdon et al., 2016). Four-arm caliper tools can be used to identify breakouts, however, the use of these tools can increase uncertainty in the orientation of  $S_{HMax}$  (Kingdon et al., 2016).

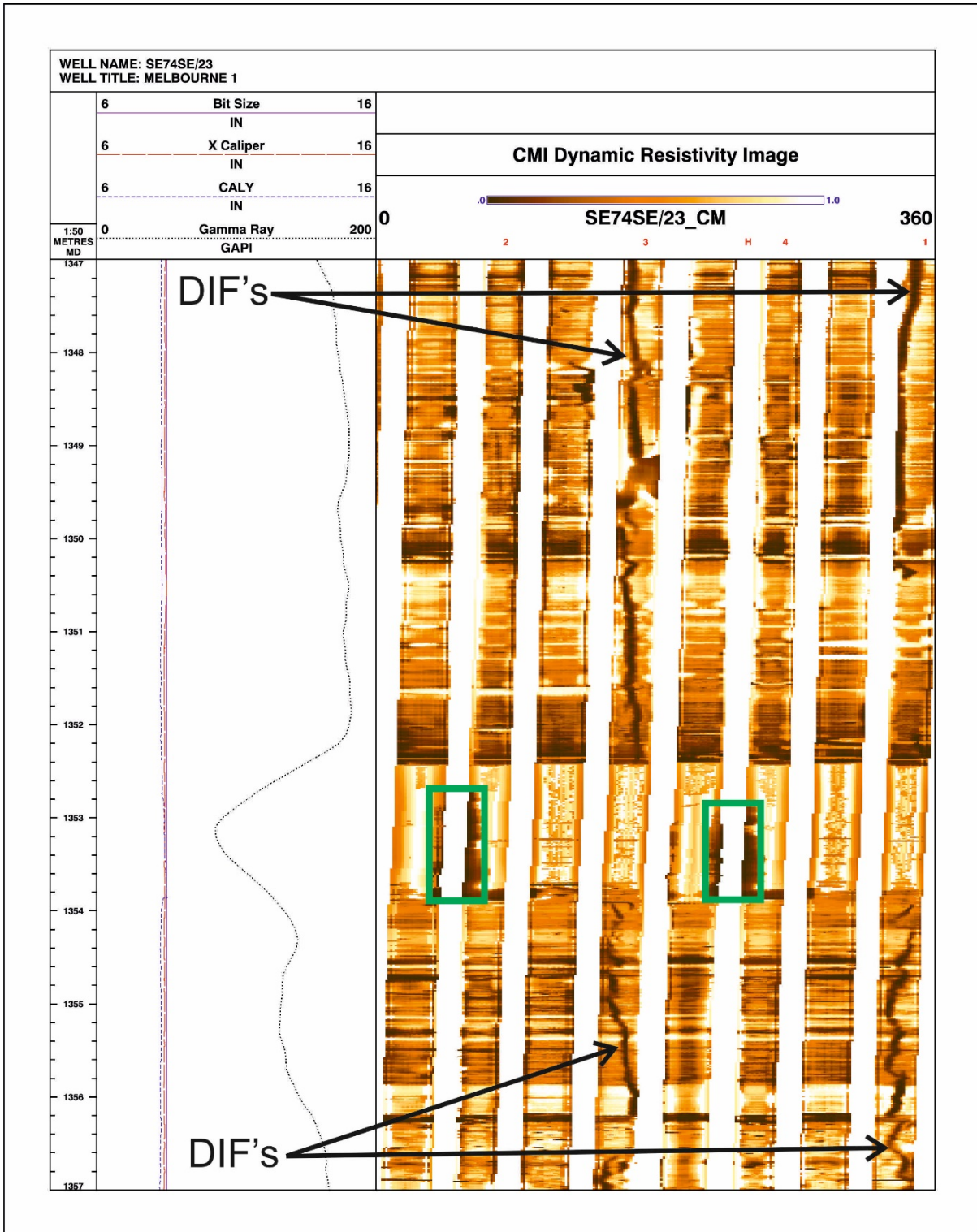


**Figure 6: A 10 m section of borehole imaging from Melbourne 1 in North Yorkshire showing both borehole breakouts and DIFs (after Kingdon et al., 2016). Left panel; conventional wireline logs including 4- arm caliper. Right Panel; Unwrapped Compact Micro Imager (CMI) resistivity image (clockwise from North), breakouts highlighted by green boxes indicate an  $S_{hmin}$  orientation of NE-SW.**

For a detailed explanation of characterising breakouts and DIFs from 4-arm caliper logs and breakouts see: Reinecker et al. (2003) and Tingay et al. (2008). For a review of the UK stress field orientation see Kingdon et al. (2016).

## 2.5 Maximum horizontal stress

The maximum horizontal stress ( $S_{HMax}$ ) is the most difficult principle stress to characterise as it requires estimates of:  $P_p$ ,  $S_{hmin}$ , rock tensile strength and depending on the technique you use: formation breakdown pressure or Unconfined Compressive Strength (UCS).

At shallow depths in mines and tunnels overcoring can be used to estimate the magnitude of  $S_{HMax}$ . This method involves the drilling of a pilot hole, and the insertion of a strain gauge, fixed in place with resin (Leeman and Hayes, 1966; Becker and Davenport, 2001). Both the strain gauge and a section of rock are then drilled out in a larger core. The strain gauge will then measure the stress relaxation of the rock. However the resin used to fix the gauge in place can have unreliable setting properties and poor adhesion (Farmer and Kemeny, 1992). In addition to this the process of drilling the gauge can induce heating which causes cell expansion. These measurements also require knowledge of the elastic rock properties, which can lead to large uncertainties and errors in the value of  $S_{HMax}$ .

Hydraulic fractures were utilised by the Coal Authority to estimate  $S_{HMax}$  in the late 80's, some of which were incorporated into the World Stress Map database release (Heidbach et al., 2016). However, no standards exist for systematic recording of these data. Consequently, there is no way to easily identify boreholes where these data were collected and if data were preserved. In addition to this Zoback (2010) questioned the use of hydraulic fractures to calculate  $S_{HMax}$  as the method was best suited to low temperatures; typically above 2 km and in rocks where borehole wall failure is not observed. Hydraulic fractures yield the most reliable results in smooth holes with no pre-existing fractures; however this is very rarely verified prior to conducting a hydraulic fracturing test (Zoback, 2010). The most serious problem with this method is that it is almost impossible to detect the pressure at which a fracture forms at the well bore wall (Zoback, 2010).

$S_{HMax}$  can be estimated from observations of breakouts and DIFs on borehole imaging using Equation 2 and Equation 3 after: Barton and Zoback (1988); Moos and Zoback (1990); Zoback et al., (2003).

For borehole breakouts:

$$S_{HMax} = \frac{(C_0 + 2P_p + \Delta P + \sigma^{\Delta T}) - S_{hmin}(1 + 2 \cos 2\theta_b)}{1 - 2 \cos 2\theta_b}$$

$$\text{Where } 2\theta_b = \pi - W_{bo}$$

### Equation 2

In Equation 2  $C_0$  is the rock strength usually from UCS tests,  $W_{bo}$  is the breakout width,  $\Delta P$  is the difference in pressure between the pore fluid pressure and the pressure exerted by a column of mud in the well bore. The thermal stress induced by the difference in temperature between the drilling fluid and formation fluid is:  $\sigma^{\Delta T}$

For DIFs:

$$S_{HMAX} = 3S_{hmin} - 2P_p - \Delta P - T_0 - \sigma^{\Delta T}$$

### Equation 3

Where  $T_0$  is the rock tensile strength.

Due to the difficulties in determining stress either through unsuitable techniques or uncertainties in calculations there are almost no readily available, reliable measurements of  $S_{HMax}$  in the UK.

## 2.6 Well Data Quality Control

All well data is typically recorded in measured depth (MD) downhole, typically relative to Kelly Bushing (KB) or Rotary Table (RT) in metres (m) or feet (ft). The KB or RT tends to be several metres above ground level. To calculate the stress at depth all observations are converted to true vertical depth below ground level in metres (TVD BGL).

To calculate TVD BGL the effect of borehole deviation must be taken into account. For FIT, LOT and RFT data where borehole deviation was  $> 10^\circ$  from vertical, deviation surveys were collected. These are often held in ASCII formats, or tabulated in end of well reports (EOWRs). True vertical depth is usually recorded but in a small number of cases was calculated using the minimum curvature method from borehole deviation and hole azimuth. If the borehole deviation was  $< 10^\circ$  the well was assumed to be vertical.

To assess  $S_v$  using the density log method, vertical wells were prioritised. It is common practice for vertical characterisation wells to be drilled to assess a potential resource target prior to development. These characterisation wells often have greater coverage of density logs over more stratigraphic units. As a result these characterisation wells were prioritised for calculating  $S_v$ . Wireline density tools require good contact with the borehole to record accurate densities. Loss of contact with the borehole wall results in the density tool recording the density of drilling muds and leads to anomalously low values. Due to the number of wells with density logs in the regions where large washouts were found the data from the well was removed from the interpretation.

### 3 Regions

The selection of UK regions in which stress field information has been collated or calculated was largely determined by the availability of data and their resource potential for unconventional shale resources, highlighted by Andrews et al. (2013). The three main areas of focus for this study are:

- East Yorkshire and North Nottinghamshire
- The Weald
- Cheshire and Lancashire.

Wells, Quarries and mines in this report are identified by name or well title, additional information is provided in Appendix 1.

#### 3.1 Eastern Yorkshire and North Nottinghamshire

The area of interest (AOI) was identified based on the availability of well data and current exploration interest for unconventional resources. This region covers the area between Doncaster, York and Scarborough. Initially 217 wells were identified though 97 mainly water wells were discarded on account of having no useful information. The remaining 120 wells were investigated for stress field information. Of these 120 wells, 54 contained information suitable for stress field characterisation and are shown in Figure 7. See Appendix 1 for details.



Market Weighton Block and the Cleveland Basin. This fault zones is the onshore component of the Dowsing Fault zone and was triggered by N-S extension in Late Jurassic to the early Cretaceous (Hawkins and Saul, 2003).

Twenty nine of the 120 wells were drilled by the Coal Authority and were mostly used for constraining density profiles in the post-Carboniferous succession. The remaining 91 hydrocarbon wells include some small oil and gas fields such as Kirby Misperton, Malton and Hatfield Moors.

### 3.1.1 Vertical Stress

To determine the vertical stress, 17 wells were selected (five Coal Authority wells, 12 hydrocarbon wells) from the initial list based on location and top and base depth of density logging. Group or Formation level stratigraphy was recorded for each well allowing average formation densities to be calculated for units including the Mercia Mudstone Group and/or the Sherwood Sandstone Group. Density logs from the hydrocarbons industry typically start below these units as they rest on the Carboniferous targets. Due to the issues highlighted in sections 2.1 and 2.6, including density logs in non-standard units and poor digitisation due to the quality of the available log plots, four of the wells were removed from the initial wells list. The final vertical stress graph is shown in Figure 8 contains information from the 13 wells used to constrain the vertical stress.

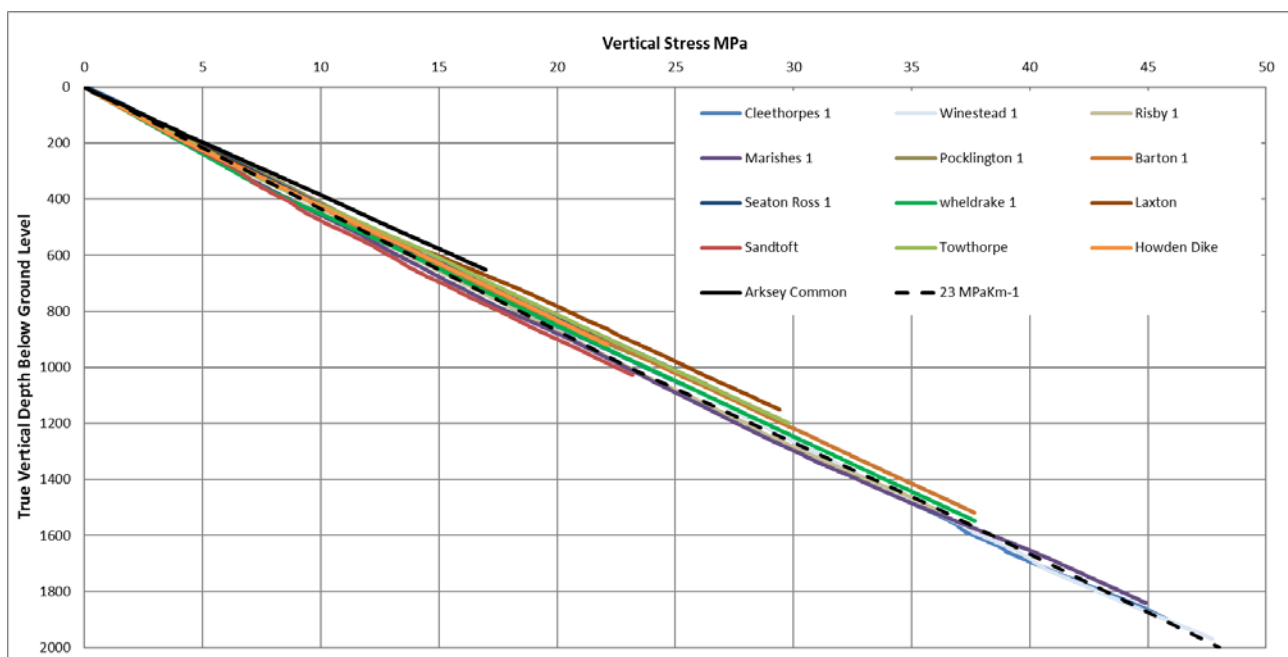


**Figure 8: Compilation of vertical stress gradients from East Yorkshire and North Nottinghamshire. Dashed black line represents a gradient of 23 MPa/km<sup>-1</sup> which is a good fit to the deepest wells in the region.**

The black dashed line in Figure 8 represents the stress gradient which has been fitted to the vertical stress data calculated from the density log inversion after Zoback (2003). The vertical stress gradient shown is between 23 MPa/km<sup>-1</sup> m and 24 MPa/km<sup>-1</sup>. Due to the consistency of the trend in vertical stress from these wells no other wells from this region were used.

### 3.1.2 Pore Pressure

Repeat Formation Test (RFT) data were available from eight wells. Wells which had drill stem test reports were also recorded but not used in this case due to incomplete reports. The pressure data were converted to MPa and plotted in Figure 9, the majority of the pressure data plot on or near the hydrostatic pressure line of 10 MPa/km<sup>-1</sup>. This indicates that pore pressure is hydrostatic with several outliers. The pore pressure data from this region plot on a gradient of 10.17 MPa/km<sup>-1</sup>.

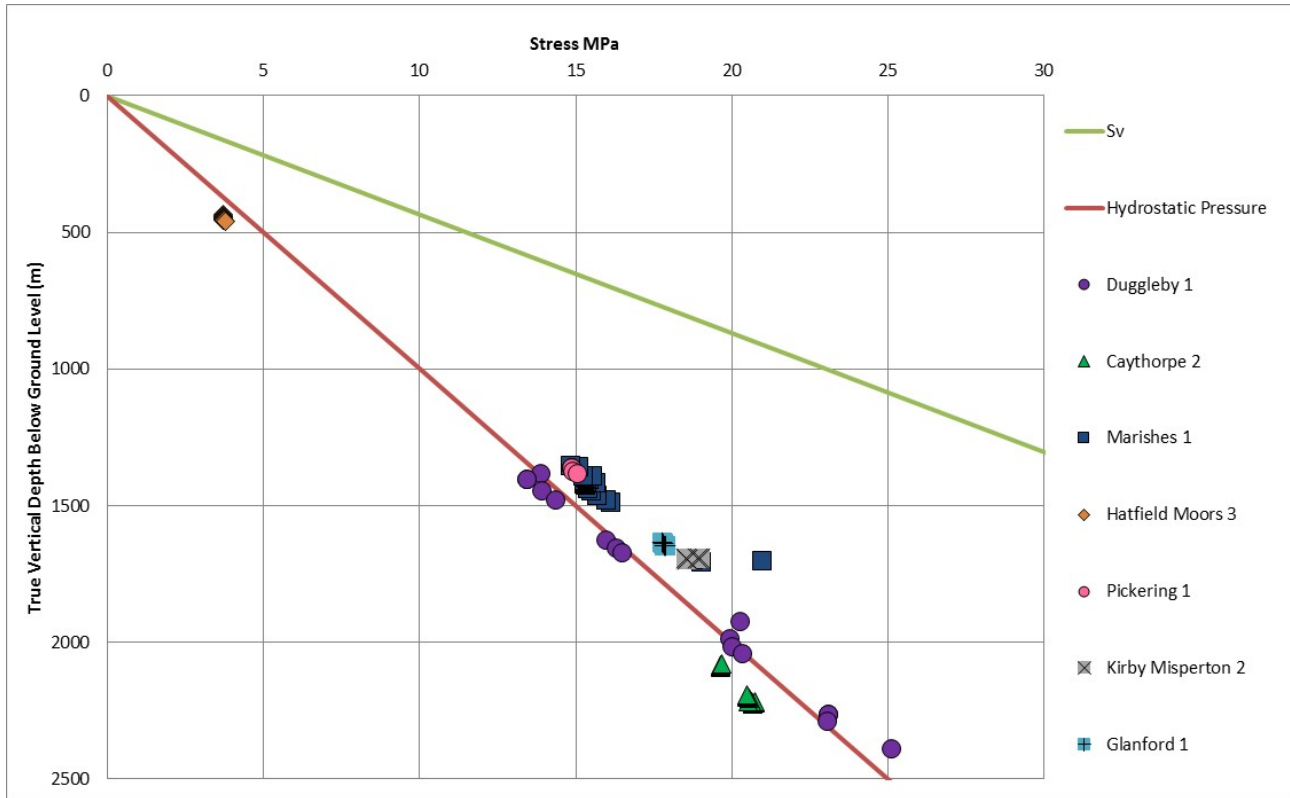


**Figure 9: Compilation of available pressure data for East Yorkshire and North Nottinghamshire. With the exception of three data points from Marishes all of the data plot on or near the hydrostatic pressure gradient of  $10 \text{ MPa km}^{-1}$ , indicating that pore pressure is hydrostatic.**

### 3.1.3 Minimum Horizontal Stress

From the 91 hydrocarbon wells studied a variety of files were investigated for any information on the stress field including: company composites, mud logs, EOWRs, log scans etc. These were interrogated for FIT's and LOT's.

Of the 84 wells, 44 had FIT's or LOT's listed with the equivalent mud weight listed (EMW) and recorded with sufficient metadata to estimate  $S_{hmin}$ . This method will only give a regional estimate of  $S_{hmin}$  due to the lack of XLOT's to validate the data. In total there were 64 FIT's/LOT's observations from 44 wells for the Eastern Yorkshire and North Nottinghamshire area. Following collection of the LOT data these were plotted alongside the RFT data and the vertical stress measurements (Figure 10).

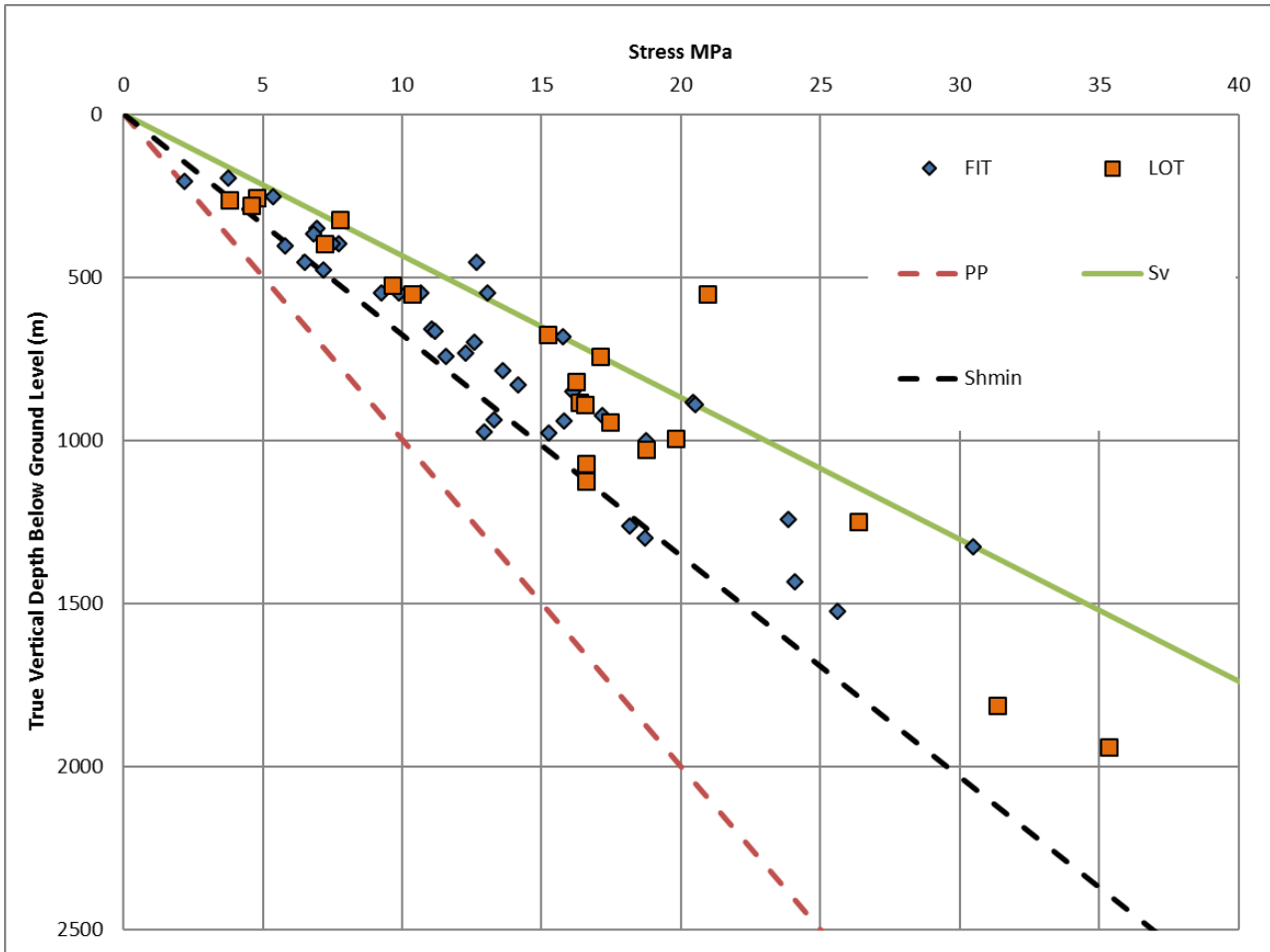


**Figure 10: Compilation of FIT, LOT and RFT data available for the East Yorkshire and North Nottinghamshire region.  $S_v$  is the vertical (lithostatic) stress for the region and corresponds to a gradient of 23 MPakm<sup>-1</sup> after Figure 8. PP is the pore pressure gradient for the area of 10.17 MPakm<sup>-1</sup> after Figure 9.  $S_{hmin}$  plotted using the lower bound of the LOT's after Addis et al (1998). These gradients are based on regional data and may not be representative of the stress field at specific sites. Above 1500 m eleven of the values recorded from both FIT's and LOT's plot on or above the  $S_v$  line. This may be the result of poor tests or it may indicate that at shallow depths  $S_{hmin} \approx S_v$ .**

### 3.1.4 Maximum Horizontal Stress

Across the region only four locations had sufficient data to calculate  $S_{HMax}$ . Overcoring data were available from North Selby Colliery (Bigby et al., 1992). Hydraulic fracturing data were available from two Coal Authority wells: Howden Dike and East Lodge (summarised in Table 2). A summary of the two hydraulic fracture reports is provided below.

**Table 2: Summary of the hydraulic fracture tests from two UK Coal Authority Boreholes in East Yorkshire and North Nottinghamshire**

Well Title	Top Depth (m)	Bottom Depth (m)	$S_{hmin}$ ( $\sigma_3$ )	$S_v$ ( $\sigma_2$ )	$S_{HMax}$ ( $\sigma_1$ )
Howden Dike	799.5	896	15.3 MPa	21 MPa	29.7 MPa
East Lodge	1023	1123	16.6 MPa	26.1 MPa	32.2 MPa

The only other borehole with sufficient data available to calculate  $S_{HMax}$  was the Melbourne 1 Coal Bed Methane well in North Yorkshire. Breakouts were observed on borehole imaging at depths of 987-988 m (Figure 11), which reveal a clear  $S_{HMax}$  direction of 144.4°. Figure 11 also illustrates DIFs between 984.8 m and 986.87 m.

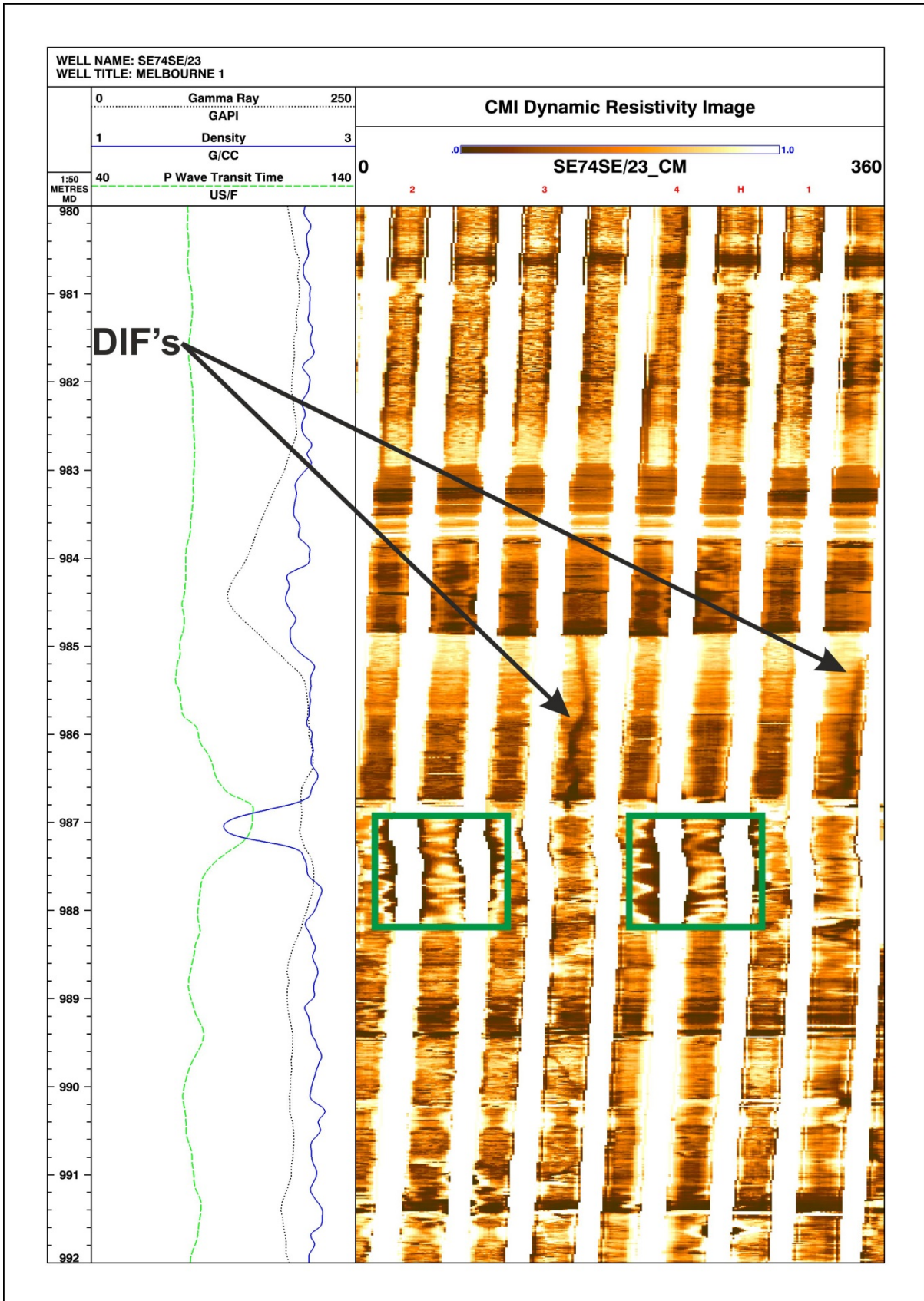


Figure 11: A 10 m section of borehole imaging from the Melbourne 1 well showing both borehole breakouts and DIFs. Left hand panel; conventional wireline logs including Gamma Ray, Density and P-Wave Velocity. Right hand Panel; Unwrapped CMI resistivity image (clockwise from North), breakouts highlighted by green boxes and showing an  $S_{HMax}$  direction of  $148.2^\circ$ .

Equation 2 and Equation 3 in section 2.5 shows how  $S_{HMax}$  can be calculated from both breakouts and DIFs. There were no UCS estimates available so  $S_{HMax}$  could not be calculated from the breakout zone. However, point load tests were carried out on this core and can be multiplied by 0.8 to give an

estimate of tensile strength (Ulusay & Hudson 2007). Equation 3 can therefore be used to calculate  $S_{HMax}$ . The list of parameters which were used to calculate  $S_{HMax}$  in Equation 3 are presented in Table 3. Due to the lack of temperature information it was not possible to estimate  $\sigma^{\Delta T}$  and it was discounted. This yielded a  $S_{HMax}$  value of 27.22 MPa at 982.08 m.

**Table 3: List of parameters from the Melbourne 1 well used in Equation 3 to calculate  $S_{HMax}$  from a unit with a DIF**

Parameter	Value	Units	Assumption
Depth	982.08	M	
$S_v$	22.59	MPa	Based on 23 MPakm <sup>-1</sup>
Point Load	2.56	MPa	
Tensile strength	2.05	MPa	0.8 * Point Load
$S_{hmin}$	16.8	MPa	Estimated from regional FIT / LOT data
Pore Pressure	9.82	MPa	Assumed to be hydrostatic
Mud Weight	11.31	MPa	Based on a mud weight of 9.6 ppg from EOWR

### 3.2 The Weald

The Weald study initially focused on vertical stress gradients to establish changes in the state of stress. Some 118 wells drilled for oil / gas purposes were initially identified as potentially containing information to characterise the stress field (Figure 12). LOT and FIT data has not yet been collated for this region. See Appendix 1 for details.

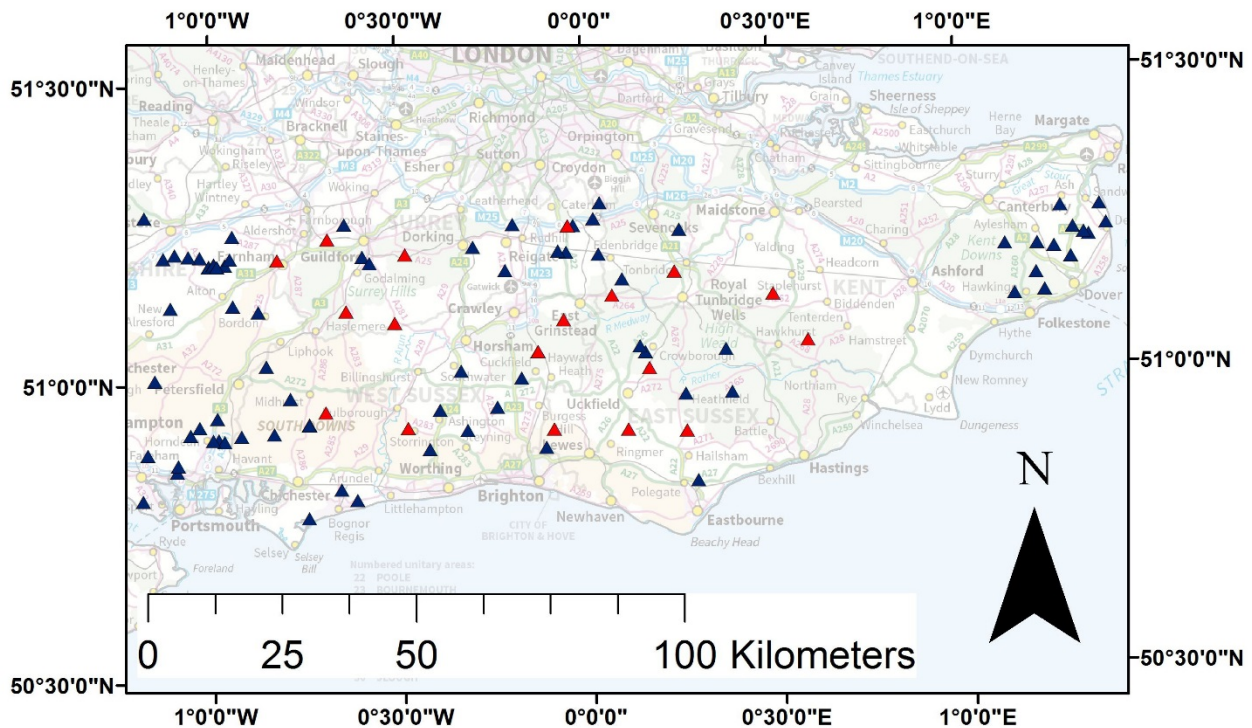


**Figure 12: Map of The Weald showing the distribution of the initial 118 wells in the area of interest screened for information to characterise the in-situ stress field (Blue) and the 18 wells used to calculate the vertical stress (Red). Contains Ordnance Survey data © Crown copyright and database rights 2017.**

The Weald is a part of the Wessex Basin, a major sedimentary basin complex in southern Britain, formed as a sinistral pull apart basin during episodes of Mesozoic extension (Lake and Karner 1987). In late Cretaceous – Early Tertiary times the basin underwent inversion as a result of Alpine compressional forces (Lake and Karner 1987). The general structure is one of a broad regional basin upwarp (the Weald Anticline or Anticlinorium), upon which are imposed zones of more localised tighter northerly-verging inversion fold pairs, including monoclines with steep to overturned northern limbs. These structures developed along former syndepositional normal faults that underwent reversal of movement during compression (Chadwick, 1986; Chadwick, 1993; Chadwick & Evans, 2005).

Initial stress field characterisation focused on the vertical stress in the core of the anticline to identify any differences in vertical stress gradients. To achieve this 13 wells were selected based on geographical distribution, top and bottom depth on density log and well TD. Figure 13 illustrates the variation in vertical stress gradients across the Weald and shows that the vertical stress at 1 km is in the range of 22 - 25 MPa. One visible deviation from this trend is Baxter's Cope 1 below circa 1100 m. This is the result of large washouts within the Kimmeridge Clay section.

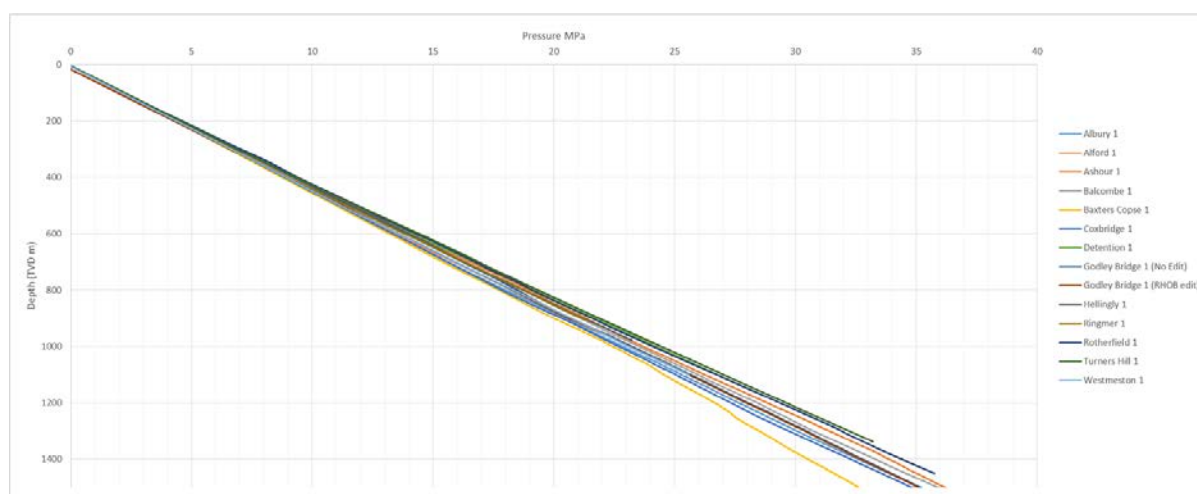


**Figure 13: Compilation of vertical stress gradients from the Weald based on 13 wells. All of the curves fall in the range of 22 – 25 MPa $\text{km}^{-1}$ . Below 1000 metres there is a sharp change in the profile of Baxter's Cope however this is associated with a large wash out rather than any change in the vertical stress gradient and the data from this well below 1100 m are excluded from the regional interpretation**

### 3.3 Cheshire and Lancashire

The Cheshire and Lancashire area was selected based on the availability of well data and current exploration interest for unconventional resources. The initial area of interest included 115 wells, 67 of which were thought to have information to characterise the in-situ stress field. Of these 67 wells only 21 had any information to characterise the stress field (Figure 14). See Appendix 1 for details.

The area of Cheshire and Lancashire with information to characterise the stress field (Figure 14) covers two main sedimentary basins. The Cheshire Basin and the West Lancashire Basin, which is an onshore extension of the East Irish Sea Basin (Smith et al 2005). Both of these basins lie unconformably on Carboniferous strata deposited in the older Pennine and Bowland basins (Kirby et al., 2000; Smith et al., 2005). Much of the Early Carboniferous extension was caused by back-arc spreading created a deep water environment across the whole region (Kirby et al., 2000). This was subsequently infilled by deltas and turbidity flows (in the Namurian – Westphalian) (Kirby et al., 2000). Following uplift and erosion driven by the Variscan orogeny, E – W extension became the dominant tectonic process (Chadwick, 1997). There is little preservation of younger strata in this region though it is thought that extension in these regions continued into the Cretaceous. This was followed by a major phase of uplift and inversion associated with continental convergence to the south (Smith et al., 2005). Detailed descriptions of the structural and stratigraphic history of the areas can be found in Kirby et al. (2000) and Smith et al (2005).

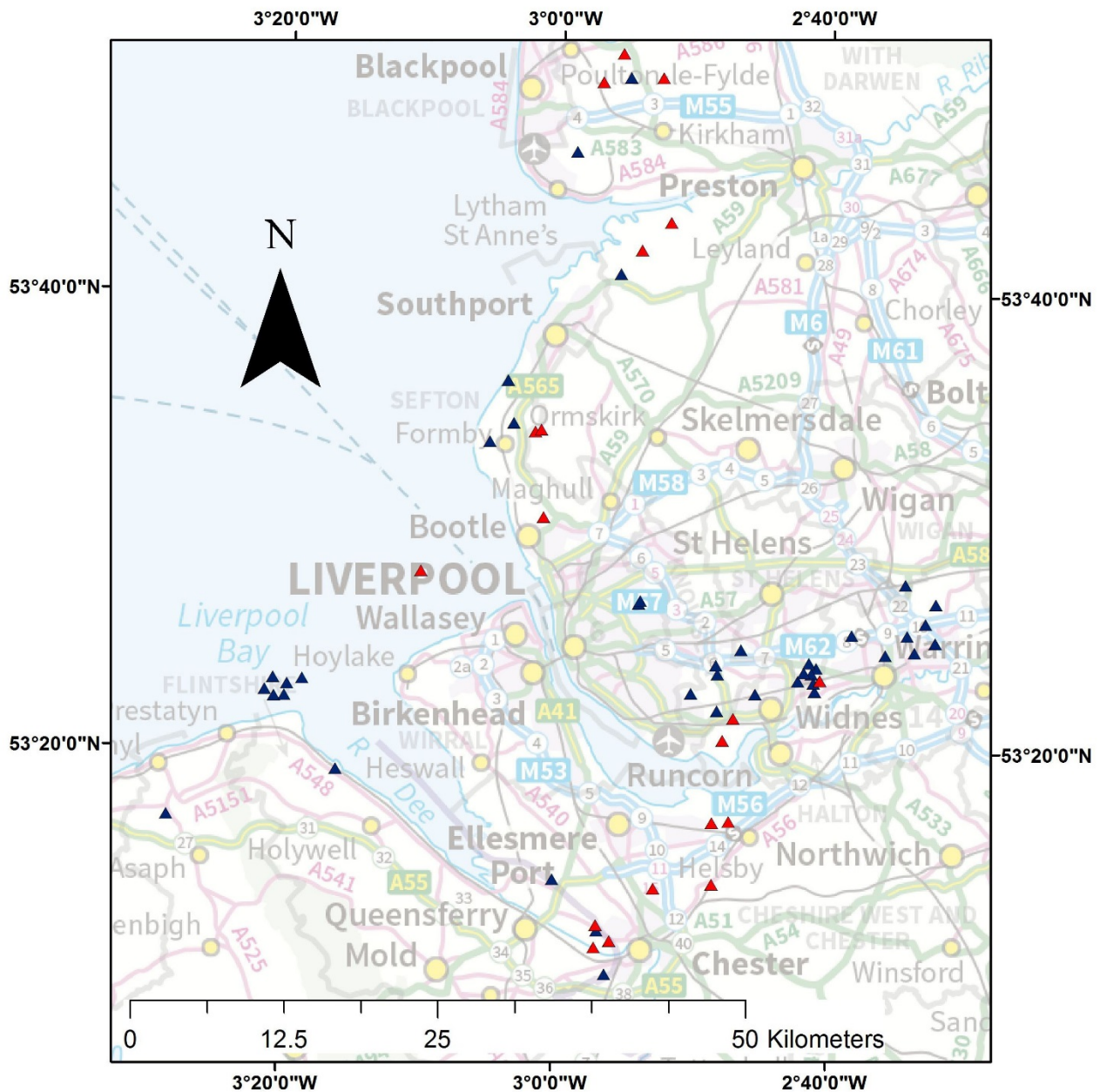
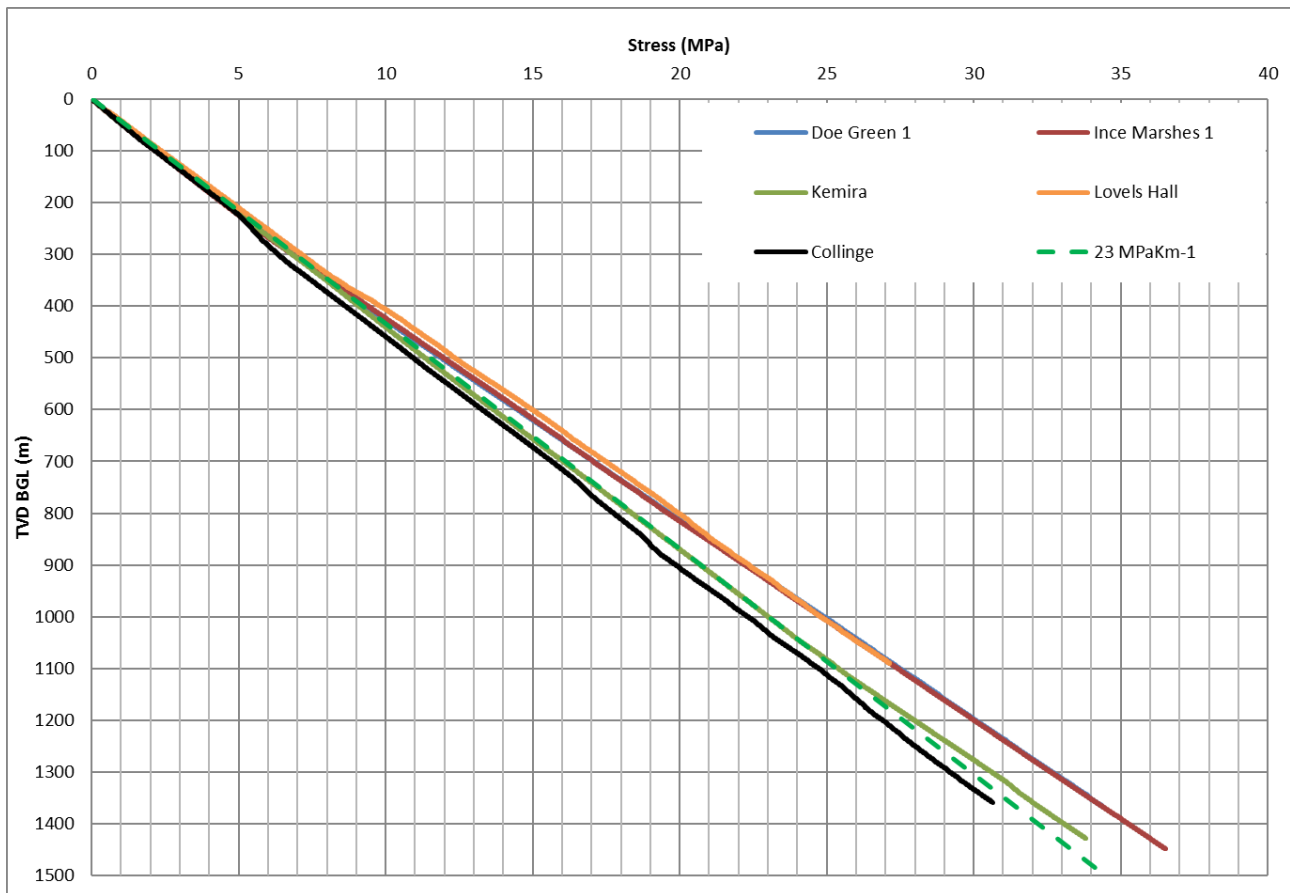


Figure 14: Map of Cheshire and Lancashire showing the distribution of the initial 67 wells in the area of interest thought to contain information to characterise the in-situ stress field (Blue) and the 21 Wells, which contained information to characterise the stress field (Red). Contains Ordnance Survey data © Crown copyright and database rights 2017.

### 3.3.1 Vertical Stress

Studies initially focussed on seven wells in the immediate area surrounding the proposed UK Geoenery Observatories (UKGEO) southern site in North East Cheshire. The vertical stress gradients derived from two Coal Authority boreholes and three hydrocarbon boreholes are shown in Figure 15. The vertical stress gradient for these wells varies between 23 and 26 MPakm<sup>-1</sup>. The stress profiles for two wells, Hale and Morley Bridge fell below 23 MPakm<sup>-1</sup>. This was a result of large washouts and possible errors in the CPS to gcm<sup>-3</sup> conversion (see section 2.1.1); as a result these wells were removed.



**Figure 15: Compilation of vertical stress gradients from the proposed UKGEO Thornton Site and surrounding areas. Dashed black line represents a gradient of 23 MPakm<sup>-1</sup>. The vertical stress gradients range from 23 – 26 MPakm<sup>-1</sup>.**

### 3.3.2 Pore Pressure

Pore pressure data from RFT tools was only available for two wells in the area: Blacon West 1, Blacon East 1 with an interpreted DST available for Elswick 1, all measurements are below 700 m depth (Figure 16). In some cases EOWR's cite pore pressure data collected in the East Irish Sea as the basis for assuming a hydrostatic pore pressure with a gradient of 10 MPakm<sup>-1</sup>, which is the value for a fluid with a density of 1 gcm<sup>-3</sup>. The pore pressure gradient for this region is 10.8 MPakm<sup>-1</sup>.

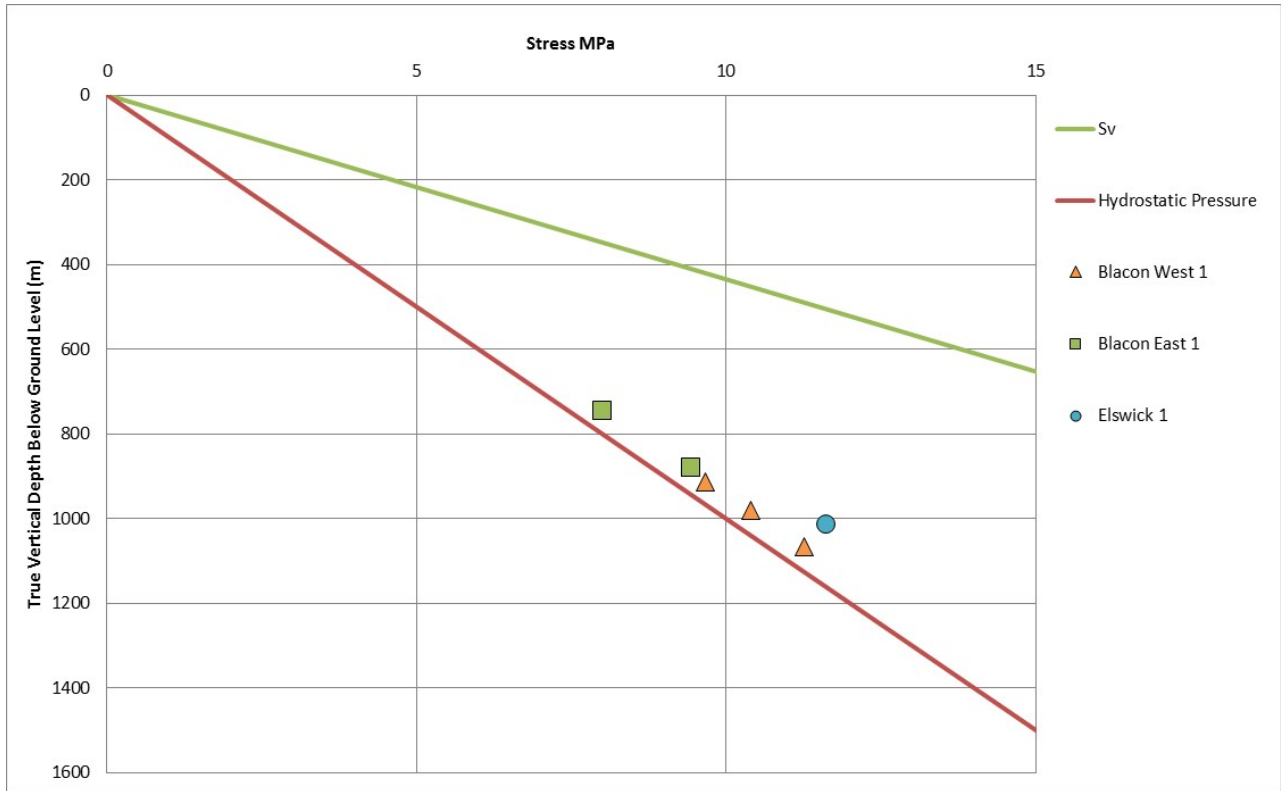


**Figure 16: Compilation of available RFT pressure data for Cheshire and Lancashire. All of the data plot on or near the hydrostatic pressure gradient of 10 MPakm<sup>-1</sup>. Indicating that pore pressure is hydrostatic.**

### 3.3.3 Minimum Horizontal Stress

Data from LOT and FIT were available from 18 wells in the region, some of these were recorded as fracture pressure gradients in psift<sup>-1</sup>. These data were converted to MPa and are shown in Figure 17. The LOT at 850 m plots above the 23 MPakm<sup>-1</sup> line is one of the tests recorded as a gradient rather than a discrete value.

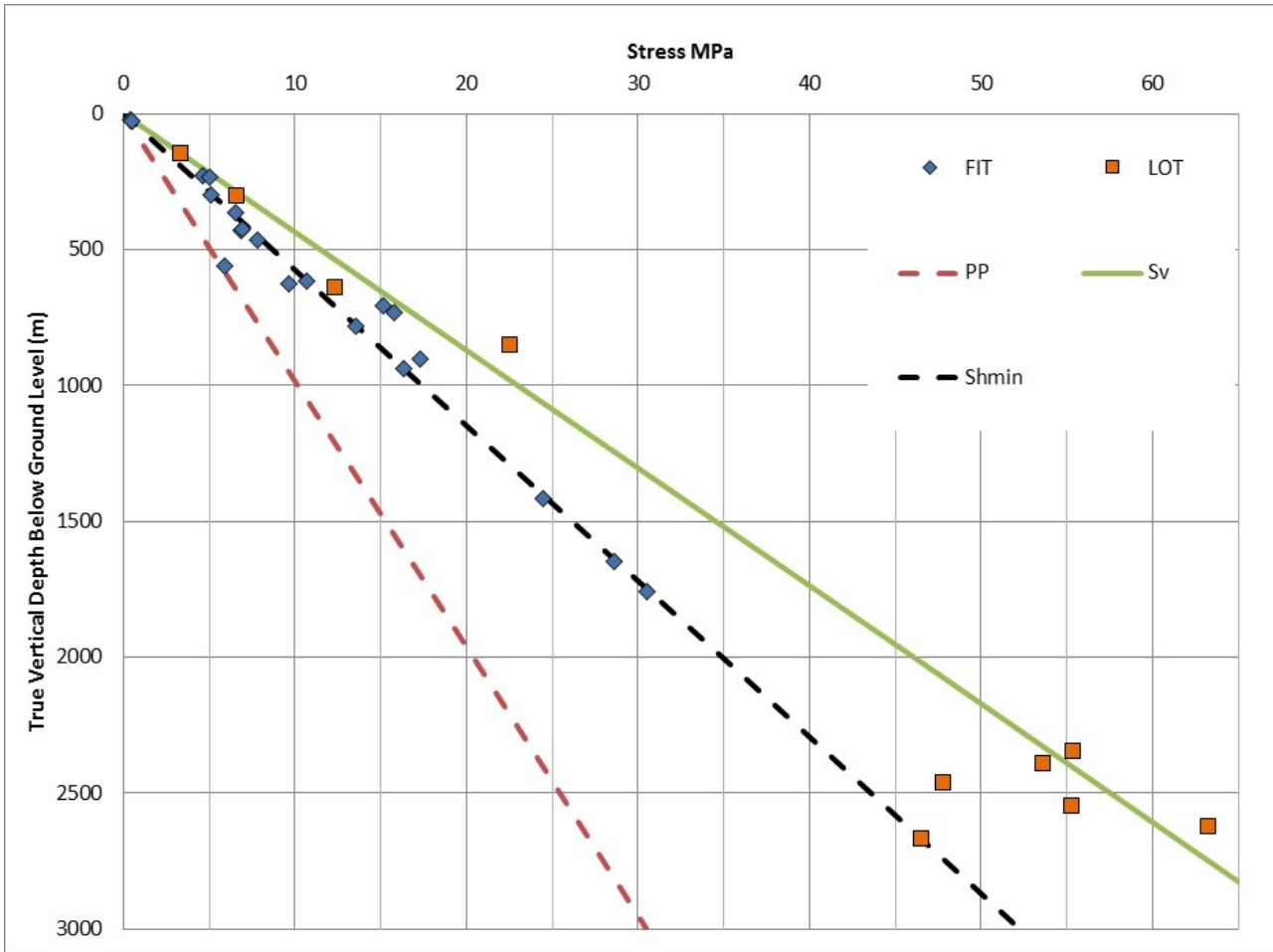


**Figure 17: Compilation of FIT and LOT data available for Cheshire and Lancashire.  $S_v$  (Green) is the vertical stress (lithostatic pressure) for the region and corresponds to a gradient of  $23 \text{ MPa km}^{-1}$  after Figure 15. PP is the pore pressure gradient for the area of  $10.80 \text{ MPa km}^{-1}$  after Figure 16.  $S_{Hmin}$  plotted using the lower bound of the LOT's after Addis et al (1998). These gradients may not be representative of the stress field at specific sites. These gradients are based on regional data and may not be representative of the stress field at specific sites.**

### 3.3.4 Maximum Horizontal Stress

$S_{HMAX}$  was estimated from borehole breakouts at 16 depths in the Preese Hall 1 well, drilled by Cuadrilla in 2010. Rock property data was estimated from geophysical log data calibrated against rock test data (Baker Hughes, 2011). The results are summarised in Table 4.

**Table 4: Summary table of  $S_{HMAX}$  data calculated using borehole breakouts from the Prees Hall 1 well (based on Baker Hughes, 2011). PPG – Pounds per Gallon.**

TVD BGL (m)	$S_{HMAX}$ (Lower)	$S_{HMAX}$ (Upper)	$S_v$	$S_{HMAX}$ Orientation	Breakout Width
	PPG (EMW)	PPG (EMW)	PPG (EMW)	Deg	Deg
1491.082	22.6	24.83	20.12	173	60
1853.184	20.9	25.7	19.94	173	45
1875.434	23.2	26.96	19.95	173	45
1926.336	25	28	19.98	173	64
2117.446	24.1	27.6	20.13	173	20
2188.464	22.65	25.52	20.17	173	50

2230.526	23.07	25.9	20.19	173	45
2305.812	22.06	23.92	20.24	173	30
2328.062	22.27	24.71	20.25	173	70
2473.757	21.17	24.25	20.34	173	60
2548.433	21.98	23.8	20.38	173	45
2552.09	21.9	23.8	20.38	173	50
2553.31	22.55	24.3	20.38	173	30
2566.721	22.18	23.8	20.39	173	40
2587.142	22.1	24.7	20.4	173	30
2630.424	22.1	25.3	20.41	173	60

### 3.4 Additional Maximum Horizontal stress data

Due to the paucity of  $S_{HMax}$  available across the UK and the lack of  $S_{HMax}$  data within the regions themselves (sections 3.1.4 and 3.3.4) the decision was made to incorporate the available legacy  $S_{HMax}$  data.

The  $S_{HMax}$  values are largely calculated from two techniques; hydraulic fracturing and overcoring. The available data was compiled from peer review papers and published reports. This yielded  $S_{HMax}$  information for 25 sites including hydraulic fracturing measurements Carnmenellis Granite in Cornwall (Pine et al., 1983) and overcoring at a quarry in Caithness in Scotland Figure 18.

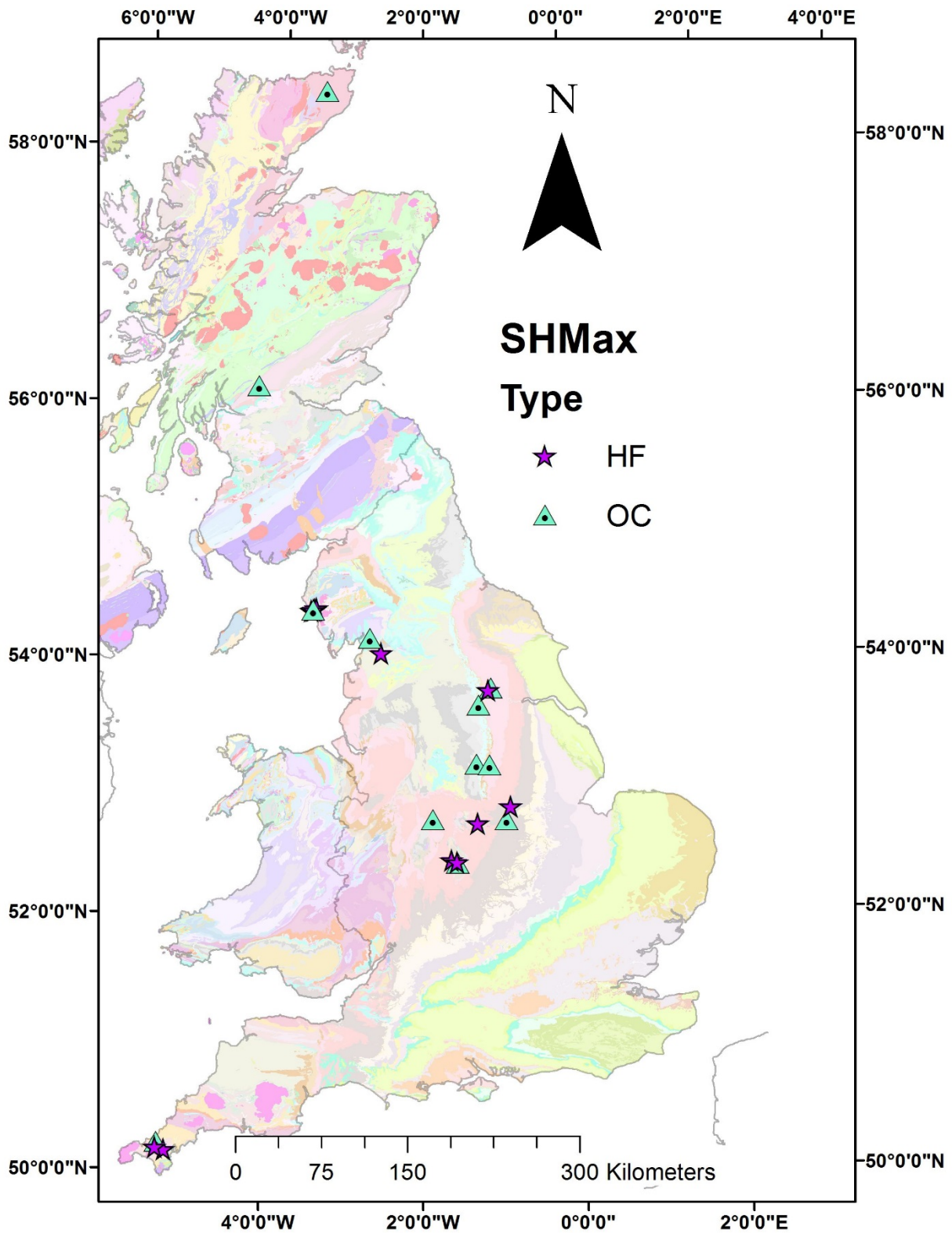
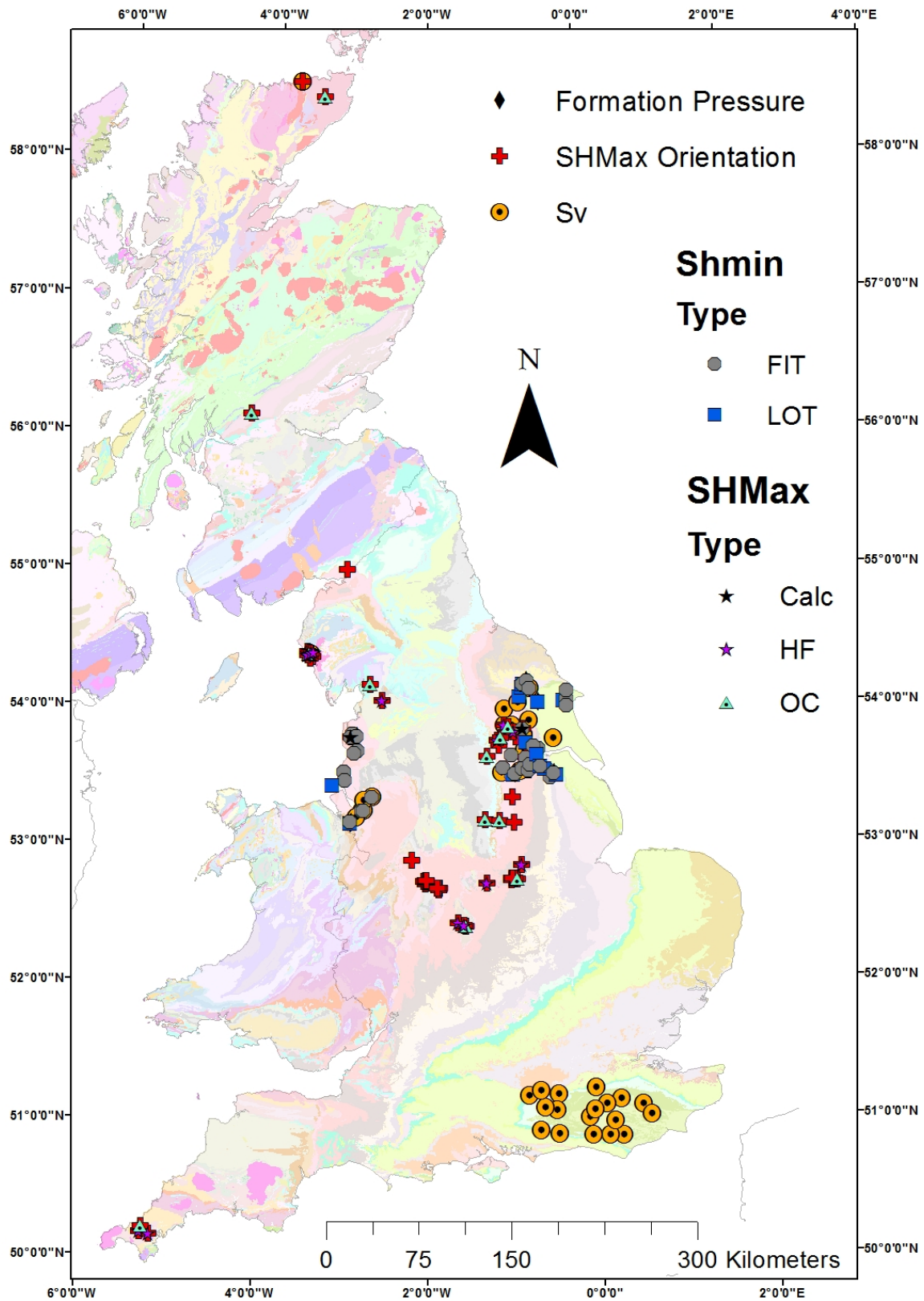


Figure 18: Distribution of additional  $S_{HMax}$  data from publish literature and Coal Authority reports across the UK: HF – Hydraulic Fracturing, OC – Overcoring. Contains British Geological Survey materials ©NERC 2017.

## 4 Discussion

Figure 19 shows the distribution of data available to characterise the UK onshore stress field.



**Figure 19: Map showing geographical location of borehole data available to characterise the UK stress field: FIT – Formation Integrity Test, LOT- Leak off test, HF – Hydraulic Fracturing, OC – Overcoring and Calc –  $S_{HMax}$  calculation from borehole breakouts and DIFs. Contains British Geological Survey materials ©NERC 2017.**

Across the UK landmass there are similarities in the state of stress between the regions investigated (Figure 10, Figure 17, Figure 20). This is despite the contrasting tectonic settings and separations of 100's of kilometres. Whilst relationships between pore pressure, vertical stress and minimum horizontal stress data are all discussed, due to the scarcity of  $S_{HMax}$  data across the UK it is difficult

to establish regional relationships. Despite variations in stress magnitude it does appear in almost all cases that  $S_{HMax} > S_v$  indicating a strike-slip / reverse faulting environment.

Much of the legacy vertical stress data is from coal industry hydraulic fracturing reports. However these data are often based on an assumed vertical stress gradient of 22-26 MPakm<sup>-1</sup>. There are only a small number of published studies on vertical stress which do support this but they are geographically constrained (Nirex, 1997; Williams et al., 2016). The vertical stress profiles from the density log inversion calculations illustrate that the vertical stress gradient ranges from 23 – 26 MPakm<sup>-1</sup> (Figure 20), supporting the assumptions made by the Coal Authority. There is a three MPakm<sup>-1</sup> difference in vertical stress gradients between North West England and Scotland when compared with Yorkshire and the Weald.

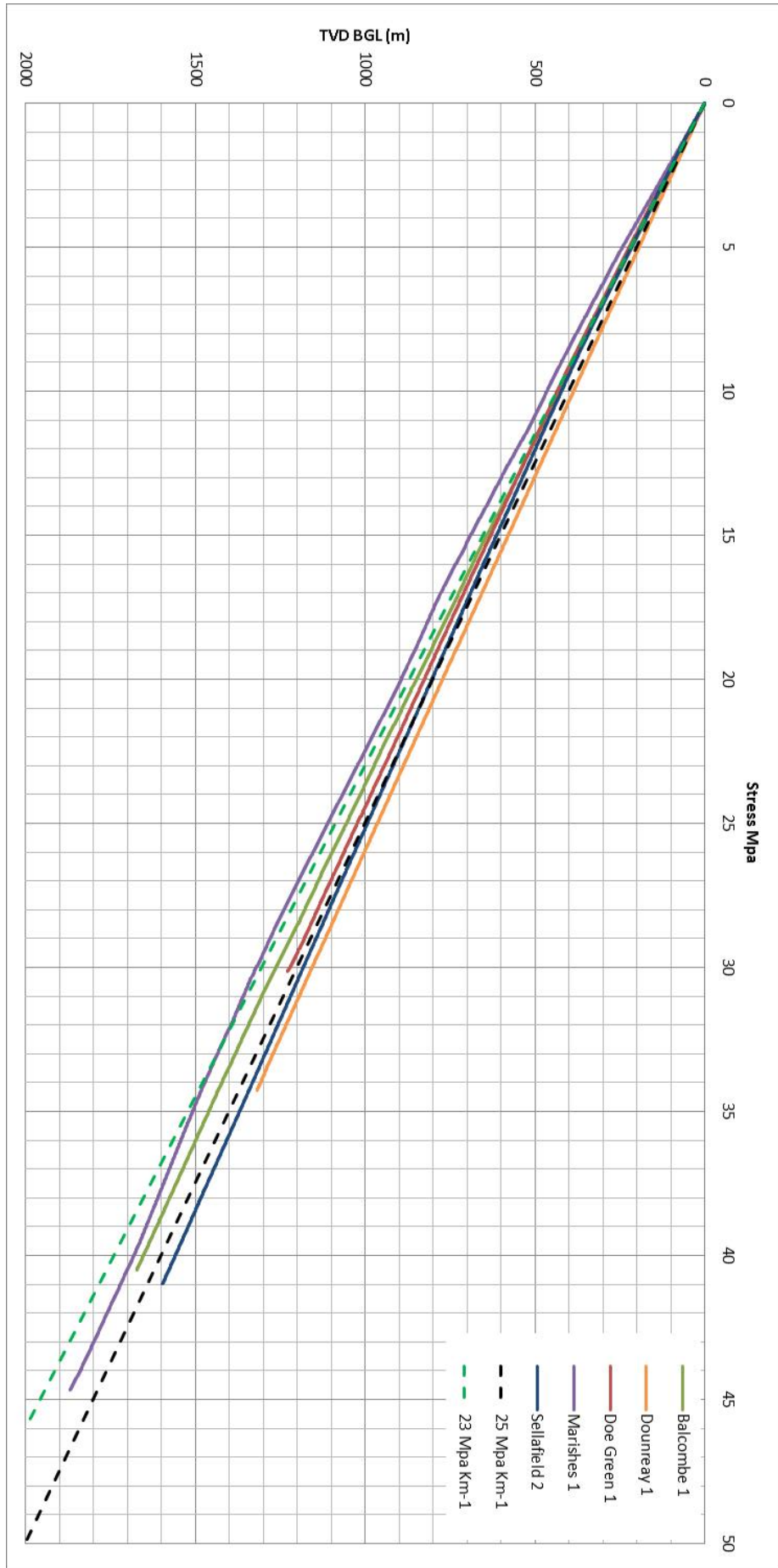
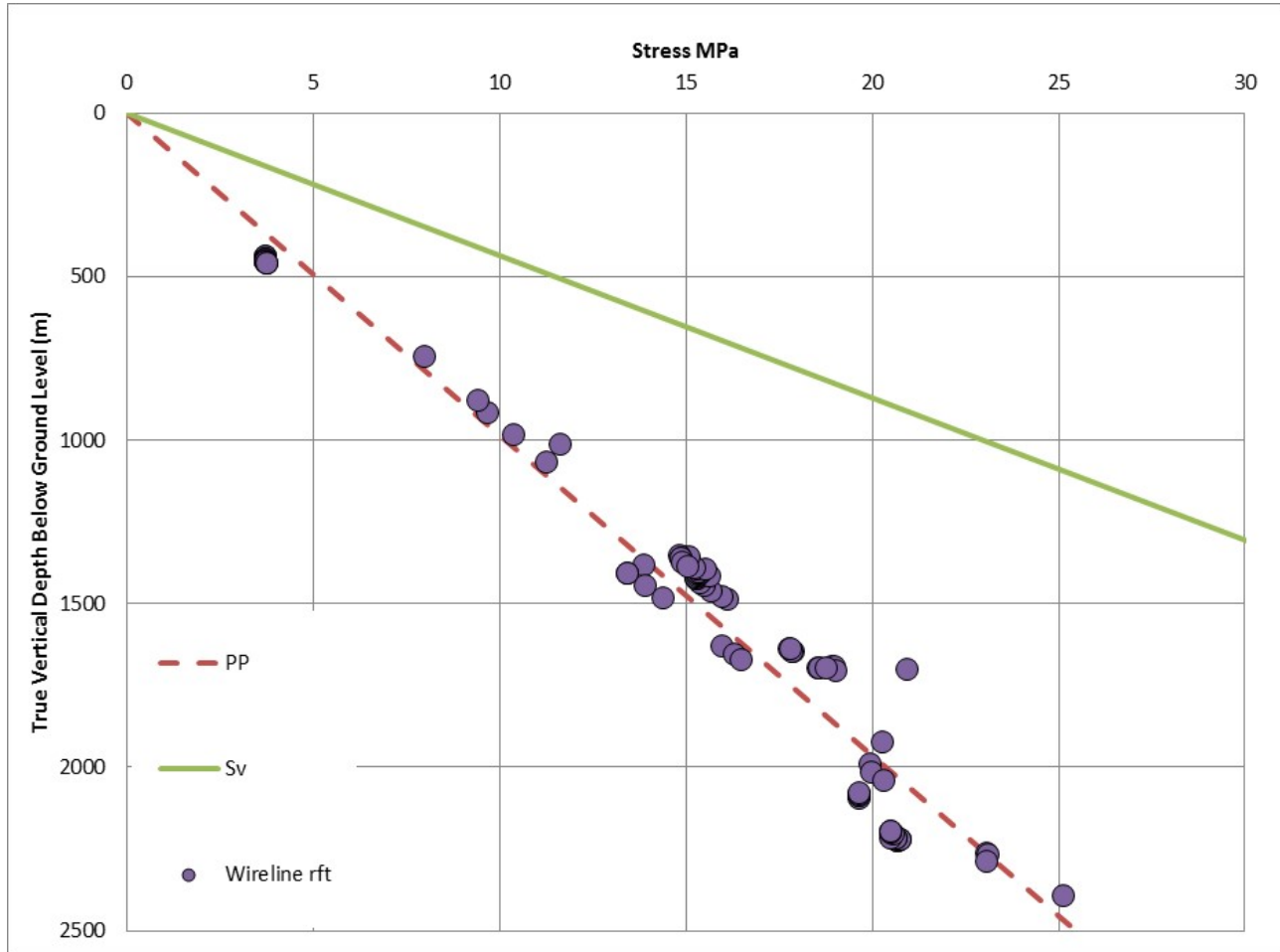


Figure 20: Vertical stress gradients for a variety of UK Regions. Dashed lines representing gradients of 23 and 26 MPakm<sup>-1</sup> are included for reference. Balcombe 1 is a well from the Weald, Marishes 1 is from North Yorkshire,

**Doe Green 1 is from Lancashire, Sellafield 2 was drilled in Cumbria and Dounreay 1 was drilled on the North Coast of Scotland.**

The pore pressure data shows no indication of over or under-pressure conditions. As both over and under pressure can affect vertical stress this data is supported by the vertical stress profiles. For this study some 227 wells were inspected for RFT data, but pressure data were only available for 10 wells (Figure 21). The available data reveal that for a small number of sites pore pressure is consistent with a gradient of  $10.19 \text{ MPakm}^{-1}$ .



**Figure 21: Diagram showing the available pressure data from Cheshire, Lancashire, East Yorkshire and North Nottinghamshire. PP corresponds to a gradient of  $10.19 \text{ MPakm}^{-1}$ . This data supports the assumption of hydrostatic pore pressure in these regions.**

The majority of the pore pressure data are hydrostatic and plot slightly above the  $10 \text{ MPakm}^{-1}$  line. Three measurements from Marishes 1 plot around 5 MPa above the hydrostatic line. After checking the log scans these measurements were collected in a Namurian Sandstone – Claystone formation. These tests were not marked as supercharged but there were a number of tool failures in this area and this may be an effect of low permeability strata. Due to the small number of occurrences it is not possible to state that there is evidence of overpressure but more data is needed to investigate this.

Despite the consistency of the pore pressure measurements there are variations in the vertical stress profiles across the UK (Figure 20). The greatest variations are between Scotland (Dounreay 1) and North Yorkshire (Marishes 1), but there also downhole variations in vertical stress which may be a result of the stratigraphy.

A compilation of FIT and LOT data from the wells included in this study are shown in Figure 22.

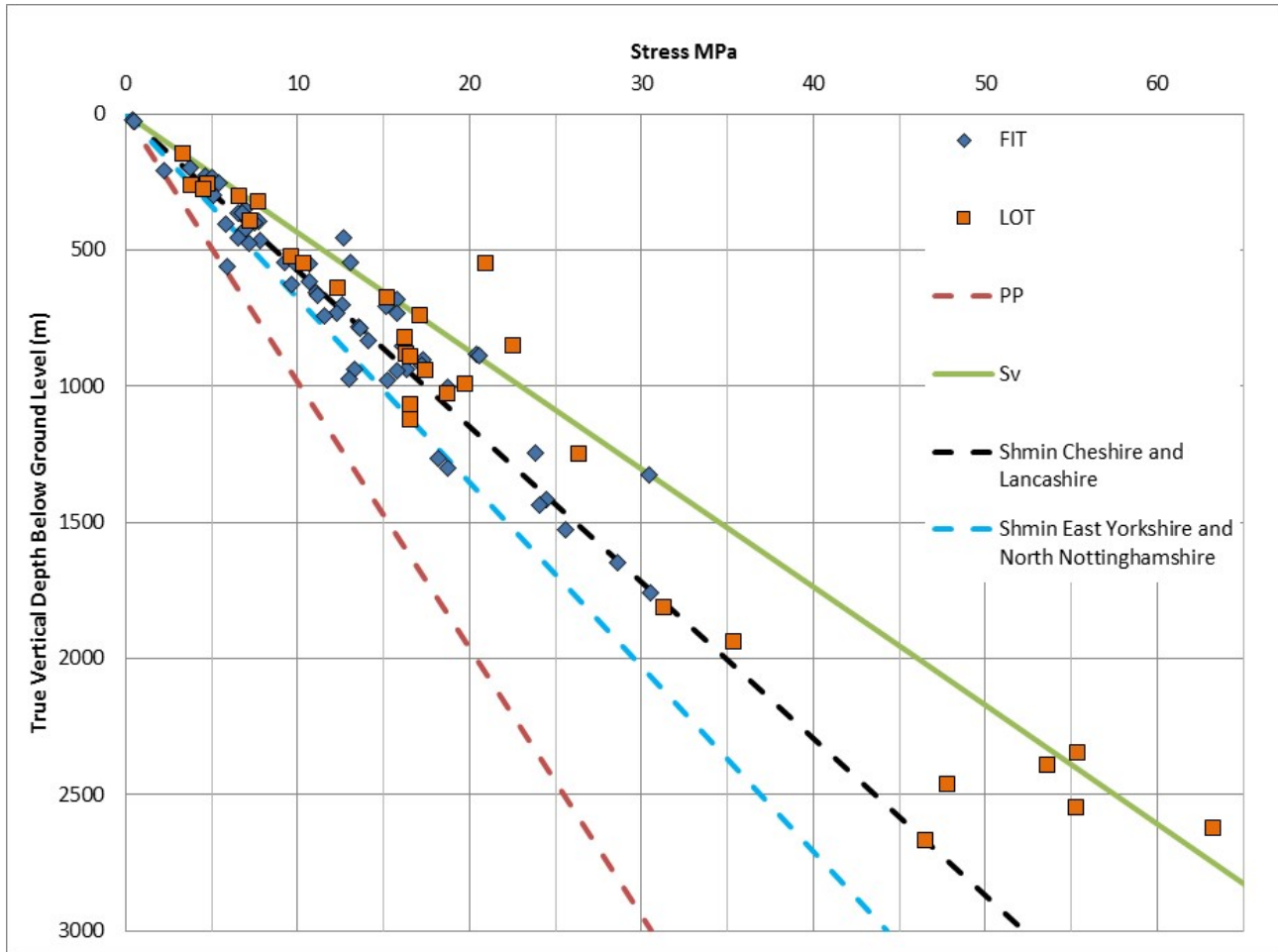


**Figure 22: Compilation of FIT and LOT data and estimates of  $S_{hmin}$  from: Cheshire, Lancashire, East Yorkshire and North Nottinghamshire,  $S_v$  is  $23 \text{ MPakm}^{-1}$  after Figure 20. Figure 21 demonstrated that the pressure data for the region corresponded to hydrostatic pressure; PP represents a gradient of  $10.19 \text{ MPakm}^{-1}$ . At depths of  $< 1000 \text{ m}$  there are 12 FIT/LOT measurements which plot at or above the vertical stress line. This indicates that  $S_{hmin} \approx S_v$  but more work is needed to confirm this. Regional  $S_{hmin}$  gradients plotted using the lower bound of the LOT's after Addis et al (1998). These gradients are based on regional data and may not be representative of the stress field at specific sites.**

The general trend on the data suggests that  $S_{hmin} < S_v$ , however a number of the tests above  $1000 \text{ m}$  plot at or above the  $23 \text{ MPakm}^{-1}$  line (Figure 22). Two FIT test plot on the hydrostatic pressure line. These anomalies may be the result of tool failure such as bleeding off.

Estimates of  $S_{hmin}$  have been derived for each of the regions from the Leak-off test data after Addis et al (1998). These gradients have been drawn to facilitate comparison between the two regions and may not be representative of the values or trend of  $S_{hmin}$  at specific sites. There are no XLOT's to validate these measurements and there is a considerable spread in the LOT data (Figure 22). This data does appear to support the trend shown in Figure 20 with the  $S_{hmin}$  estimate for Cheshire and Lancashire greater than East Yorkshire and North Nottinghamshire.

Out of the 91 FIT/LOT data points compiled in this study only 11 exceed the estimate  $S_v$  ( $23 \text{ MPakm}^{-1}$ ), this data strongly supports a strike slip faulting environment. Nine of the 11 measurements that plot above the  $23 \text{ MPakm}^{-1}$  line, were collected at depths of  $< 1000 \text{ m}$  (Figure 23) which may indicate more variability in the stress field at these depths. Eight of the 11 measurements were collected in Permo – Triassic strata and in particular the Mercia Mudstone and the Zechstein Groups. These are highly heterogeneous formations with muds, sand, silts and variable thicknesses of evaporites. This heterogeneity may also be a factor in the increased variability of  $S_{hmin}$ .

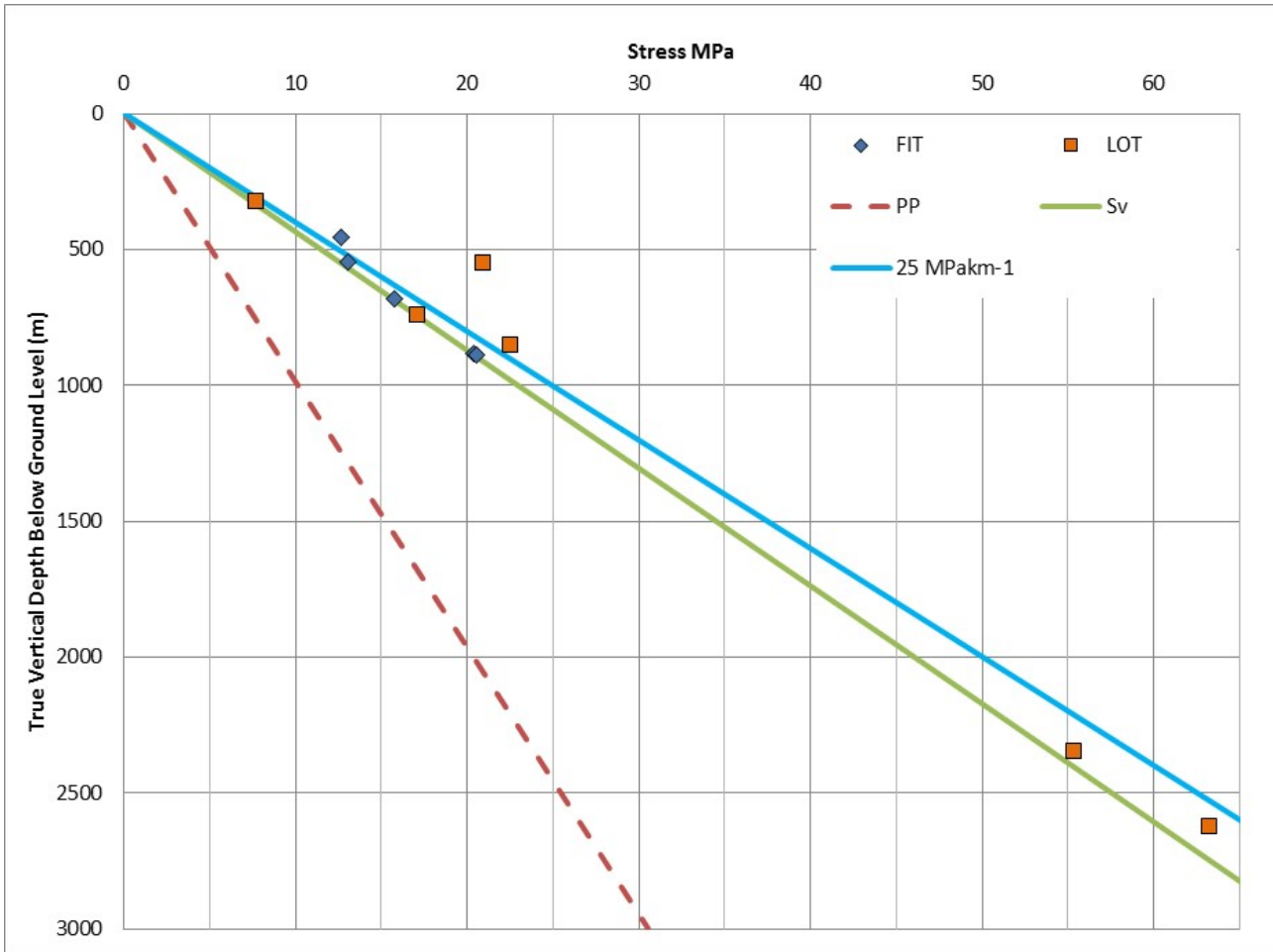


Figure 23: Compilation of all FIT, LOT and RFT data Which exceeds  $S_v$  shown by the green line which corresponds to a gradient of  $23 \text{ MPakm}^{-1}$ . Figure 21 demonstrated that the RFT data for the region corresponded to hydrostatic pressure and has not been plotted. PP represents a gradient of  $10.19 \text{ MPakm}^{-1}$ . Nine of the eleven measurements were collected at depths of  $< 1000 \text{ m}$  suggesting either changes in the stress field at this point of less heterogeneity in the strata.

With a single exception (Melbourne 1), all of the  $S_{\text{HMax}}$  magnitude data across the UK were compiled from legacy data (Pine et al., 1983; Cooling et al 1988; Bigby et al., 1992; Nirex 1997; Becker and Davenport, 2001; Baker Hughes, 2011). Figure 24 shows the spatial distribution of  $S_{\text{HMax}}$  magnitude estimates across the UK. There are currently 93 estimates from 30 sites including: boreholes, quarries, collieries and Mines. The stress magnitude data are mainly calculated from overcoring and hydraulic fracturing tests, but several measurements were calculated from borehole breakouts in the Preese Hall 1 well.

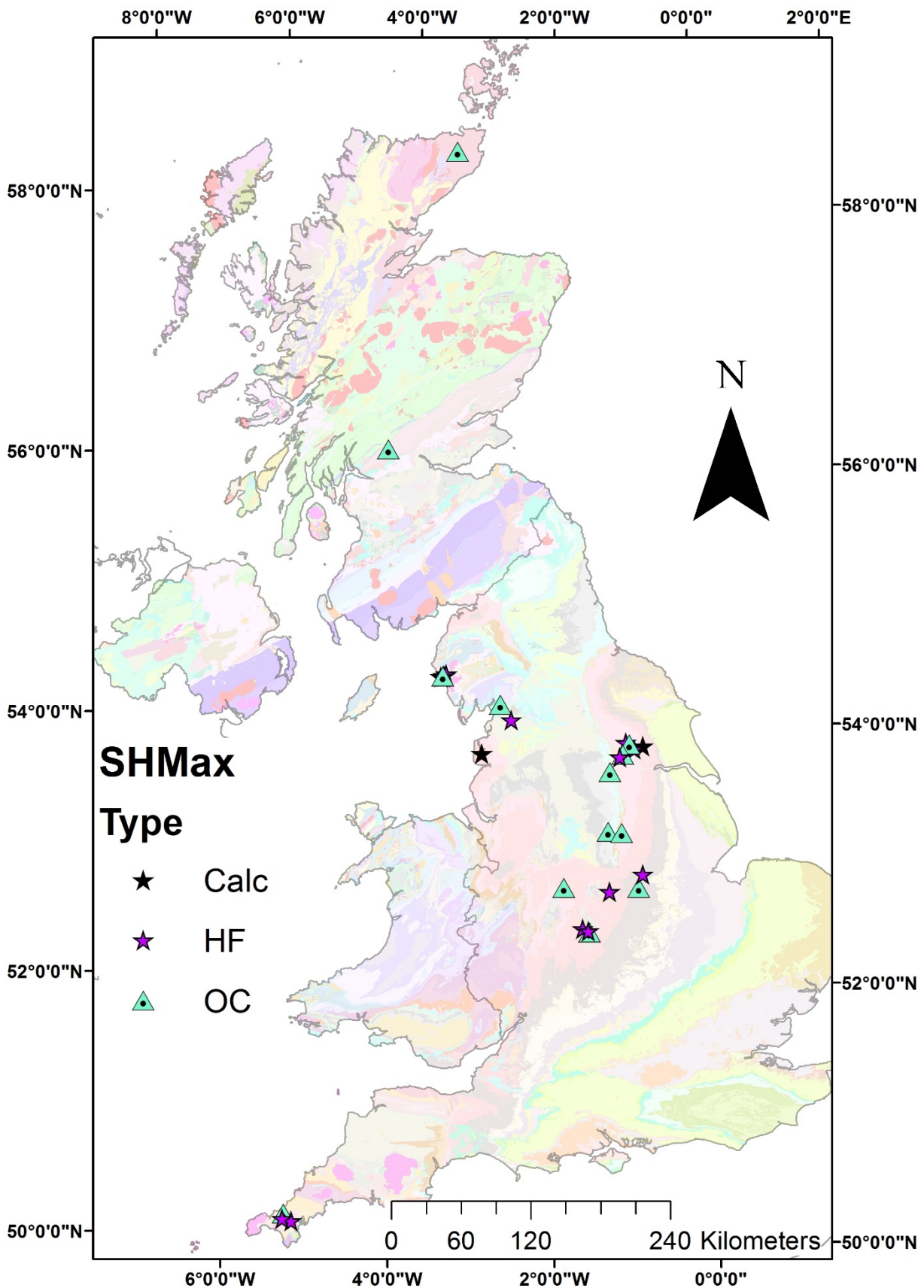
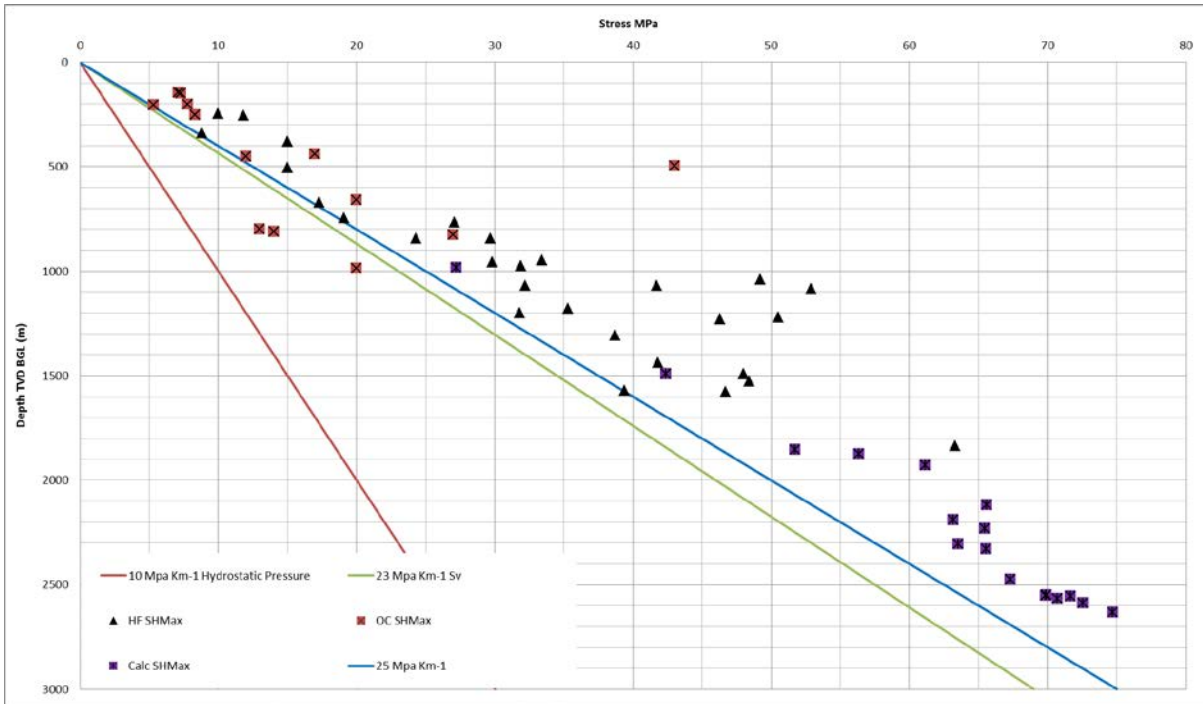


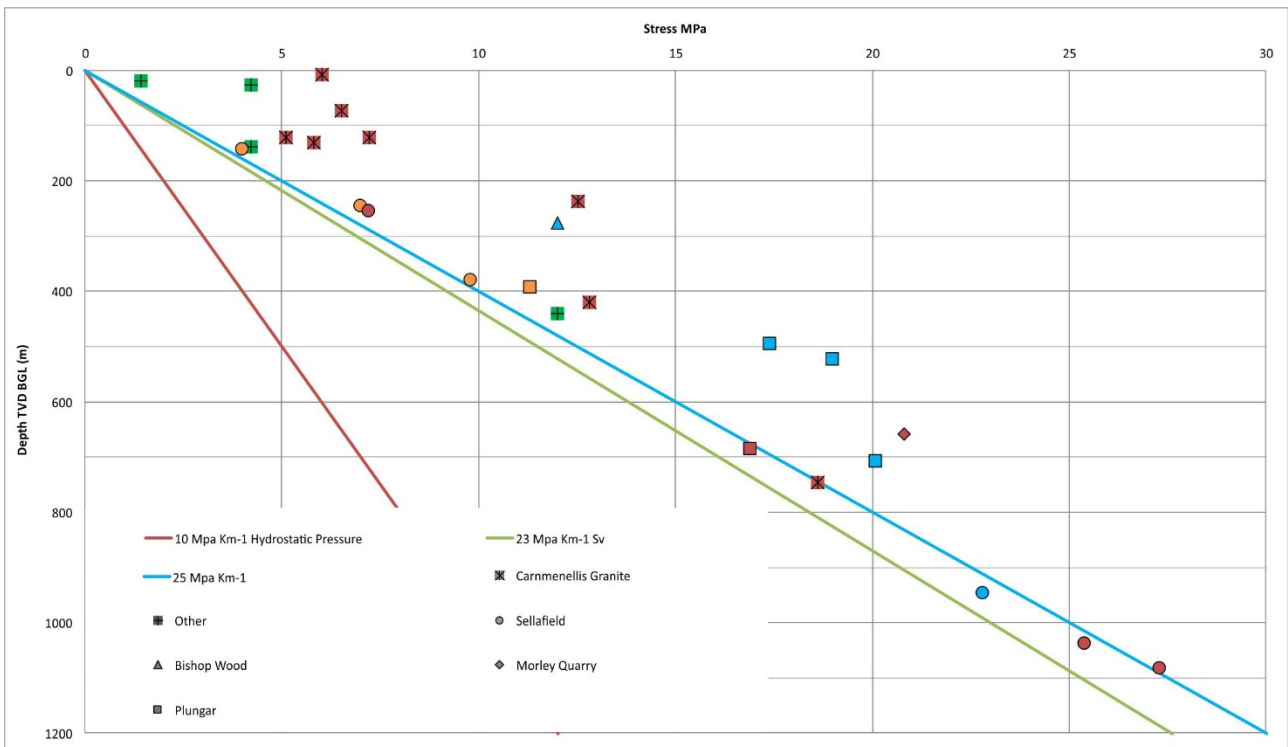
Figure 24: Location of all of the measurements of  $S_{HMax}$  magnitude across the UK. These magnitudes have been estimated using: Overcoring (OC), Hydraulic Fracturing (HF) and calculations from observations of borehole breakouts and DIFs (Calc). Contains British Geological Survey materials ©NERC 2017.

Figure 25 compares the magnitudes of  $S_{HMax}$  from legacy data against the estimates of UK vertical stress (Figure 20).



**Figure 25: Compilation of all  $S_{HMax}$  magnitudes from: Overcoring (OC), Hydraulic Fracturing (HF) and calculations from observations of borehole breakouts and DIFs (Calc). With the exception of three overcoring measurements  $S_{HMax}$  magnitude is greater than the  $S_v$  of 23 MPakm<sup>-1</sup> suggesting that  $S_{HMax} \geq S_v$  however this is based on data from a small number of locations.**

Figure 25 shows that with three exceptions, all of the  $S_{HMax}$  estimates plot above 23 MPakm<sup>-1</sup> and on, or above 25 MPakm<sup>-1</sup>, a high value of  $S_v$  for the regions studied (Figure 20). Based on the available data  $S_{HMax}$  is  $\geq S_v$  indicating a predominately strike slip / reverse environment, supporting the conclusions of Baptie (2010). There is evidence of reverse faulting regimes in the data largely from hydraulic fracturing measurements (Figure 26).



**Figure 26:  $S_{hmin}$  values which exceed the vertical stress gradient of 23 MPakm<sup>-1</sup> indicating possible reverse Faulting regimes.  $S_{hmin}$  values derived from hydraulic fracturing and overcoring methods. Values have been shaded broadly by lithology and age. Green: Unknown source and age, Red: Igneous source, Orange: Triassic Sediments, Blue: Carboniferous sediments**

The majority of the data indicating a possible thrust faulting environment was collected either as part of the Hot Dry Rock (HDR) research project in the Cornish Granite (Parker, 1999), or shallow quarry measurements e.g. Gatur and Spittal in Scotland (Becker and Davenport, 2001). As such they are outside the main focus of this report. This dataset is limited both spatially and stratigraphically but does indicate possible reverse / strike slip faulting regimes from Sellafield in Cumbria, Plungar in Nottinghamshire and Bishop Wood in North Yorkshire.

As discussed in Section 2.5 there are significant issues with  $S_{HMax}$  magnitudes from both hydraulic fracturing and overcoring techniques. At Rosemanowes there is an uncertainty of  $15 \text{ MPakm}^{-1}$  in the values of  $S_{HMax}$  (Pine et al., 1983).

Much of the published literature on the UK stress field relates to the orientation of  $S_{HMax}$  and focuses mainly on the North Sea (Klein and Barr, 1986; Williams et al., 2015). Kingdon et al (2016) reviewed previous studies of stress field orientation onshore and characterised the stress field orientation using a borehole imaging dataset. The results of the study indicated a consistent  $S_{HMax}$  orientation of  $150.9^\circ$  (with a circular standard deviation of  $13.1^\circ$ ). This orientation was attributed to ridge-push stresses associated with the Mid Atlantic Ridge system (Klein and Barr, 1986).

Of the 93  $S_{HMax}$  observations, 29 had  $S_{HMax}$  orientations recorded, which are illustrated in a rose diagram (Figure 27).

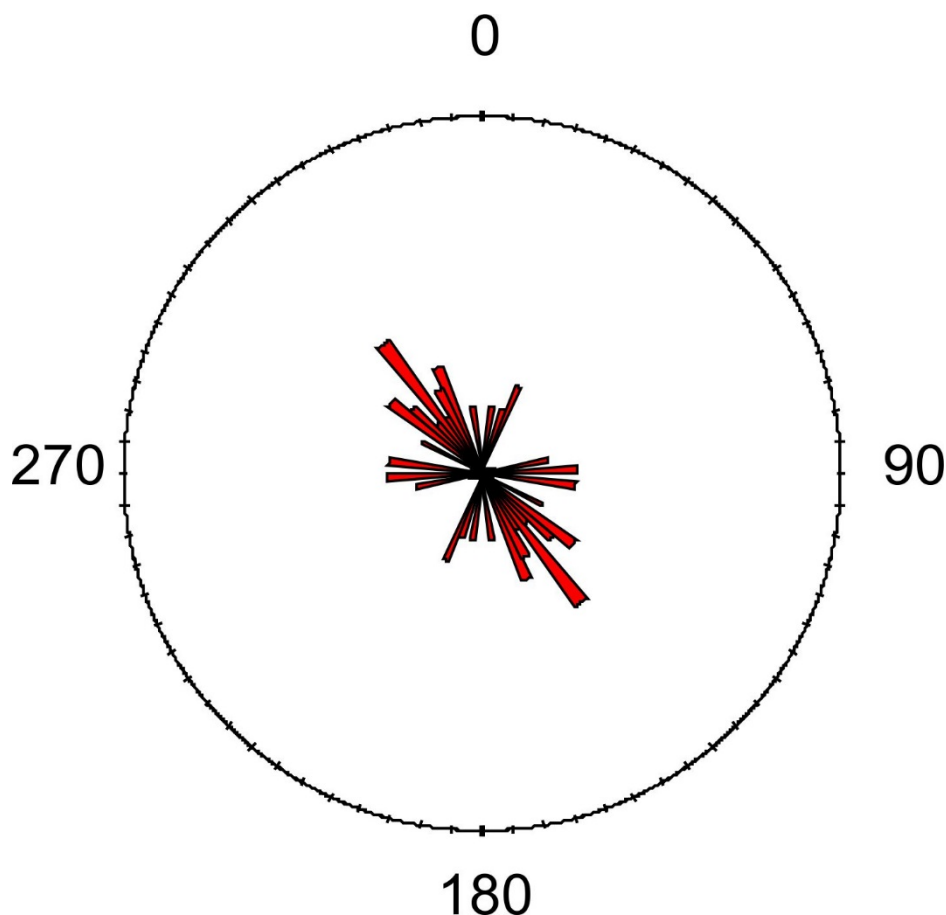


**Figure 27:  $S_{HMax}$  orientations from Hydraulic Fracturing and Overcoring binned at  $5^\circ$  intervals**

The dominant  $S_{HMax}$  orientation for these observations is  $141^\circ$  (with a circular standard deviation of  $32^\circ$ ) (Figure 27). The large standard deviation of these measurements (shown on Figure 27) results from nine observations: four indicating a NNE – SSW direction of  $S_{HMax}$  and five an E – W trend of  $S_{HMax}$ . Observations indicating an E-W direction of  $S_{HMax}$  were recorded in two boreholes in the Midlands: Morley Quarry 1 and a single observation in Back Lane Plungar. The single observation at Plungar was from Carboniferous volcanic strata and is  $> 60^\circ$  different to the other three observations from this well. The observations from Morley Quarry were recorded in Precambrian foliated lavas or tuffs. This would appear to indicate that pre-Variscan igneous strata is preserving

relic stress orientations. By comparison, the orientations from the Permian Carnmenellis granites are predominantly NW – SE. As these strata are not prospective for hydrocarbons there is very little additional data available to investigate if stress orientations are being preserved by igneous strata. The E – W orientations are different to the vast majority of those documented in Kingdon et al (2016) though this may be due to the geographic and stratigraphic constraints on the available data. The majority of the remaining observations support the NE-SW trend of  $S_{HMax}$  as recorded in Kingdon et al (2016).

Su et al., (2001) have shown that coal cleats form in the orientation of  $S_{HMax}$  when  $\sigma_1 > \sigma_2$ . In an attempt to assess palaeo stress orientation, Rippon et al (2006) following on from: Ellison (1997); Jones, (2004) mapped the coal cleats across the UK. This method has been utilised in other locations ahead of potential coal bed methane developments where there is an absence of borehole data (Paul and Chatterjee, 2011). The palaeo stress orientations identified by Rippon et al (2006) and Ellison (1997) are predominately NW-SE and are thought to result from compression due to the Variscan orogeny. There were significant deviations in cleat orientations in both South Wales and the Midland Valley, which are thought to be the result of fault block rotations (Rippon et al., 2006). Given the similarities between the stress field orientation in the Variscan and the present day, it is difficult to say if the coals are preserving a palaeo-stress orientation. Where significant differences the palaeo-stress orientation existed (e.g. the Midland Valley and the south Wales coalfield) there is insufficient borehole data to characterise the  $S_{HMax}$  orientation.

## 5 Conclusions

Despite some variability in  $S_{hmin}$  and  $S_{HMax}$  due to the strata and measurement techniques the available data indicates that the UK landmass is predominantly a strike slip faulting environment with possible indicators of reverse faulting above 1200 m (though these are largely confined to igneous rocks in Cornwall, Cumbria and Leicestershire).

Pore pressure observations across all regions studied, largely support the assumption of hydrostatic pore pressure with a gradient of  $10.19 \text{ MPakm}^{-1}$ , with only a small number of measurements indicating overpressure e.g. Marishes 1 (1700 m). However, given that there data is constrained both spatially and stratigraphically these may have be from isolated or impermeable units. These data do not show significant or under pressure in Cheshire, Lancashire, East Yorkshire or North Nottinghamshire.

Vertical stress gradients (Figure 20) and values from LOT's and FIT's across the different regions show that the gradient of both  $S_v$  and  $S_{hmin}$  is two to three  $\text{MPakm}^{-1}$  higher in Cheshire and Lancashire when compared to East Yorkshire or North Nottinghamshire. However, XLOT's or laboratory test data are required to validate the estimates of  $S_{hmin}$ .

The general trend of  $S_{hmin}$  from the leak off tests appears to show the  $S_{hmin} < S_v < S_{HMax}$  indicating a predominantly strike-slip regime. There is a larger variation in the recorded values of  $S_{hmin}$  in the Permo - Triassic strata of the UK than the Carboniferous, with  $S_{hmin}$  approaching the value of  $S_v$  and in some cases  $\geq S_v$ .

There are observations from hydraulic fracturing and overcoring which may suggest greater variation in stress field orientation than recorded in Kingdon et al (2016). However this study focused on borehole imaging datasets which are stratigraphically limited. Borehole imaging data from within the Carboniferous succession indicates that across the areas of interest the  $S_{HMax}$  orientation is likely to be NW – SE.

The  $S_{HMax}$  data from hydraulic fracturing, overcoring and borehole breakouts data plot above  $S_v$  ( $23 \text{ MPakm}^{-1}$ ) with a three exceptions. This is indicative of a strike-slip regime. However, there are substantial variations in the overcoring data and there are errors associated with hydraulic fracturing data, particularly when used to estimate  $S_{HMax}$  (Zoback, 2010).

From the available data there appears to be similarities in the stress field across the UK, pore pressure is hydrostatic with a gradient of  $10.19 \text{ MPakm}^{-1}$ . The vertical stress gradient for the Weald, East Yorkshire and North Nottinghamshire is  $23 \text{ MPakm}^{-1}$  and varies from values of  $25 - 26 \text{ MPakm}^{-1}$  recorded for areas of Cheshire and Lancashire and Scotland. Data derived from LOT, hydraulic fracture data and  $S_{\text{HMax}}$  calculated from borehole breakouts, collectively indicate a strike-slip faulting regime ( $S_{\text{hmin}} < S_v < S_{\text{HMax}}$ ). However at depths of  $< 1 \text{ km}$  there is greater uncertainty in the relation between  $S_v$ ,  $S_{\text{hmin}}$  and  $S_{\text{HMax}}$ . Stress magnitude data from the Triassic appears to show a greater variation than data from Carboniferous successions.

Much of the data is geographically constrained and sourced from legacy data, and more information will help to better characterise the UK stress field.

## 6 Further Work

Compiled information on the UK stress field shows differences of up to two to three  $\text{MPakm}^{-1}$  in  $S_v$  and  $S_{\text{hmin}}$  between areas of Cheshire, Lancashire and East Yorkshire North Nottinghamshire. Data from Cheshire and Lancashire region have provided estimates of  $S_v$  pore pressure and  $S_{\text{hmin}}$  near the Proposed UKGEO southern site. Pore pressure is likely to be between  $10.19$  and  $10.8 \text{ MPakm}^{-1}$ ,  $S_v$  between  $23 - 26 \text{ MPakm}^{-1}$  and  $S_{\text{hmin}}$  has been estimated using leak-off test data to have a value of  $17.4 \text{ MPakm}^{-1}$ .

The conclusions of this report are based on the integration of published legacy data and information from the BGS archives. Locally it has allowed characterisation of the stress field and in particular  $S_v$ ,  $S_{\text{hmin}}$  and  $P_p$ . There are no locations within the regions studied which contain sufficient data to study trends or variations in:  $S_v$ ,  $S_{\text{hmin}}$  or  $S_{\text{HMax}}$  with depth, with the exception of studies at Preese Hall and Sellafield (Baker Hughes, 2011; Nirex, 1997).

The UKGEO project provides a unique opportunity to study the relationships between  $S_v$ ,  $P_p$ ,  $S_{\text{hmin}}$  and  $S_{\text{HMax}}$  at a variety of depths at a single locality in the UK subsurface. It could also provide an example of how these stresses affect borehole stability over an extended period of time.

Collecting drill core, XLOT's, wireline RFT, borehole imaging and density logs from surface would allow detailed investigation of the stress field at the site. This would then form the basis for a geomechanical model, which aid the design and implementation of innovative subsurface energy technologies.

## Appendix 1

This section contains the meta data for the wells, mines and quarries used in this report to characterise the UK onshore stress field.

### 1.1 Wells with Stress field information

Meta data for the wells initially identified as potentially containing information to characterise the stress field detailed in sections 3.1, 3.2 and 3.3

#### 1.1.1 East Yorkshire and North Nottinghamshire

Name	PURPOSE	SOBI	BGS ID	EASTING	NORTHING	TD
ARKSEY COMMON	Coal Authority Well	SE50NE/40	115042	459722	407264	653
MOSS	Hydrocarbon Well	SE51SE/19	116558	459977	413897	1098

POLLINGTON BH3	Coal Authority Well	SE52SE/38	117089	459905	420698	870
MANOR FIELD HOUSE	Coal Authority Well	SE53NE/44	117985	459614	435247	534
WIGGINTON	Hydrocarbon Well	SE55NE/226	19199843	459372	456193	1231
CLIFTON AIRFIELD	Coal Authority Well	SE55SE/128	119375	459450	454977	1186
HATFIELD 1	Hydrocarbon Well	SE60NE/21	119970	469313	406965	1615
HATFIELD 2	Hydrocarbon Well	SE60NE/22	119971	467244	406745	1394
HATFIELD WEST 1	Hydrocarbon Well	SE60NE/68	120019	467656	406041	479
HATFIELD MOORS 4	Hydrocarbon Well	SE60NE/75	120026	468972	406259	694
WORMLEY HILL	Coal Authority Well	SE61NE/18	120926	466901	416383	933
BEEVERS BRIDGE	Coal Authority Well	SE61NE/19	120927	466302	418765	963
CROSS HILL	Coal Authority Well	SE61NW/1	120959	460132	418962	801
PARK HOUSE FARM	Coal Authority Well	SE61NW/17	120997	464307	419060	948
BALNE LODGE	Coal Authority Well	SE61NW/18	120998	461759	418251	807
Trumfleet 4	Hydrocarbon Well	SE61SW/104	19370644	460550	411910	1158
FENWICK GRANGE	Coal Authority Well	SE61SW/33	121243	461473	414445	716
TRUMFLEET 1	Hydrocarbon Well	SE61SW/4	121186	460520	412640	1580
TRUMFLEET 6	Hydrocarbon Well	SE61SW/98	18062904	460561	411925	1158
TRUMFLEET 6Z	Hydrocarbon Well	SE61SW/99	18062907	460561	411925	1180
RUSHOLME GRANGE	Coal Authority Well	SE62NE/31	121328	469694	426603	928
BARLOW 3	Coal Authority Well	SE62NE/32	121329	465580	428455	916
CAMBLESFORTH 1	Coal Authority Well	SE62NW/1	121483	464868	425580	934
BARLOW 1	Hydrocarbon Well	SE62NW/15	121499	463347	427857	1215
CAMBLESFORTH 2	Coal Authority Well	SE62NW/26	121515	464058	427634	877
MILL FARM 1	Hydrocarbon Well	SE62SE/263	18275472	467930	422155	830
DRAX NO.4	Coal Authority Well	SE62SE/28	121589	467260	424241	948
COWICK GRANGE	Coal Authority Well	SE62SE/32	121593	465413	421718	981
GOWDALL	Coal Authority Well	SE62SW/23	121823	461542	422379	938
SNAITH	Coal Authority Well	SE62SW/45	121845	464384	422707	948
RICCALL NO.2	Coal Authority Well	SE63NW/41	121988	461807	438246	734
WHELDRAKE 1	Hydrocarbon Well	SE64NE/4	122640	467660	446082	1558
Howden Dike	Coal Authority Well	SE64NW/202	122854	461723	446080	923
East Lodge	Coal Authority Well	SE64SE/20	122964	469019	440612	1138
OLD BRIDGE DYKE	Coal Authority Well	SE64SW/37	123006	461978	442352	885
TOWTHORPE	Coal Authority Well	SE65NW/23	123204	461824	459071	1198
WHENBY 1	Hydrocarbon Well	SE67SE/7	124355	465409	472457	1832

BRIER HILLS	Coal Authority Well	SE70NW/11	124527	471081	408504	927
SANDTOFT	Coal Authority Well	SE70NW/13	124529	474590	409206	1025
ROE CARR SANDTOFT	Hydrocarbon Well	SE70NW/14	124530	473867	405048	1079
HATFIELD MOORS 1	Hydrocarbon Well	SE70NW/15	124531	470353	406680	484
HATFIELD MOORS 2	Hydrocarbon Well	SE70NW/16	124532	471744	406750	518
HATFIELD MOORS 3	Hydrocarbon Well	SE70NW/17	124533	470380	406670	1828
HATFIELD MOORS 6	Hydrocarbon Well	SE70NW/98	12701627	470359	406684	745
AXHOLME 1	Hydrocarbon Well	SE70SE/5	124617	479133	404056	1526
AXHOLME 2	Hydrocarbon Well	SE70SE/6	124618	479338	402977	1433
SWINEFLEET 1	Hydrocarbon Well	SE71NE/10	18407548	479243	419793	1319
EALAND 1	Hydrocarbon Well	SE71SE/38	18958646	476914	410614	1010
LAXTON	Coal Authority Well	SE72NE/9	124831	478195	425699	1150
NEWSHOLME	Coal Authority Well	SE72NW/14	124936	472444	429336	1067
SEATON ROSS 1	Hydrocarbon Well	SE73NE/4	125283	477014	438593	1036
Derwent Bridge	Coal Authority Well	SE73NW/11	125300	470890	436103	1060
BRIND COMMON WRESSLE	Coal Authority Well	SE73SE/2	125306	475200	431294	994
SPALDINGTON 1	Hydrocarbon Well	SE73SE/6	125310	479275	432455	1850
MELBOURNE 1	Hydrocarbon Well	SE74SE/23	18405086	476315	443088	1477
HIGH HUTTON 1	Hydrocarbon Well	SE76NW/14	125667	474423	469412	2745
HIGH HUTTON 2	Hydrocarbon Well	SE76NW/169	18455717	473600	469120	1253
WHITWELL ON THE HILL 1	Hydrocarbon Well	SE76NW/8	125660	472780	465760	2008
BARTON 1	Hydrocarbon Well	SE76SW/22	125862	472199	464674	1573
MALTON 1	Hydrocarbon Well	SE77NE/13	125945	479982	475778	1935
MALTON 2	Hydrocarbon Well	SE77NE/14	125946	476100	476100	1591
MALTON 3	Hydrocarbon Well	SE77NE/15	125947	479990	475992	1722
MALTON 4	Hydrocarbon Well	SE77NE/16	125948	476127	476797	2072
KIRBY MISPERTON 1	Hydrocarbon Well	SE77NE/17	125949	477105	478933	3421
KIRBY MISPERTON 2	Hydrocarbon Well	SE77NE/18	125950	476331	479261	1761
KIRBY MISPERTON 3	Hydrocarbon Well	SE77NE/19	125951	477108	478943	1837
KIRBY MISPERTON 4	Hydrocarbon Well	SE77NE/63	19393807	476331	479261	1755

KIRBY MISPERTON 5	Hydrocarbon Well	SE77NE/64	19407253	476340	479254	1972
KIRBY MISPERTON 6	Hydrocarbon Well	SE77NE/65	19407254	476366	479218	1493
PICKERING 1	Hydrocarbon Well	SE78SE/14	126173	479658	482158	2046
PICKERING 2	Hydrocarbon Well	SE78SE/84	99991111	479673	482161	2284
BUTTERWICK 1	Hydrocarbon Well	SE80NW/1	131525	484210	405630	1700
ALTHORPE1	Hydrocarbon Well	SE80NW/100	18407556	481398	409417	1319
BURTON-ON-STATHER 1	Hydrocarbon Well	SE81NE/2	131735	487865	418829	1858
LUDDINGTON 1	Hydrocarbon Well	SE81SW/95	18538083	482617	414407	1295
BROOMFLEET 1	Hydrocarbon Well	SE82NE/10	132161	489324	427706	2024
NEWPORT 1	Hydrocarbon Well	SE82NE/17	18407553	485704	429309	1207
ALKBOROUGH 1	Hydrocarbon Well	SE82SE/3	132197	488345	422644	1999
SOUTH CLIFFE 1	Hydrocarbon Well	SE83NE/8	132253	487911	435220	1070
POCKLINGTON 1	Hydrocarbon Well	SE84NW/26	132370	481658	449925	1082
DUGGLEBY 1	Hydrocarbon Well	SE86NE/3	132562	488950	465049	3058
BURDALE P3	Hydrocarbon Well	SE86SE/8	18201310	487957	461790	47
MARISHES 1	Hydrocarbon Well	SE87NW/30	132690	482070	475803	1879
Marishes 2	Hydrocarbon Well	SE87NW/44	19204459	482070	475803	1657
MARISHES 2Z	Hydrocarbon Well	SE87NW/45	19204460	482070	475803	1729
Marishes 3	Hydrocarbon Well	SE87NW/47	19436878	482070	475803	1503
HIBALDSTOW 1	Hydrocarbon Well	SE90SE/112	133438	498943	403924	1879
WRESSLE 1	Hydrocarbon Well	SE91SE/139	125320	496770	411106	2240
BROUGHTON B1	Hydrocarbon Well	SE91SW/456	134540	494627	410760	1920
CROSBY WARREN 1	Hydrocarbon Well	SE91SW/457	134541	491219	412872	1854
CROSBY WARREN 2	Hydrocarbon Well	SE91SW/465	134549	491187	412908	2050
CROSBY WARREN 3	Hydrocarbon Well	SE91SW/501	134585	491192	412922	1707
CROSBY WARREN 3Z	Hydrocarbon Well	SE91SW/502	134586	491192	412922	1780
TOP PLANTATION	Hydrocarbon Well	SE93SE/80	18201343	495902	430411	120
NORTH DALTON 1	Hydrocarbon Well	SE95SW/6	135318	493815	452770	1699
LANGTOFT 1	Hydrocarbon Well	SE96NE/4	135324	499340	465196	1993
BRIGG 1	Hydrocarbon Well	TA00NW/122	456311	503370	406391	1933
BRIGG 2	Hydrocarbon Well	TA00NW/123	456312	503770	406390	1991
GLANFORD 1	Hydrocarbon Well	TA00NW/124	456313	501745	407278	2012
GLANFORD 1Y	Hydrocarbon Well	TA00NW/126	456315	501745	407278	2059
GLANFORD 1Z	Hydrocarbon Well	TA00NW/127	456316	501745	407278	1920
RISBY 1	Hydrocarbon Well	TA03NW/83	458615	501057	435778	1504
RUDSTON 1	Hydrocarbon Well	TA06NE/15	459977	509340	466320	2514

FORDON 1	Hydrocarbon Well	TA07NE/1	460083	505830	475710	2303
FORDON 2	Hydrocarbon Well	TA07SE/19	460181	506890	473604	2445
DALE FARM	Hydrocarbon Well	TA14NW/58	18201314	510119	447902	75
GREAT HATFIELD 1	Hydrocarbon Well	TA14SE/10	463623	518999	443278	2298
ATWICK 4	Hydrocarbon Well	TA15SE/11	463704	517260	451770	1861
ATWICK 9	Hydrocarbon Well	TA15SE/43	463736	518670	452020	1915
HORNSEA 1	Hydrocarbon Well	TA15SE/8	463701	518460	450620	2060
ATWICK 2	Hydrocarbon Well	TA15SE/9	463702	518350	451710	1902
CAYTHORPE 1	Hydrocarbon Well	TA16NW/10	463900	512222	467920	2067
CAYTHORPE 2	Hydrocarbon Well	TA16NW/13	463903	511069	467737	2316
BARMSTON 1	Hydrocarbon Well	TA16SE/5	463913	515455	460622	1954
BURTON AGNES 1	Hydrocarbon Well	TA16SW/36	18275481	512274	461985	2290
HUNMANBY 1	Hydrocarbon Well	TA17NW/10	463974	513010	475880	2252
WILLOWS 1	Hydrocarbon Well	TA17SW/24	18126679	512027	474868	2405
WINESTEAD 1	Hydrocarbon Well	TA22SE/7	466012	527410	424334	2003
CLEETHORPES 1	Hydrocarbon Well	TA30NW/51	466355	530237	407090	2100

### 1.1.2 The Weald

Name	PURPOSE	SOBI	BGS ID	EASTING	NORTHING	TD
CROCKERHILL 1	Hydrocarbon Well	SU50NE/201	415305	458320	109740	2145
LEE-ON-SOLENT 1	Hydrocarbon Well	SU50SE/51	415902	457430	101150	2085
LOMER 1	Hydrocarbon Well	SU52SE/18	416722	459587	123564	2115
HOOK LANE 1	Hydrocarbon Well	SU55SE/20	417381	457535	153872	1328
PORTSDOWN 1	Hydrocarbon Well	SU60NW/76	420261	463800	106520	1998
POTWELL 1	Hydrocarbon Well	SU60NW/83	420268	463990	107731	2128
HORNDEAN 4	Hydrocarbon Well	SU61SE/82	421436	466298	113464	2065
HINTON MANOR 1	Hydrocarbon Well	SU61SE/83	421437	467951	114885	2094
OLD ALRESFORD 1	Hydrocarbon Well	SU63NW/20	421745	462448	137078	1638
HERRIARD 1	Hydrocarbon Well	SU64NE/11	421870	467876	146551	1556
HERRIARD 2	Hydrocarbon Well	SU64NE/12	421871	465780	146730	1521
INWOOD COPSE 1	Hydrocarbon Well	SU64NW/49	421922	461098	146373	1951
FARLEIGH WALLOP 1	Hydrocarbon Well	SU64NW/50	421923	463212	147031	1683
HUMBLY GROVE C1	Hydrocarbon Well	SU64SE/18	421959	469620	144870	1322
HUMBLY GROVE C3 (P3)	Hydrocarbon Well	SU64SE/19	421960	469621	144876	1353
HUMBLY GROVE C2	Hydrocarbon Well	SU64SE/21	421962	469619	144869	1453
CLANFIELD 1	Hydrocarbon Well	SU71NW/3	425829	471324	116541	2012

MARKWELLS WOOD	Hydrocarbon Well	SU71SE/32	18715554	475819	113270	1825
HORNDEAN 1A (X1)	Hydrocarbon Well	SU71SW/59B	425930	471537	112602	2013
HORNDEAN 2	Hydrocarbon Well	SU71SW/60	425932	472620	112240	1594
HORNDEAN 3	Hydrocarbon Well	SU71SW/61	425933	470550	112530	1828
BORDON 1	Hydrocarbon Well	SU73NE/48	426155	478853	136423	2447
EAST WORLDHAM	Hydrocarbon Well	SU73NW/28	426248	474061	137568	2351
HUMBLY GROVE A3 (S2)	Hydrocarbon Well	SU74NW/10	426389	470538	145304	1417
HUMBLY GROVE A4 (G1 1)	Hydrocarbon Well	SU74NW/11	426390	470532	145291	1334
HUMBLY GROVE A5 (H1)	Hydrocarbon Well	SU74NW/12	426391	470527	145281	1451
HUMBLY GROVE A6 (G2)	Hydrocarbon Well	SU74NW/16	426395	470527	145281	1446
HUMBLY GROVE 2	Hydrocarbon Well	SU74NW/5	426384	470530	145280	1506
HUMBLY GROVE 3	Hydrocarbon Well	SU74NW/6	426385	472610	145190	1610
HESTERS COPSE	Hydrocarbon Well	SU74NW/8	426387	473547	146241	1577
HUMBLY GROVE A10	Hydrocarbon Well	SU74NW/88	18276657	470535	145298	1506
HUMBLY GROVE A12	Hydrocarbon Well	SU74NW/89	18276658	470538	145304	1601
HUMBLY GROVE A11	Hydrocarbon Well	SU74NW/90	18276659	470524	145271	1628
HUMBLY GROVE A14	Hydrocarbon Well	SU74NW/91	18292616	470534	145294	1807
HUMBLY GROVE A15	Hydrocarbon Well	SU74NW/92	18689076	470534	145294	1929
HUMBLY GROVE 1	Hydrocarbon Well	SU74SW/1	426525	471150	144840	1528
HUMBLY GROVE X2 (G1)	Hydrocarbon Well	SU74SW/11	426535	471151	144830	1966
HUMBLY GROVE X4 (H3)	Hydrocarbon Well	SU74SW/12	426536	471150	144819	1590
HUMBLY GROVE X5 (H4)	Hydrocarbon Well	SU74SW/13	426537	471151	144834	1824
HUMBLY GROVE X3 (L2)	Hydrocarbon Well	SU74SW/14	426538	471151	144830	1347
ODIHAM 1	Hydrocarbon Well	SU75SW/99	426906	473917	150479	1439
SINGLETON X11	Hydrocarbon Well	SU81NE/28	18689063	488411	115419	2846
SINGLETON X9	Hydrocarbon Well	SU81NE/31	18815337	488411	115419	2996
SINGLETON X12	Hydrocarbon Well	SU81NE/32	19199774	488402	115455	1718
SINGLETON X12V	Hydrocarbon Well	SU81NE/33	19199777	488402	115455	2168

SINGLETON X12W	Hydrocarbon Well	SU81NE/34	19199778	488402	115455	2772
SINGLETON X12X	Hydrocarbon Well	SU81NE/35	19199779	488402	115455	3807
SINGLETON X12Y	Hydrocarbon Well	SU81NE/36	19199781	488402	115455	3811
SINGLETON X12Z	Hydrocarbon Well	SU81NE/37	19199784	488402	115455	2743
CHILGROVE 1	Hydrocarbon Well	SU81SW/16	430268	481876	113725	2142
ROGATE 1	Hydrocarbon Well	SU82NW/16	430298	480342	126314	2146
MINSTED 1	Hydrocarbon Well	SU82SW/26	430378	484867	120287	2128
COXBRIDGE 1	Hydrocarbon Well	SU84NW/60	431078	482306	146066	2124
MIDDLETON 1	Hydrocarbon Well	SU90SE/5	434383	497394	101505	2124
LIDSEY 1	Hydrocarbon Well	SU90SW/58	434489	494443	103401	1173
BAXTERS COPSE 1	Hydrocarbon Well	SU91NW/10	434555	491496	117731	2365
GODLEY BRIDGE 1	Hydrocarbon Well	SU93NE/21	434721	495230	136636	2584
SHALFORD 1	Hydrocarbon Well	SU94NE/2	434799	498210	146800	1743
BRAMLEY 1	Hydrocarbon Well	SU94NE/74	434872	499560	145609	1147
NORMANDY 1	Hydrocarbon Well	SU94NW/25	434954	491649	149980	1358
STRAT A1	Hydrocarbon Well	SU95SW/5	435538	494780	152780	963
PAGHAM 1	Hydrocarbon Well	SZ89NE/5	456073	488408	98034	1076
STORRINGTON 1	Hydrocarbon Well	TQ01SE/27	570390	506868	114892	2084
ALFOLD 1	Hydrocarbon Well	TQ03SW/5	570473	504337	134437	1256
ALBURY 2Z	Hydrocarbon Well	TQ04NE/101	18621042	506184	147198	4608
ALBURY 1	Hydrocarbon Well	TQ04NE/46	570576	506182	147192	1845
ASHINGTON 1	Hydrocarbon Well	TQ11NW/25	578054	512750	118230	1723
HENFIELD 1	Hydrocarbon Well	TQ11SE/9	578223	517990	114570	1556
WASHINGTON 1	Hydrocarbon Well	TQ11SW/50	578165	510899	110936	1439
SOUTHWATER 1	Hydrocarbon Well	TQ12NE/94	578414	516736	125587	2342
BROCKHAM 1	Hydrocarbon Well	TQ14NE/95	578836	518832	148653	2176
WINEHAM 1	Hydrocarbon Well	TQ21NW/13	584202	523478	118851	1824
BOLNEY 1	Hydrocarbon Well	TQ22SE/17	584588	528011	124269	2440
COLLENDEAN FARM 1	Hydrocarbon Well	TQ24SW/1	584866	524800	144290	1755
LOWER KINGSWOOD 1	Hydrocarbon Well	TQ25SE/286	585890	526200	152920	2188
STANMER 1	Hydrocarbon Well	TQ31SW/13	594545	532631	111423	1343
WESTMESTON 1	Hydrocarbon Well	TQ31SW/14	594546	534065	114749	1547
BALCOMBE 1	Hydrocarbon Well	TQ32NW/5	594587	531031	129242	1725
BALCOMBE 2	Hydrocarbon Well	TQ32NW/74	19380505	531021	129243	829
BALCOMBE 2Z	Hydrocarbon Well	TQ32NW/75	19380506	531021	129243	1344
TURNERS HILL	Hydrocarbon Well	TQ33NE/4	594770	535792	135116	1416
BLETCHINGLEY 1	Hydrocarbon Well	TQ34NE/9	594989	536225	147727	1853
BLETCHINGLEY 5	Hydrocarbon Well	TQ34NW/148	18024798	534721	147995	2458
PALMERS WOOD 5	Hydrocarbon Well	TQ35SE/106	595843	537508	152679	1286

PALMERS WOOD 7	Hydrocarbon Well	TQ35SE/248	595985	536446	152624	1263
PALMERS WOOD 1	Hydrocarbon Well	TQ35SE/94	595831	536445	152623	1458
PALMERS WOOD 2	Hydrocarbon Well	TQ35SE/95	595832	536445	152622	1394
RINGMER 1	Hydrocarbon Well	TQ41SE/17	638577	547936	114823	1387
HOLTYE 1 (A)	Hydrocarbon Well	TQ43NW/6	619766	544743	139773	2207
EDEN BRIDGE 1	Hydrocarbon Well	TQ44NW/4	606495	542254	147333	1822
COWDEN 1	Hydrocarbon Well	TQ44SE/1	607394	546680	142778	1840
TATSFIELD 1	Hydrocarbon Well	TQ45NW/5	621099	542420	156990	1405
PALMERS WOOD 4	Hydrocarbon Well	TQ45SW/115	760523	541188	154031	1140
HELLINGLY 2	Hydrocarbon Well	TQ51SE/19	640269	558872	114656	981
ASHDOWN 2	Hydrocarbon Well	TQ52NW/12	624146	551070	129240	1740
ROTHERFIELD 1	Hydrocarbon Well	TQ52NW/16	624150	551850	126249	1447
HEATHFIELD 7	Hydrocarbon Well	TQ52SE/7	621327	558590	121490	271
ASHDOWN 1	Hydrocarbon Well	TQ53SW/3	614078	550050	130350	1383
ASHOUR 1	Hydrocarbon Well	TQ54SE/67	1097251	556400	144239	1646
SHIPBOURNE 1	Hydrocarbon Well	TQ55SE/9	611072	557290	152025	1693
WESTHAM 1	Hydrocarbon Well	TQ60NW/13	654060	560970	105350	1597
WALLCROUCH 1	Hydrocarbon Well	TQ62NE/3	616829	566058	129779	1493
BRIGHTLING 1	Hydrocarbon Well	TQ62SE/1	686828	567250	121820	1505
DETENTION 1	Hydrocarbon Well	TQ74SW/4	608607	574781	140200	1172
IDEN GREEN 1	Hydrocarbon Well	TQ83SW/1	608588	581350	131570	1087
LITTLE DUSKIN 1	Coal Authority Well	TR14NE/4	615361	617989	149650	702
PADDLESWORTH COURT	Coal Authority Well	TR14SE/3	612565	619904	140410	1141
GOLGOTHA 1	Coal Authority Well	TR24NE/6	629013	627182	149214	1129
WOOLAGE FARM 1	Coal Authority Well	TR24NW/4	621376	624005	149735	1040
Meggat Farm	Coal Authority Well	TR24SE/10	645037	625446	141066	1349
Swanton Court Farm	Coal Authority Well	TR24SW/2	615480	623865	144309	1263
BARNSOLE	Coal Authority Well	TR25NE/122	743655	628246	156781	836
EASTLING WOOD	Coal Authority Well	TR34NW/3	621349	630330	147290	1270
TOLL GATE	Coal Authority Well	TR35NE/2	607375	635581	157140	518
NORTHWALL ROAD 1	Coal Authority Well	TR35SE/22	647267	636810	153560	279
LITTLE MONGEHAM	Coal Authority Well	TR35SW/22	656571	633652	151463	761
NORTHBOURNE	Coal Authority Well	TR35SW/23	656572	632679	151856	833
VENSON	Coal Authority Well	TR35SW/24	656573	630688	152766	863

### 1.1.3 Cheshire and Lancashire

Name	Purpose	SOBI	BGS ID	EASTING	NORTHING	TD
FORMBY 4	Hydrocarbon Well	SD20NE/1	1	328220	407480	1183

FORMBY 5	Hydrocarbon Well	SD21SE/1	67	329730	412460	1327
FORMBY 6	Hydrocarbon Well	SD30NW/1	101	330183	408977	1614
FORMBY EAST 1	Hydrocarbon Well	SD30NW/134	18968198	332412	408435	170
FORMBY 7	Hydrocarbon Well	SD30NW/135	19361075	331936	408270	138
LITTLE CROSBY 1	Hydrocarbon Well	SD30SW/46	503	332585	401299	1141
BANKS 1	Hydrocarbon Well	SD32SE/8	1405	338927	421042	2170
THISTLETON 1	Hydrocarbon Well	SD33NE/17	1427	339760	437000	2140
Grange Hill 1Z	Hydrocarbon Well	SD33NE/37	19341129	339179	438938	3266
Preese Hall 1	Hydrocarbon Well	SD33NE/38	19341130	337531	436627	2789
ANNA'S ROAD 1	Hydrocarbon Well	SD33SE/37	19851006	335374	430979	632
HESKETH 1	Hydrocarbon Well	SD42NW/6	4392	343001	425197	1295
BECCONSALL 1Z	Hydrocarbon Well	SD42SW/11	19346066	340636	422976	3213
ELSWICK 1	Hydrocarbon Well	SD43NW/15	1889	342380	436965	1615
RHUDDLAN 1	Hydrocarbon Well	SJ07NW/28	696145	301859	377303	1143
POINT OF AYR 3	Coal Authority Well	SJ08NE/1	17499344	309894	387424	446
POINT OF AYR 1	Coal Authority Well	SJ18NW/18	17499334	311492	386947	373
POINT OF AYR 2	Coal Authority Well	SJ18NW/19	17499342	310590	388402	560
POINT OF AYR 4	Coal Authority Well	SJ18NW/20	17499352	312938	388283	896
POINT OF AYR 5	Coal Authority Well	SJ18NW/21	17499357	310632	386888	515
POINT OF AYR 6	Coal Authority Well	SJ18NW/22	17499359	311706	387885	546
MOSTYN QUAY 1	Hydrocarbon Well	SJ18SE/22	18357132	315636	380921	243
Liverpool Bay	Hydrocarbon Well	SJ29NW/1	18292600	322632	396984	2085
BLACON	Coal Authority Well	SJ36NE/22	155899	336825	367728	857
BLACON EAST 1	Hydrocarbon Well	SJ36NE/23	155900	337890	366860	2266
BLACON WEST 1	Hydrocarbon Well	SJ36NE/24	155901	336617	366341	1339
SEALAND 1 (YEW TREE FARM)	Hydrocarbon Well	SJ36NE/53	155930	336760	368160	1074
ECCLESTONE	Coal Authority Well	SJ36SE/17	156621	337465	364176	739
SHOTWICK	Coal Authority Well	SJ37SW/10	157271	333232	371908	702
INCE MARSHES 1	Hydrocarbon Well	SJ47NE/100	19206308	346211	376439	1577
KEMIRA 1	Hydrocarbon Well	SJ47NE/101	19411190	347595	376550	1438
MORLEY BRIDGE	Coal Authority Well	SJ47SE/15	163544	346181	371455	1217
COLLINGE	Coal Authority Well	SJ47SW/23	163603	341429	371112	1362
GREENBRIDGE	Coal Authority Well	SJ48NE/432	164207	346640	385530	758

CRONTON 1	Hydrocarbon Well	SJ48NE/487	18871155	346690	388510	657
CRONTON 2	Hydrocarbon Well	SJ48NE/488	18871156	346561	389233	447
DITTON	Coal Authority Well	SJ48NE/7	163782	349750	386910	900
FOXHILL FARM 1	Hydrocarbon Well	SJ48NW/210	18357142	344532	386962	642
HALE	Coal Authority Well	SJ48SE/18	164424	347077	383134	1156
Levels Hall	Coal Authority Well	SJ48SE/201	164607	347964	384935	1095
BLUNDELL'S HILL	Coal Authority Well	SJ49SE/72	165701	348630	390509	223
CROXTETH 1	Hydrocarbon Well	SJ49SW/5	165928	340310	394270	1285
CROXTETH 2	Hydrocarbon Well	SJ49SW/6	165929	340440	394510	799
DOE GREEN 1	Hydrocarbon Well	SJ58NE/1616	18274419	355011	387959	1394
DOE GREEN 2	Hydrocarbon Well	SJ58NE/1617	18275432	355011	387959	1318
DOE GREEN 3	Hydrocarbon Well	SJ58NE/1639	19206293	355014	387967	1271
DOE GREEN 3T	Hydrocarbon Well	SJ58NE/1641	19206295	355014	387967	1079
DOE GREEN 3U	Hydrocarbon Well	SJ58NE/1642	19206296	355014	387967	1239
DOE GREEN 3V	Hydrocarbon Well	SJ58NE/1643	19206297	355014	387967	1207
DOE GREEN 3W	Hydrocarbon Well	SJ58NE/1644	19206298	355014	387967	1124
DOE GREEN 3Y	Hydrocarbon Well	SJ58NE/1645	19206299	355014	387967	1024
DOE GREEN 3Z	Hydrocarbon Well	SJ58NE/1646	19206300	355014	387967	1045
PENKETH	Coal Authority Well	SJ58NW/40	168324	354723	388975	975
HEATH SIDE	Coal Authority Well	SJ58NW/476	168762	354140	389400	912
HAYFIELD FARM	Coal Authority Well	SJ58NW/477	168763	354321	388514	1132
FOUR OAK	Coal Authority Well	SJ58NW/71	168357	354586	387095	1150
BARROWS GREEN	Coal Authority Well	SJ58NW/72	168358	353219	387928	934
SOUTH LANE	Coal Authority Well	SJ58NW/723	16098768	353710	388630	948
FOUROAK 1	Hydrocarbon Well	SJ58NW/752	19488357	354491	387787	1216
JACKLEGS	Coal Authority Well	SJ59SE/49	171293	357617	391651	1103
Dollys Bridge	Coal Authority Well	SJ69NW/108	761783	361991	395730	766
BIRCHWOOD	Coal Authority Well	SJ69SW/1399	945047	364381	390995	1527
Fearnhead	Coal Authority Well	SJ69SW/50	943687	362720	390200	1413
Longford	Coal Authority Well	SJ69SW/51	943688	360330	390010	1261
Eaves Brow	Coal Authority Well	SJ69SW/52	943689	363620	392540	1207
BROOKHOUSE	Coal Authority Well	SJ69SW/55	943692	364475	394132	1437
Houghton Green	Coal Authority Well	SJ69SW/64	943712	362131	391574	1311

## 1.2 Wells with Stress field information

Wells with information used to categorise the UK onshore stress field, see Glossary for definitions of abbreviations.

Name	Purpose	SOBI	BGS ID	Easting	Northing	TD	PP Data	SHMax Orientation Data	SHMax Data	Sv Data	shmin Data
DOUNREAY 1	NIREX Site Characterisation Well	NC96NE/1	613396	298589	966923	1327		Borehole Imaging		Density Log Inversion	
SELLAFIELD 14A	NIREX Site Characterisation Well	NY00NW/451	875069	302488	505692	970		Borehole Imaging			
SELLAFIELD 2	NIREX Site Characterisation Well	NY00SE/28	656998	305554	503430	1610			HF	Density Log Inversion	
SELLAFIELD 5	NIREX Site Characterisation Well	NY00SE/30	657000	305168	503886	1260			HF		
SELLAFIELD 11A	NIREX Site Characterisation Well	NY00SE/34	657004	306792	501633	1170		Borehole Imaging			
SELLAFIELD RCF3	NIREX Site Characterisation Well	NY00SE/37	657007	305565	503932	990		Borehole Imaging			
SELLAFIELD 8A	NIREX Site Characterisation Well	NY00SE/38	657008	307209	504981	1000			HF		
SELLAFIELD 3	NIREX Site Characterisation Well	NY00SW/35	818356	302596	502650	1953		Borehole Imaging	HF		
SELLAFIELD 7A	NIREX Site Characterisation Well	NY00SW/36	818357	303857	504903	1010		Borehole Imaging			
SELLAFIELD 10A	NIREX Site Characterisation Well	NY00SW/38	818359	304312	503061	1607		Borehole Imaging	HF		
SELLAFIELD 12A	NIREX Site Characterisation Well	NY00SW/39	818360	304933	502644	1150		Borehole Imaging			
SELLAFIELD 10B	NIREX Site Characterisation Well	NY00SW/40	818361	304268	503080	252			OC		
SELLAFIELD 13A	NIREX Site Characterisation Well	NY00SW/41	818362	304521	500146	1740		Borehole Imaging			
BECKLEES 2	Hydrocarbon Well	NY37SE/19	18530580	335163	571557	1386		Borehole Imaging			
FORMBY EAST 1	Hydrocarbon Well	SD30NW/134	18968198	332412	408435	170					FIT
FORMBY 7	Hydrocarbon Well	SD30NW/135	19361075	331936	408270	138					FIT
LITTLE CROSBY 1	Hydrocarbon Well	SD30SW/46	503	332585	401299	1141					FIT
Grange Hill 1Z	Hydrocarbon Well	SD33NE/37	19341129	339179	438938	3266					FIT
Preese Hall 1	Hydrocarbon Well	SD33NE/38	19341130	337531	436627	2789		Calc	Calc		FIT
HESKETH 1	Hydrocarbon Well	SD42NW/6	4392	343001	425197	1295					FIT
BECCONSALL 1Z	Hydrocarbon Well	SD42SW/11	19346066	340636	422976	3213					FIT

ELSWICK 1	Hydrocarbon Well	SD43NW/15	1889	342380	436965	1615	DST					FIT
Wray	Geothermal Well	SD66NW/5	18294	363200	465700	304		HF	HF			
ARKSEY COMMON	Coal Authority Well	SE50NE/40	115042	459722	407264	653					Density Log Inversion	
Gateforth New Road	Coal Authority Well	SE52NE/25	116857	457220	429564	378		Borehole Imaging				
BISHOP WOOD 6	Coal Authority Well	SE53SE/26	118151	456355	433757	291		HF	HF			
HATFIELD WEST 1	Hydrocarbon Well	SE60NE/68	120019	467656	406041	479						FIT
HATFIELD MOORS 4	Hydrocarbon Well	SE60NE/75	120026	468972	406259	694						LOT
Trumfleet 4	Hydrocarbon Well	SE61SW/104	19370644	460550	411910	1158						FIT
TRUMFLEET 6	Hydrocarbon Well	SE61SW/98	18062904	460561	411925	1158						FIT
MILL FARM 1	Hydrocarbon Well	SE62SE/263	18275472	467930	422155	830						FIT
WHELDRAKE 1	Hydrocarbon Well	SE64NE/4	122640	467660	446082	1558					Density Log Inversion	
Howden Dike	Coal Authority Well	SE64NW/202	122854	461723	446080	923		Borehole Imaging	HF		Density Log Inversion	
East Lodge	Coal Authority Well	SE64SE/20	122964	469019	440612	1138		Borehole Imaging	HF			
TOWTHORPE	Coal Authority Well	SE65NW/23	123204	461824	459071	1198					Density Log Inversion	
SANDTOFT	Coal Authority Well	SE70NW/13	124529	474590	409206	1025					Density Log Inversion	
HATFIELD MOORS 3	Hydrocarbon Well	SE70NW/17	124533	470380	406670	1828	RFT					FIT
SWINEFLEET 1	Hydrocarbon Well	SE71NE/10	18407548	479243	419793	1319		Borehole Imaging				FIT
EALAND 1	Hydrocarbon Well	SE71SE/38	19199843	476914	410614	1231						FIT
LAXTON	Coal Authority Well	SE72NE/9	124831	478195	425699	1150					Density Log Inversion	
SEATON ROSS 1	Hydrocarbon Well	SE73NE/4	125283	477014	438593	1036					Density Log Inversion	
Derwent Bridge	Coal Authority Well	SE73NW/11	125300	470890	436103	1060		Borehole Imaging				
SPALDINGTON 1	Hydrocarbon Well	SE73SE/6	125310	479275	432455	1850						LOT
MELBOURNE 1	Hydrocarbon Well	SE74SE/23	18405086	476315	443088	1477		Borehole Imaging	Calc			FIT
HIGH HUTTON 1	Hydrocarbon Well	SE76NW/14	125667	474423	469412	2745						FIT
HIGH HUTTON 2	Hydrocarbon Well	SE76NW/169	18455717	473600	469120	1253						LOT
BARTON 1	Hydrocarbon Well	SE76SW/22	125862	472199	464674	1573					Density Log Inversion	
MALTON 4	Hydrocarbon Well	SE77NE/16	125948	476127	476797	2072						LOT
KIRBY MISPERTON 1	Hydrocarbon Well	SE77NE/17	125949	477105	478933	3421						FIT
KIRBY MISPERTON 2	Hydrocarbon Well	SE77NE/18	125950	476331	479261	1762	RFT					LOT



DOE GREEN 1	Hydrocarbon Well	SJ58NE/1616	18274419	355011	387959	1394				Density Log Inversion	FIT
DOE GREEN 2	Hydrocarbon Well	SJ58NE/1617	18275432	355011	387959	1318					FIT
DOE GREEN 3	Hydrocarbon Well	SJ58NE/1639	19206293	355014	387967	1271					FIT
Washdale Lane No.3	Coal Authority Well	SJ83NE/283	781403	386693	336257	644		Borehole Imaging			
Bank	Coal Authority Well	SJ91NE/101	17499257	398527	318291	632		Borehole Imaging			
Deerlawn	Coal Authority Well	SJ91NE/102	17499307	398487	319778	691		Borehole Imaging			
Dry Pits No.5	Coal Authority Well	SJ91NE/106	17499318	396262	319330	680		Borehole Imaging			
Quarry Littleton	Coal Authority Well	SJ91NE/108	17499363	397820	318957	766		Borehole Imaging			
SLEES	Coal Authority Well	SJ91NE/109	181881	398847	319531	613		Borehole Imaging			
Ansons Bank	Coal Authority Well	SJ91NE/83	181932	397904	317170	621		Borehole Imaging			
Chase Road	Coal Authority Well	SJ91NE/84	181933	398093	318670	723		Borehole Imaging			
Harts	Coal Authority Well	SJ92SE/34	182785	398099	320199	823		Borehole Imaging			
Stepping Stones	Coal Authority Well	SJ92SE/47	17499398	398743	320097	622		Borehole Imaging			
Lysways No.1	Coal Authority Well	SK01SE/29	190714	408727	313785	835		Borehole Imaging			
BEN BROOK	Coal Authority Well	SK01SE/52	17101712	408600	312680	878		Borehole Imaging			
LYSWAYS LODGE	Coal Authority Well	SK01SE/54	17101721	409141	312610	851		Borehole Imaging			
Bilson Brook	Coal Authority Well	SK01SE/55	17156094	409647	313962	787		Borehole Imaging			
Borough Lane	Coal Authority Well	SK01SE/56	17156095	407406	313612	860		Borehole Imaging			
Smithy Lane	Coal Authority Well	SK01SE/57	190231	407779	313806	862		Borehole Imaging			
MORLEY QUARRY 1	Geothermal Well	SK41NE/30	216505	447650	317870	836		HF	HF		
AYLESFORD COVERT	Coal Authority Well	SK62SE/25	232827	467553	320791	584		Borehole Imaging			
WINDY RIDGE	Coal Authority Well	SK62SE/28	232830	468250	321748	634		Borehole Imaging			
THE SALTWAY	Coal Authority Well	SK62SE/31	232833	467486	321696	589		Borehole Imaging			
Mattersey Quarry	Coal Authority Well	SK68NE/53	235848	468280	387871	1048		Borehole Imaging			
Fishponds Asfordby	Coal Authority Well	SK72SW/101	238306	470183	321859	746		Borehole Imaging			
Back Lane Plugnar	Coal Authority Well	SK73SE/65	238530	476255	332789	731		HF	HF		
WESTWOOD FARM	Coal Authority Well	SK76NW/46	239484	470055	367304	903		Borehole Imaging			
DANIELS WOOD	Coal Authority Well	SP28NW/258	318103	424670	285832	889		HF	HF		
WALL HILL	Coal Authority Well	SP28SE/136	318335	429624	283864	857		HF	HF		
COXBRIDGE 1	Hydrocarbon Well	SU84NW/60	431078	482306	146066	2124				Density Log Inversion	
BAXTERS COPSE 1	Hydrocarbon Well	SU91NW/10	434555	491496	117731	2365				Density Log Inversion	

GODLEY BRIDGE 1	Hydrocarbon Well	SU93NE/21	434721	495230	136636	2584				Density Log Inversion	
NORMANDY 1	Hydrocarbon Well	SU94NW/25	434954	491649	149980	1358				Density Log Inversion	
CARWYNNEN AEC8	Geothermal Well	SW63NE/44	689097	165849	36609	703		HF	HF		
Rosemanowes Quarry RH15	Geothermal Well	SW73SW/11	625306	173555	34590	2610		HF	HF		
BRIGG 1	Hydrocarbon Well	TA00NW/122	456311	503777	406391	1933					LOT
BRIGG 2	Hydrocarbon Well	TA00NW/123	456312	503770	406390	1991					LOT
GLANFORD 1	Hydrocarbon Well	TA00NW/124	456313	501745	407278	2012	RFT				FIT
RISBY 1	Hydrocarbon Well	TA03NW/83	458615	501057	435778	1504				Density Log Inversion	
RUDSTON 1	Hydrocarbon Well	TA06NE/15	459977	509340	466320	2514					LOT
CAYTHORPE 1	Hydrocarbon Well	TA16NW/10	463900	512222	467920	2067					FIT
CAYTHORPE 2	Hydrocarbon Well	TA16NW/13	463903	511069	467737	2316	RFT				
BURTON AGNES 1	Hydrocarbon Well	TA16SW/36	18275481	512274	461985	2290					FIT
WILLOWS 1	Hydrocarbon Well	TA17SW/24	18126679	512027	474868	2405					FIT
STORRINGTON 1	Hydrocarbon Well	TQ01SE/27	570390	506868	114892	2084				Density Log Inversion	
ALFOLD 1	Hydrocarbon Well	TQ03SW/5	570473	504337	134437	1256				Density Log Inversion	
ALBURY 1	Hydrocarbon Well	TQ04NE/46	570576	506182	147192	1845				Density Log Inversion	
WESTMESTON 1	Hydrocarbon Well	TQ31SW/14	594546	534065	114749	1547				Density Log Inversion	
BALCOMBE 1	Hydrocarbon Well	TQ32NW/5	594587	531031	129242	1725				Density Log Inversion	
TURNERS HILL	Hydrocarbon Well	TQ33NE/4	594770	535792	135116	1416				Density Log Inversion	
PALMERS WOOD 1	Hydrocarbon Well	TQ35SE/94	595831	536445	152623	1458				Density Log Inversion	
RINGMER 1	Hydrocarbon Well	TQ41SE/17	638577	547936	114823	1387				Density Log Inversion	
HOLTYE 1 (A)	Hydrocarbon Well	TQ43NW/6	619766	544743	139773	2207				Density Log Inversion	
HELLINGLY 2	Hydrocarbon Well	TQ51SE/19	640269	558872	114656	981				Density Log Inversion	
ROTHERFIELD 1	Hydrocarbon Well	TQ52NW/16	624150	551850	126249	1447				Density Log Inversion	
ASHOUR 1	Hydrocarbon Well	TQ54SE/67	1097251	556400	144239	1646				Density Log Inversion	
DETENTION 1	Hydrocarbon Well	TQ74SW/4	608607	574781	140200	1172				Density Log Inversion	
IDEN GREEN 1	Hydrocarbon Well	TQ83SW/1	608588	581350	131570	1087				Density Log Inversion	

### 1.3 Stress field information from Mines and Quarries

Legacy information from mines and quarries used to characterise the UK onshore stress field.

Name	Purpose	Easting	Northing	SHMax Orientation Data	SHMax Data
ASFORDBY	Mine/Quarry	472818	320970	OC	OC
BOLSOVER	Mine/Quarry	446312	369271	OC	OC
COVENTRY	Mine/Quarry	430400	282790	OC	OC
Gartur	Mine/Quarry	257400	698330	OC	OC
Holme Park Quarry	Mine/Quarry	353620	478550	OC	OC
LEA HALL	Mine/Quarry	430400	282790	OC	OC
NORTH SELBY	Mine/Quarry	464752	444388	OC	OC
PRINCE OF WALES	Mine/Quarry	448066	420741	OC	OC
South Crofty	Mine/Quarry	166913	40892	OC	OC
Spittal	Mine/Quarry	316790	954405	OC	OC
WELBECK	Mine/Quarry	457994	368433	OC	OC
WISTOW	Mine/Quarry	458968	435580	OC	OC

## Glossary

Unit / Abbreviation	Full Name
BGS	British Geological Survey
Calc	Calculation of $S_{HMax}$ from borehole breakouts and drilling induced tensile fractures.
CPS	Counts per second
DIF	Drilling induced tensile fracture
EOWR	End of well report
FIT	Formation integrity test
$gcm^{-3}$	Grams per cubic centimetre
HF	Hydraulic fracture measurement
Km	Kilometre
LOT	Leak off test
LT	Limit test
m	Metres
Mpa	Mega Pascals
$MPakm^{-1}$	Mega Pascals per kilometre
NERC	Natural Environment Research Council
OC	Overcoring measurement
$P_p$	Pore pressure

PPG	Pounds per gallon
psift <sup>-1</sup>	Pounds Per square inch per foot
RFT	Repeat Formation Tester
S <sub>HMax</sub>	Maximum Horizontal Stress
S <sub>hmin</sub>	Minimum Horizontal Stress
S <sub>v</sub>	Vertical Stress / Lithostatic Pressure
SOBI	Single Onshore Borehole Index
TVD BGL	True vertical depth below ground level
UCS	Unconfined Compressive Strength
UKGEO	UK Geoenergy Observatories Project
XLOT	Extended Leak off test

## References

Addis, M., Yassir, N., Willoughby, D. & Enever, J. 1998. Comparison off leak-off test and extended leakoff test data for stress estimation. SPE/ISRM Eurock'98, Trondheim, Norway.

Agostinelli, C and Lund, U. 2013. R package 'circular': Circular Statistics (version 0.4-7). URL <https://r-forge.r-project.org/projects/circular/>

Baptie, B. 2010. Seismogenesis and state of stress in the UK. *Tectonophysics*, 482 (1-4). 150-159. 10.1016/j.tecto.2009.10.006

Baker Hughes, 2011. Wellbore Failure Analysis and Geomechanical Modelling in the Bowland Shales, Blackpool, UK, GMI. Preliminary Technical Report. Cuadrilla Resources. Last Accessed 04-Feb-2017.

Barton, C.A. & Zoback, M. D. 1988. In-situ stress orientation and magnitude at the Fenton Geothermal Site, New Mexico, determined from wellbore breakouts. *Geophysical Research Letters*, 15, 467–470.

Becker, A., & Davenport, C. A., 2001. Contemporary in situ stress determination at three sites in Scotland and northern England, *Journal of Structural Geology*, 23, 407-419.

Bell, J. S. & Gough, D. I. 1979, Northeast-Southwest Compressive Stress. In: *Alberta: Evidence From Oil Wells*, *Earth and Planetary Science Letters*, 45, 475-482.

Bigby, D. N., Cassie, J. W. & Ledger, A. R., 1992. Absolute stress and stress change measurements in British Coal Measures. In: Hudson, J.A. (Ed.), *Rock Characterisation: Proceedings of the International Symposium on Rock Stress*. United Kingdom, Chester, pp. 390-395.

Brudy, M. & Zoback, M. D. 1999. Drilling-induced tensile wall-fractures: Implications for determination of in-situ stress orientation and magnitude. *International Journal of Rock Mechanics*, 36, 191-215.

- Chadwick, R. A. 1986. Extension Tectonics in the Wessex Basin, Southern England. *Journal of the Geological Society*, 143, 465-488.
- Chadwick, R. A. 1993. Aspects of Basin Inversion in Southern Britain. *Journal of the Geological Society*, 150, 311-322.
- Chadwick, R.A. Fault analysis of the Cheshire Basin, NW England. In: Meadows, N. S., Trueblood, S. E, Hardman, M. & Cowan, G. (eds), 1997, *Petroleum Geology of the Irish Sea and Adjacent Areas*, Geological Society Special Publication No. 124, pp. 297-313
- Chadwick, R.A., & Evans, D. J. 2005 *A seismic atlas of southern Britain : images of subsurface structure*. Nottingham, UK, British Geological Survey, 196pp. (British Geological Survey Occasional Publication, 7).
- Cooling, C. M., Hudson, J. A. & Tunbridge, L. W. 1988. In situ Rock Stresses and Their Measurement in the UK .2. Site Experiments and Stress-Field Interpretation. *International Journal of Rock Mechanics and Mining Sciences & Geomechanics Abstracts* 25(6): 371-382.
- Dickinson, G. 1953. Geological aspects of abnormal reservoir pressure in the Gulf Coast Louisiana. *Bulletin of the American Association of Petroleum Geologists*, 37, 410-432.
- Ellison, R. A. 1997. Observations of coal cleat in British coalfields. British Geological Survey Technical Report WA/97/58 (Keyworth: British Geological Survey.)
- Farmer, I. W. & Kemeny, J. M. 1992. Deficiencies in rock test data. In: Hudson, J.A. (ed), *Rock Characterisation: Proceedings of the International Symposium on Rock Stress*, Chester, United Kingdom, 298-303.
- Fraser, A. J. & Gawthorpe, R. L. Tectono-stratigraphic development and hydrocarbon habitat of the Carboniferous in northern England In: Hardman, R. F. P. & Brooks, J. (eds), 1990, *Tectonic Events Responsible for Britain's Oil and Gas Reserves*, Geological Society Special Publication No 55, pp 49-86.
- Hawkins, T. R. W. & Saul, L. G. H. 2003. Complex extensional faulting of Triassic rocks north of York, North Yorkshire, UK. *Proceedings of the Yorkshire Geological Society*, 54, 257-267.
- Heidbach, O., Rajabi, M., Reiter, K., Ziegler, M. & WSM Team (2016): World Stress Map Database Release 2016. GFZ Data Services. <http://doi.org/10.5880/WSM.2016.001>
- Hillis, R. 2000. Pore pressure/stress coupling and its implications for seismicity. *Exploration Geophysics*, 31, 448-454.
- Holford, S. P., Tassone, D. R., Stoker, M. S. & Hillis, R. R. 2016. Contemporary stress orientations in the Faroe-Shetland region. *Journal of the Geological Society*, 173, 142-152.
- Jones, N. S., Holloway, S., Creedy, D. P., Garner, K., Smith N. J. P., Browne, M. A. E. & Durucan S. 2004. UK Coal Resource for New Exploitation Technologies. Final Report. British Geological Survey Commissioned Report CR/04/015N.
- Kent, P. E. 1980. Subsidence and Uplift in East Yorkshire and Lincolnshire: A Double Inversion. *Proceedings of the Yorkshire Geological Society*, 42(28), 505-524.
- Kingdon, A, Fellgett, M. W. and Williams, J. D. O, 2016. Use of borehole imaging to improve understanding of the in-situ stress orientation of Central and Northern England and its implications

- for unconventional hydrocarbon resources. *Marine and Petroleum Geology*, 73, 1-20. DOI: 10.1016/j.marpetgeo.2016.02.012
- Kirby, G. A., and Swallow, P. W. 1987. Tectonism and sedimentation in the Flamborough Head region of north-east England. *Proceedings of the Yorkshire Geological Society*, 46, Part 4: 301-309.
- Kirby, G. A., Baily, H. E., Chadwick, R. A., Evans, D. J., Holliday, D. W., Holloway, S., Hulbert, A. G., Pharaoh, T. C., Smith, N. J. P., Aitkenhead, N. & Birch, B. 2000. The structure and evolution of the Craven Basin and adjacent areas. *Subsurface Memoir of the British Geological Survey*.
- Klein, R. J. & Barr, M. V. 1986. Regional state of stress in Western Europe. In: Stephansson, O. (Editor.) *Proceedings of the International Symposium on Rock Stress and Rock Stress Measurements*, Stockholm, 1–3 September 1986. Centek, Lulea, 33–44.
- Lake, S. D. & Kamer, G. D., 1987. The structure and evolution of the Wessex Basin, southern England: an example of inversion tectonics. In: P.A. Ziegler (Editor), *Compressional Intra-Plate Deformations in the Alpine Foreland*. *Tectonophysics*, 137: 347-378.
- Leeman, E. R. & Hayes, D. J., 1966, A technique for determining the complete state of stress in rock using a single borehole. *Proceedings of the 1st congress of the international society of Rock Mechanics*, Lisbon, Part 2, 17-23
- Moos, D., & Zoback, M. D. 1990. Utilization of observations of well bore failure to constrain the orientation and magnitude of crustal stresses: Application to continental, Deep Sea Drilling Project, and Ocean Drilling Program boreholes. *Journal of Geophysical Research*, 95(B6), 9305– 9325, doi:10.1029/JB095iB06p09305.
- Nirex, 1997. *Sellafield Geological and Hydrogeological Investigations: Assessment of In-situ Stress Field at Sellafield*. Nirex Report S/97/003.
- Parker, R. 1999. The Rosemanowes HDR project 1983-1991. *Geothermics*, 28, 603-615.
- Paul, S. & Chatterjee, R. 2011. Mapping of cleats and fractures as an indicator of in-situ stress orientation, Jharia coalfield, India. *International Journal of Coal Geology*, 88, 113-122.
- Pine, R. J., Ledingham, P. & Merrifield, C. M. 1983. In situ Stress Measurement in the Carnmenellis Granite .2. Hydrofracture Tests at Rosemanowes Quarry to Depths of 2000-M. *International Journal of Rock Mechanics and Mining Sciences* 20(2): 63-72.
- Plumb, R. A. and Hickman, S. H. 1985. Stress-Induced Borehole Elongation: A Comparison Between the Four-Arm Dipmeter and the Borehole Televiwer in the Auburn Geothermal Well. *Journal of Geophysical Research*, 90(B7), 5513–5521
- Reinecker, J., Tingay, M. & Müller, B., 2003. Borehole breakout analysis from four-arm caliper logs, World Stress Map Project. WSM website: [http://dc-app3-14.gfz-potsdam.de/pub/guidelines/WSM\\_analysis\\_guideline\\_breakout\\_caliper.pdf](http://dc-app3-14.gfz-potsdam.de/pub/guidelines/WSM_analysis_guideline_breakout_caliper.pdf)
- Rippon, J. H., Ellison, R. A. & Gayer, R. A. 2006. A review of joints (cleats) in British Carboniferous coals: indicators of palaeostress orientation. *Proceedings of the Yorkshire Geological Society*, 56, 15-30.
- Smith, N. J. P., Kirby, G. A. & Pharaoh, T. C. 2005. Structure and evolution of the south-west Pennine Basin and adjacent area. *Subsurface Memoir of the British Geological Survey*.

- Su, X. B., Feng, Y. L., Chen, J. F. & Pan, J. N. 2001. The characteristics and origins of cleat in coal from Western North China. *International Journal of Coal Geology*, 47, 51-62.
- Tingay, M. R. P., Hillis, R. R., Morley, C. K., Swarbrick, R. E., Okpere, E. C. 2003a. Variation in vertical stress in the Baram Basin, Brunei: tectonic and geomechanical implications. *Marine and Petroleum Geology*, 20, 1201-1212.
- Tingay, M. R. P., Hillis, R.R., Morley, C. K., Swarbrick, R. E., Okpere, E. C. 2003b. Pore pressure and stress coupling in Brunei Darussalam - implications for shale injection. In: Van Rensbergen, P., Hillis, R. R., Maltman, A. J. & Morley, C. K. (eds) 2003. *Subsurface Sediment Mobilization*. Geological Society, London, Special Publications, 216, 369-379.
- Tingay, M., Muller, B., Reinecker, J., Heidbach, O., Wenzel, F. & Fleckenstein, P. 2005. Understanding tectonic stress in the oil patch: The World Stress Map Project. *The Leading Edge*, 24 (12), 1276-1282.
- Tingay, M., Reinecker, J. & Müller, B. 2008. Borehole breakout and drilling-induced fracture analysis from image logs [online], in World Stress Map Project—Guidelines: Image Logs, Helmholtz Cent. Potsdam, GFZ German Research Centre for Geosciences, Potsdam, Germany. (Available at: [http://dc-app3-14.gfz-potsdam.de/pub/guidelines/WSM\\_analysis\\_guideline\\_breakout\\_image.pdf](http://dc-app3-14.gfz-potsdam.de/pub/guidelines/WSM_analysis_guideline_breakout_image.pdf)).
- Ulusay, R. and Hudson, J. A. 2007. The complete ISRM suggested methods for rock characterization, testing and monitoring: 1974-2006. *International Society for Rock Mechanics*, 2007. 628p.
- Verweij, J. M., Boxem, T. A. P. & Nelskamp, S. 2016. 3D spatial variation in vertical stress in on- and offshore Netherlands; integration of density log measurements and basin modelling results. *Marine and Petroleum Geology*. 78. 870-882. DOI: 10.1016/j.marpetgeo.2016.06.016
- White, A. J., Traugott, M. O. & Swarbrick, R. E. 2002. The use of leak-off tests as means of predicting minimum in-situ stress. *Petroleum Geoscience*, 8, 189-193.
- Williams, J. D. O., Fellgett, M. W., Kingdon, A. & Williamson, P. J. 2015. In-situ stress orientations in the UK Southern North Sea: Regional trends, deviations and detachment of the post- Zechstein stress field. *Marine and Petroleum Geology*. 67. 769-784. DOI: 10.1016/j.marpetgeo.2015.06.008
- Williams, J. D. O., Fellgett, M. W. & Quinn, M. F. 2016. Carbon dioxide storage in the Captain Sandstone aquifer: determination of in situ stresses and fault-stability analysis. *Petroleum Geoscience*, 22, 211-222. DOI: 10.1144/petgeo2016-036
- Zoback, M. D. 2010. *Reservoir Geomechanics*. Cambridge University Press
- Zoback, M. D., Barton, C. A., Brudy, M., Castillo, D. A., Finkbeiner, B. R., Grollmund, B. R., Moos, D. B., Peska, P., Ward, C. D. & Wiprut, D. J. 2003. Determination of stress orientation and magnitude in deep wells. *International Journal of Rock Mechanics & Mining Sciences*., 40, 1049 – 1076.